Doctoral Dissertation

Syntheses and Characterizations of Diketopiperazine Monomers and Corresponding Polyamides

Hongrong YIN

Supervisor: Tatsuo KANEKO

Graduate School of Advanced Science and Technology

Japan Advanced Institute of Science and Technology

Materials Science

March 2021

Abstract

Chirality and self-assembly are basic attributes of nature and closely related life activity. In materials science, chirality and self-assembly of biopolymers also inspire the development of functional materials, especially in cases of amino acids and polypeptides. Synthetic polypeptides have been studied in many fields, especially in medical applications such as nanoparticles, drug delivery system, and tissue engineering.

2,5-Diketopiperazines (DKPs), which are cyclic dipeptides, are common in nature or easily synthesized by the condensation of α-amino acids. Based on two symmetrical amide groups in a six-membered ring, DKPs have four sites able to form hydrogen bond, which result in highly molecular arrangement properties. Due to the strong hydrogen bonding and chiral structure, DKPs have been studied in medicine design, chiral catalyst, low molecular weight gelators, and annexing agent for polymers. However, though DKPs have many interesting properties, only a few DKP-based polymers were reported and the effects of DKP moiety on the corresponding properties of polymers are not clear. Otherwise, the synthesis of DKP monomer is challenging and important for the synthesis of polymers.

The aim of this work is to study chirality and self-assembly properties of DKP monomers and resulting polyamides. This work is divided into three parts: (1) syntheses and configurational studies of diketopiperazine stereoisomers; (2) syntheses and solvent-controlled self-assembly of diketopiperazine-based polyamides from aspartame; (3) syntheses and stereochemistry-property studies of diketopiperazine-based polyamides.

In chapter II, to synthesize AB-type DKP monomers, cyclo(aspartyl-4-amino-phenylalanyl) (ADKP), step-wise protection and deprotection of (L/D)-aspartic acid and (L/D)-4-nitro phenylalanine was performed. Caused by the solubility problem of precursors of trans-ADKPs, LD- and DL-ADKP were synthesized in low yield. No racemization occurred during the synthesis. Structural characterizations and studies of stereoisomers were performed by 1H NMR, ROESY, FTIR, and CD. In DMSO solution, configurations of cis- and trans-ADKP were confirmed, in which DKP ring was in planer structure, and the folded benzene ring was stabilized by C_β-H…π interaction in cis-structures and C_α-H…π interaction in trans-structures. Self-assemble behavior of stereoisomer was studied by solvent displacement method. LL- and DD-ADKP show similar chrysanthemum-like morphology, while LD-ADKP shows rose-like morphology. The present study provides a synthesis method for stereoisomers of DKP, and structural insight of phenylalanine-aspartic acid-based DKP, which have potential for drug and catalyst design.

In chapter III, LL-type ADKP was synthesized from aspartame and subsequently utilized in the polycondensation of homo-polyamide (PA1) with high molecular weights. By using various amino acid, dicarboxylic acid, and diamine, random DKP-based copolymers were also synthesized. The self-assembly properties of ADKP and PA1 were studied via the solvent displacement method. Notably, PA1 self-assembled into particles with various morphologies in different solvent systems, such as irregular networks, ellipsoids, and vesicles. The morphological transformation was also confirmed by dropping acetone and toluene onto the PA1 particles. Furthermore, infrared spectra and Hansen solubility parameters of PA1 and different solvents revealed the particle formation mechanism, which provided more insights into the relationship between the morphology and strength of the hydrogen bonding of each solvent.

In chapter IV, Homo-polyamides and co-polyamides from ADKP stereoisomers were synthesized. Due to same chemical structure, all PAs showed similar molecular weight, thermal properties and solubility. Determined by CD spectroscopy, all PAs showed optical activity. Moreover, solvent/third molecule effect on LL-PA was investigated by adding other solvents into the LL-PA DMSO solution. When water and ethanol were added, LL-PA in DMSO became optical inactivity. It is suggested that water or ethanol disturbed hydrogen bond between DKP units in polymer chain, which played an important role in stabilizing secondary structure of polymer. Self-assembly of PAs were investigated. LL-PA, DD-PA and LLcoDD-PA self-assembled into vesicles, while LD-PA self-assembled into cubic structure in toluene and acetone. The present study provides structural insights of DKP-based polymers with stereochemistry, and reveals their optical and self-assemble properties.

As conclusions, DKP unit is an important building block for medicines, catalysts, supramolecules, and has enormous potential for development of functional materials. However, polymers carrying DKP unit in backbone have not been well explored and are lack of study. In this study, novel AB-type DKP monomers and relative polyamides with stereochemistry were successfully synthesized. Chirality and self-assembly properties of obtained monomers and polyamides were well studied. This study creates a new insight on stereochemistry and self-assembly of DKP monomers and polymers, which could lead to the development of functional materials.

Keywords: bio-based polymers, diketopiperazine, self-assembly, nanoparticles, stereochemistry

Acknowledgements

I, the author of this dissertation, would like to express my deepest gratitude to my respected supervisor *Professor Tatsuo Kaneko* for his valuable guidance, supervision, encouragement, and support during my study in Japan Advanced Institute of Science and Technology (JAIST).

I would like to extend my appreciation to my thesis committee: my second supervisor *Professor Toshiaki Taniike, Professor Kazuaki Matsumura, Associate Professor Kosuke Okeyoshi* at JAIST and *Professor Michiya Matsusaki* from Osaka University.

I am very grateful to my advisor for minor research *Associate Professor Shun Nishimura, Professor Kohki Ebitani, Assistant Professor Kenji Takada,* and *Dr. Maiko Okajima* for their excellent guidance and kind encouragement at professional and personal level. This work would never have performed without their great supporting.

Finally, I would like to give his sincere thanks to my family and members of Kaneko laboratory for their supporting.

January 2021

Hongrong YIN

Contents

CHAPTER I

General introduction

1.1 Bio-based polymers

Since the first man-made plastic Celluloid was created by Thomas Hancock in1855[1], uncountable plastics has been synthesized and developed. Benefited from the low cost, manufacturing and functionality, plastics are widely used in multifarious fields. Since 1989, production of plastics has been passed the production of steel by volume, and in 2015, about 322 million tons of plastics were produced[2]. Nowadays, from industries to basic necessities of life, even aerospace, plastics are considered as essential materials.

However, most of the plastics are derived from petroleum, consuming more than half of the petroleum which is used in chemistry. In the contrary of the convenience of plastics, the production of petroleum-based plastics has been raising serious global environmental issues and resource problems such as garbage-related problem, air pollution, and oil shortage.[3,4] Facing with these issues, many approaches have been coming up with. Under the concept of sustainable society, recycling of plastic products is one of the preferable options while energy recovery also become an alternative option.[5,6]

From the view of the raw material of plastics, to reduce and substitute petroleum, bio-based polymers are in needed, which are based on renewable resources, such as plants, animals, bacteria.[7,8] Bio-based polymers are normally divided into two types: first is the direct obtained polymers and their derivatives, like cellulose and chitosan; second is polymers derived by bio-based monomer like poly(lactic acid) (PLA)[8].

1.1.1 Commercial bio-based polymers

Academia and industry have been playing effort for development of bio-based polymers, and successfully produce commercially available high performance-bio-based polymers, such as Sorona® of Dupont, Planext® of Teijin, and Torayca® of Toray. Nowadays, bio-based polymers have been produced more than 2.11 million tonnes a year in 2019, which occupies around 1 % of total plastic production.[9] Various types of bio-based polymers are produced and available in the market, for example, bio-based PP (polypropylene), PE (polyethylene), PET (polyethylene terephthalate), PA (polyamide), and innovative PHAs (polyhydroxyalkanoates).[10–12] Various bio-based polymers have been widely accepted and used in industry and family, from packing agriculture, automotive, construction to electrics (Figure 1.1)[9].

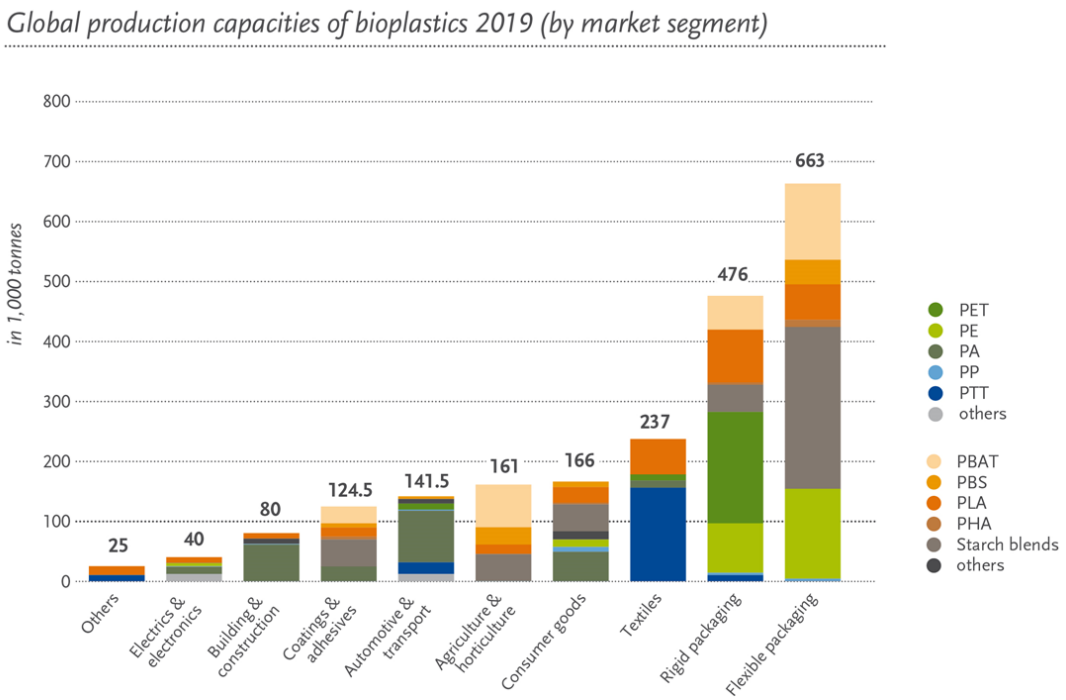

Figure 1.1 Global production capacities of bio-based polymers.

1.1.2 Functional bio-based polymers

Bio-based polymers are not only used as direct materials, but also as functional bio-based polymers. Bio-based polymers have been studied in many fields, especially in medical applications such as nanoparticles, drug delivery system, and tissue engineering[13–15]. Based on the chemical structure of bio-based polymers, such as the sugar structure peptide structure, and aliphatic ester structure, many bio-plastics are considered as ideal biomaterial for food, medicine, and personal care, because they have properties of non-toxicity, biocompatibility, biodegradability, and self-assembly (Figure 1.2)[13,14,16–18]. Naturally derived bio-based polymers included polysaccharides such as cellulose, chitosan, and amino acid-based protein such as gelatin, wool, have been used since ancient time[13,19,20]. However, they have disadvantage of poor mechanical properties. On the other hand, synthetic bio-based polymers, such as PLA, poly(hydroxy butyrate) (PHB), poly(lysine), and poly(aspartic acid), have enhanced mechanical properties, predictable and controllable functionalities, which can be used in more complicated situations.[15,21–24] To achieve a certain function, composition or blend of naturally derived bio-based polymers and synthetic bio-based polymers, also inorganic materials has been applied.

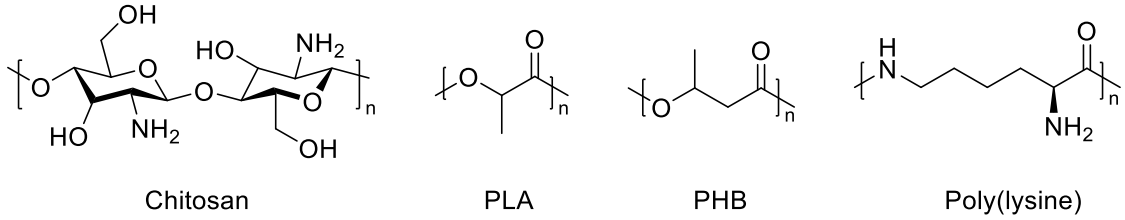

Figure 1.2 Structures of representative functional bio-based polymers.

Nano-/micro-particles

Polysaccharide and amino acid-based bio-based polymers have advantages of biocompatibility and biodegradability, also, they have multiple functional groups for noncovalent bond formation, such as hydroxyl group, carboxyl group, sulfonyl group, amine, aromatic ring and amide bond.[25,26] As a result, these bio-based polymers can form particle system through self-assembly. Several important factors should be counted in the selection of bio-based polymers for particulation: (1) self-assemble ability; (2) particles functionalities, such as size, morphology, stability or sensitivity to environment.[18,27–29] The formation of particles can be divided into two type: spontaneous method through physiochemistry and induced method through processing method. In practice, particulation of bio-based polymers is a combination of these methods. Spontaneous method includes segregative system (for example, phase separation, resulting in core-shell particles) and aggregative system (for example, self-assembly, resulting in homogeneous particles) (Figure 1.3). To form bio-based polymers particles, processing methods are also important, for examples, molding techniques, solvent desorption, injection, gelation, and emulsion-templating methods. Various bio-based polymers particles have been widely utilized in many fields, such as food, encapsulating, personal care, and medical use.

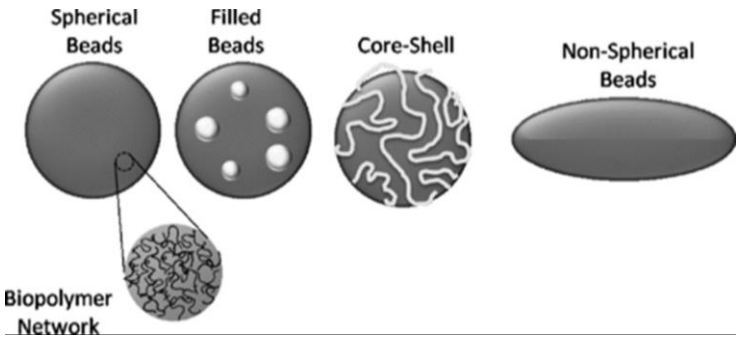

Figure 1.3 bio-based polymers particles systems.

Tissue engineering scaffolds

Tissue engineering refers to the use of materials to rebuild or repair organs and tissues through in vitro culture or construction. Materials for Tissue engineering scaffold are basically required for biocompatibility, biodegradability, porosity, and mechanical performance.[30–32] Thus, many bio-based polymers have been investigated as tissue engineering scaffold. Some naturally derived polysaccharides and proteins such as hyaluronan, and collagen, are components of extracellular matrix, which have regulation effect of division, migration of cells. On the other hand, synthetic bio-based polymers such as PLA, polycaprolactone (PCL), have higher mechanical properties, which is similar to mechanical properties of tissue.[22,33] In many cases, blends or compositions of natural and synthetic bio-based polymers have been studied for both advantages. As tissues are three-dimensional structure, materials for scaffolds needs high porosity and appropriate pore size to support tissues and transport mass.[15,19,30] Therefore, to produce porous scaffolds, many approaches such as hydrogel, particulate leaching, thermally induced phase separation, and electrospinning have been developed (Figure 1.4).

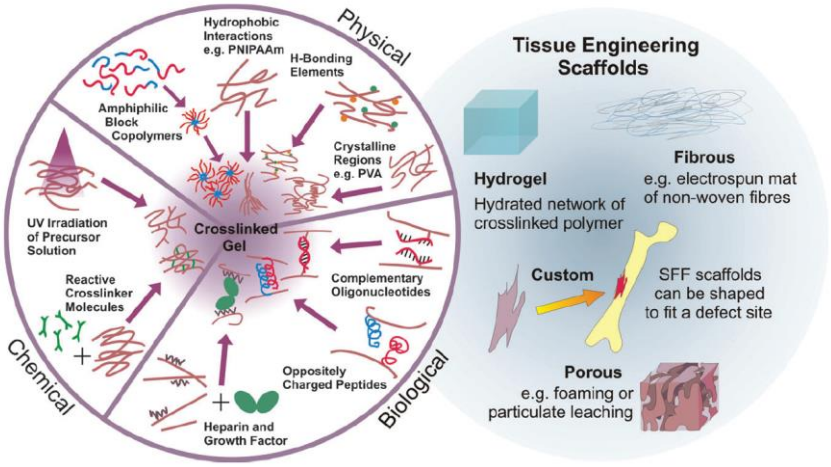

Figure 1.4 (Left) Crosslinking of hydrogel. (Right) Tissue engineering scaffolds forms.

1.2 Biomass

Biomass is a kind of materials from various organisms formed through photosynthesis, including animals, plants and microorganisms.[34] Biomass is important energy resource and raw materials for human since ancient time. Under problems of oil peak and global warming, biomass is attached great important form all over the world, as renewable resource for carbon neutrality. It is estimated that lignin and cellulose, which are the main components of plant biomass, are regenerated at a rate of about 164 billion tons per year, which is 15-20 times the oil output per year in terms of energy conversion. The main sources of biomass are mainly from wood waste, agricultural straw, livestock manure, sugar crop waste, aquatic plants, etc. From chemocatalytic or biocatalytic route, cellulose or other carbohydrates have been derived into various monomers in industry scale, such as furan derivatives, lactic acid derivatives, aliphatic acids, resin acids, ethene, and aliphatic diols (Figure 1.5).[35,36] Thus, some conventional petroleum-based monomers can be derived from biomass, such as ethene, and propene, for productions of PE and PP. Not only in conventional plastics, biomass-derived monomers also can be applied in functional polymers. Lactic acid and lactide are monomers of polylactic acid, which has biodegradability and biocompatibility.[37–39] Furan derivatives are used in synthesis of poly(ethylene furanoate), which has better mechanical and thermal properties than polyethylene terephthalate, and shows self-healing property.[40,41]

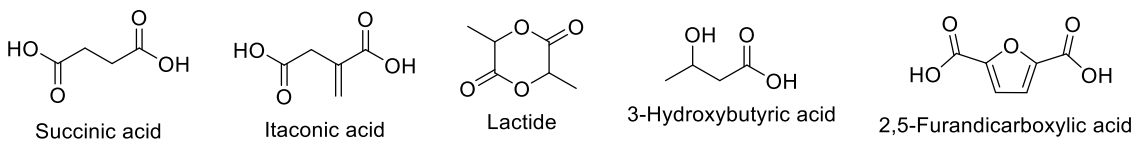

Figure 1.5 Representative biomass-derived monomers.

Moreover, amino acids, which are basic building block of proteins, play a vital role in biological activities in life. Although amino acids are plenty in world, protein-derived amino acids were considered as important nutrient, which were not largely used as materials as much as cellulose-based biomass. Recently, study on amino acid production form biomass-based feedstocks has been developed. Various proteinogenic and non-proteinogenic amino acids are synthesized from biomass-derived hydroxyl acids through chemocatalitic and biocatalytic methods (Figure 1.6).[42]

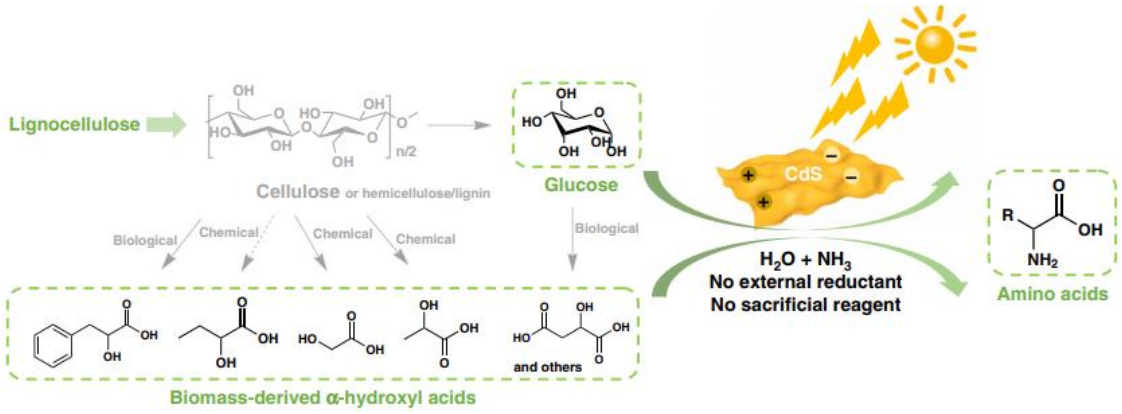

Figure 1.6 Catalytic synthesis of amino acid from plant-based biomass.

As a result, researches on amino acid-based bio-based polymers have attracted interest from scientists.[43] For examples, aspartic acid is used for the synthesis of poly(aspartic acid), which has ability of calcium abortion for water treatment.[44,45] 4-Amino phenylalanine and its derivatives have been applied in syntheses of high-performance polyamides, polyimides, polyurea (Figure 1.7).[46,47]

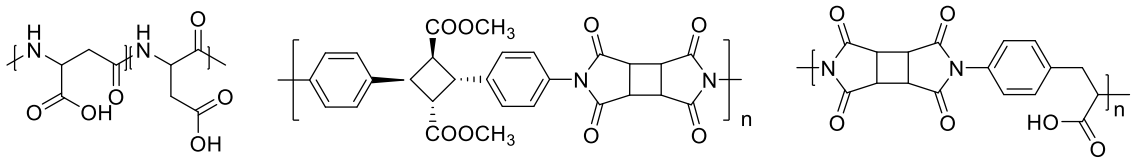

Figure 1.7 Representative amino acid-based bio-based polymers.

1.3 2, 5-Diketopiperazines (DKPs)

2,5-Diketopiperazines (DKPs), which are the cyclic dipeptides, contain two amide bonds where the two nitrogen atoms and the two carbonyls are at opposite sites in a six-membered ring. DKPs-based compounds are naturally occurring, which widely exist from fungi, bacteria, plants, and animals.[48–50] Meanwhile, DKPs are usually synthesized by three methods of cyclization: amide bond formation, C-N bond formation, and C-C bond formation. DKPs are usually obtained as by-products in peptide synthesis, or degradation products from peptides or nylons.[51,52]

1.3.1 Structure features of DKP unit

DKP ring is a six-membered ring, which provide six available positions for modification, resulting in a diversity of DKP-containing molecules. As dipeptides, DKPs have two chiral carbons according to original amino acids, resulted in *cis*- and *trans*-stereoisomers.[53] Furthermore, in cases of asymmetric DKPs from different type of amino acids, DKPs have four kinds of stereoisomers: two *cis*-structures (RR or SS) and two *trans*-structures (RS and SR) (Figure 1.8.a). DKP ring is a semirigid core, and it mainly has two conformations, planer form and boat from, which have very small caloric difference between these two forms (Figure 1.8.b).[50] Substituted side chains deeply affect the conformation of DKPs, for example, DKPs with aromatic side chain prefer in planar conformation, in which aromatic ring tend to overlap with the DKP ring.[54] *Cis*- and *trans*-stereochemistry also have been investigated on conformation. All configurations of DKP unit are calculated within a few kcal/mol, which is important for their bioactivity and the understanding of peptide folding.[55]

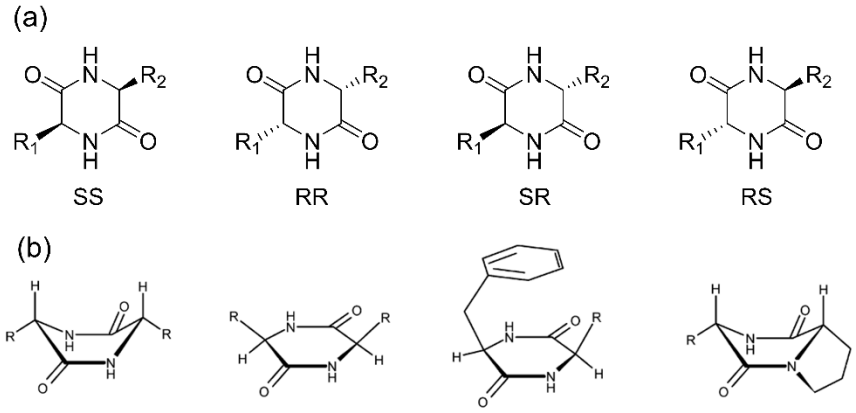

Figure 1.8 (a) Stereoisomers of DKPs, and (b) conformation examples of DKPs.

DKP ring contains two centrosymmetric s-*cis*-amide bonds, which provide two hydrogen bonding acceptor sites and two donor sites. DKPs enable to form intermolecular hydrogen bonding between adjacent molecules, which could cause highly ordered molecular aggregation. Compared to linear dipeptides, DKPs could provide four hydrogen bond sites, and due to the rigidity of ring structure, DKPs have unique self-assembly patterns in liquid state and solid state (Figure 1.9).[52,56,57] Besides the hydrogen bond, other noncovalent forces could be introduced by various side chains in DKP compounds. Since the first crystal structure of DKPs was determined, DKPs has been studied and applied in crystal engineering for their hydrogen bonding properties.

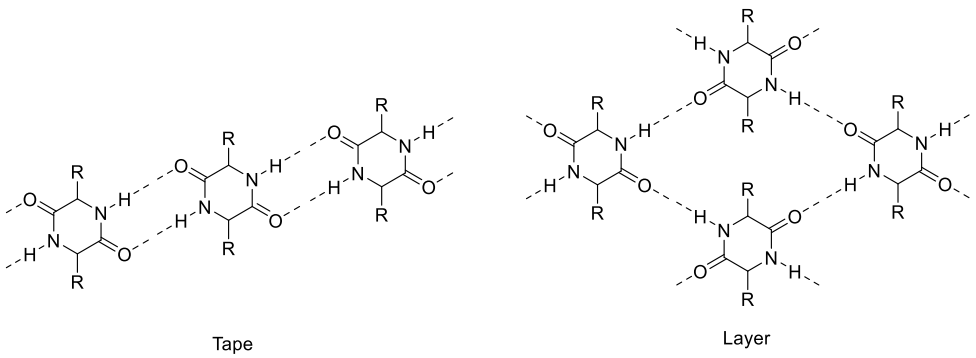

Figure 1.9 Schematic view of hydrogen bonding patterns of DKPs

1.3.2 Functionalities of DKPs

Medicine chemistry

There are many biologically active molecules that contain a DKP unit obtained from nature compounds. The chirality and the molecular configuration of DKPs are important in their bioactivity, and the configuration and structure–activity relationship has been studied in numerous DKPs, which is a significant factor for drug design (Figure 1.10).[58] Compared to liner dipeptides, DKPs as cyclic peptide, are much more rigidity and inflexibility, which could resist rapid enzymatic degradation. Six modifiable sites enlarge the family of DKPs and medical potential. The structural features of the DKPs described above not only allow them to bind to a large number of receptors with strong affinity, exhibiting a wide range of biological activities, but also have the potential development for the drug-like properties required for the multi-objective optimization of pharmaceuticals. DKP containing compounds have been studied and utilized in medicinal chemistry as oxytocin antagonists, cancer inhibitors, antivirals, bioherbicides, anxiolytic agents, and so on.

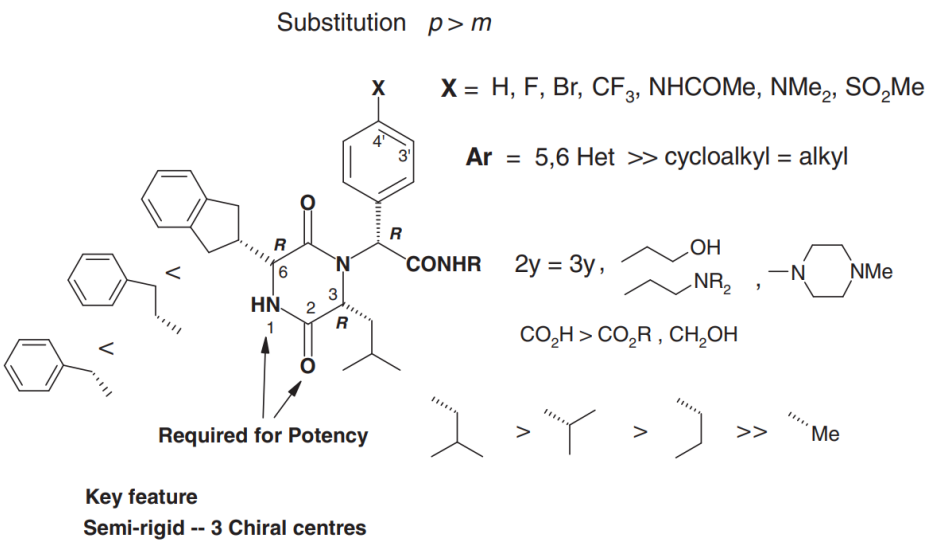

Figure 1.10 Structure–activity relationship of DKP.

Chiral catalyst

Due to the chiral structure and hydrogen bond site, DKPs are considered as a useful template for chiral synthesis. And the structural diversity provides DKPs adapted in various reactions. DKPs are found to have chiral catalytic effect on many asymmetric syntheses such as cyanohydrin formation, Reformatsky reaction, Micheal addition, Diels-Alder reaction ,and so on[59]. For instant, in the hydrocyanation of aldehydes, hydrogen bond site of DKP is presumed to settle reagent in an initial transition state, which allow the side chain with stereochemistry to subsequently attack the reagent for asymmetric autocatalysis (Scheme 1.1). The optical purity of DKPs was found to be important for the enantioselectivity of products.

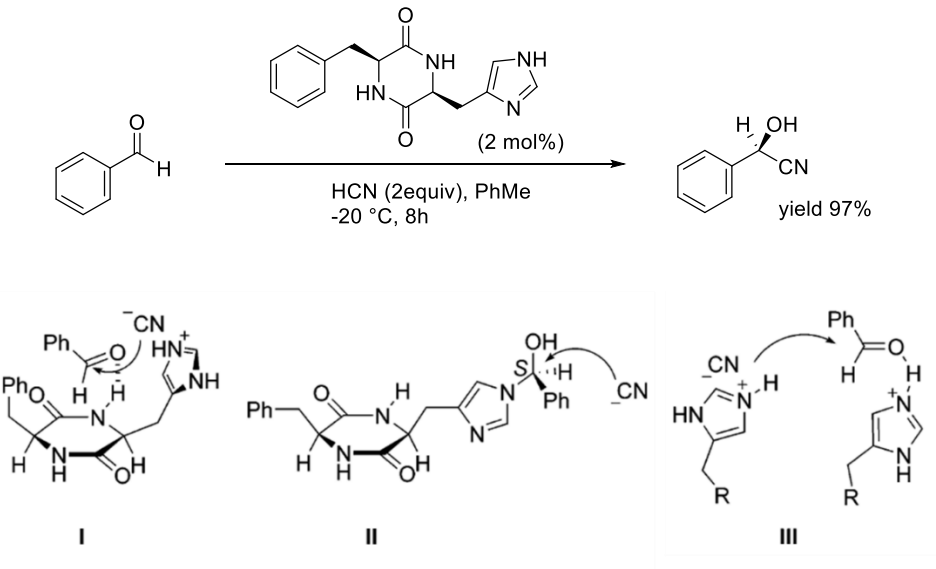

Scheme 1.1 Proposed mechanism for DKP-catalyzed hydrocyanation of aldehydes.

Self-assembly

Self-assembly is a process of the formation of ordered system from molecules via certain, local interactions, which is important not only in the life chemistry (for examples, DNA double helix and structural proteins), but also in the development of functional materials (for examples, soft materials, and drug delivery system). Driving forces of molecules in self-assembly system are mainly non-covalent interactions such as hydrogen bond, π-π interaction, electrostatic force, dipole-dipole force and dispersion force. Based on two *cis*-amide bonds, DKPs can form hydrogen bond and other interactions which depends on side chains from corresponding amino acids, are an ideal building block for fabricate self-assembly systems.

Since the first DKP crystal was studied by R. B. Corey, various DKPs crystal have been investigated. DKPs are considered as useful template for studying influences of interactions and stereochemistry on molecular conformation (Figure 1.11). Besides, the self-assembled DKP crystals are also helpful to understanding the formation of some amyloid disease. Optical waveguiding property is also founded in simple cyclo(phenyl-phenylalanine) crystal.

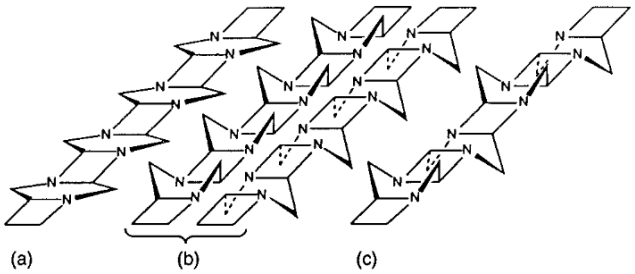

Figure 1.11 Different molecular tapes formed by DKP with stereochemistry.

DKPs as small dipeptides, have been studied as low-molecular-wight-gelators with various additional functionalities. Gelation abilities on organic fluids of DKP family were systematically studied by Hanabusa et. al., in which intermolecular hydrogen bond plays an important role in the formation of three-dimensional network. Thermo-responsive reversible organogels were produced from cyclo(gycine-L-lysine) derivates.[60] Azobenzene-containing DKP gelator was developed by K.Schneider et. al, which has self-healing property and UV-responded DNA/drug release property (Scheme 1.2).[61]

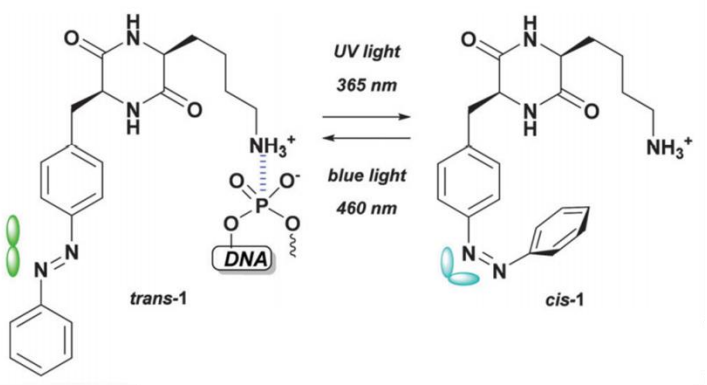

Scheme 1.2 UV-responded DKP.

Methyl L-α-aspartyl-L-phenylalaninate (aspartame) is a methyl ester of aspartic acid and phenylalanine dipeptide which is one of the most common artificial sweeteners in use today (Figure 1.12). [62,63]Through heating, intramolecular cyclocondensation of aspartame occurs and produces cyclo(L-aspartyl-L-phenylalanyl) (APM-DKP). The structure of APM-DKP contains an aromatic ring, a diketopiperazine moiety and a carboxylic group, which is expected to cause strong hydrogen-bonding and π-π stacking.

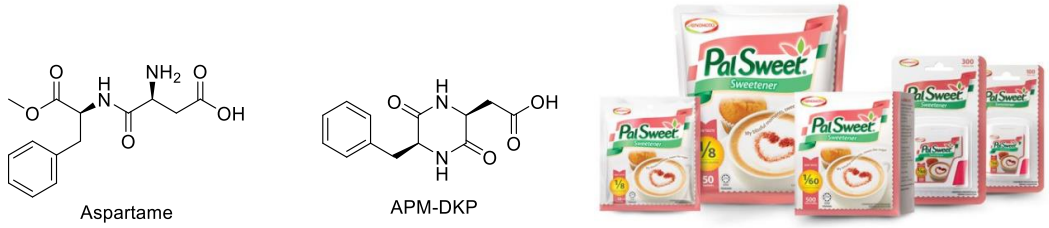

Figure 1.12 Chemical structures of Aspartame and APM-DKP.

APM-DKP has been a most studied DKP core in gelation. For instance, APM-DKP was studied as thixotropic hydrogelators, which showed thermally/isothermally reversible properties in various solvents. Hydrogen bonding and van der Waals force were considered as driving force of the formation of hydrogel (Figure 1.13).[56]

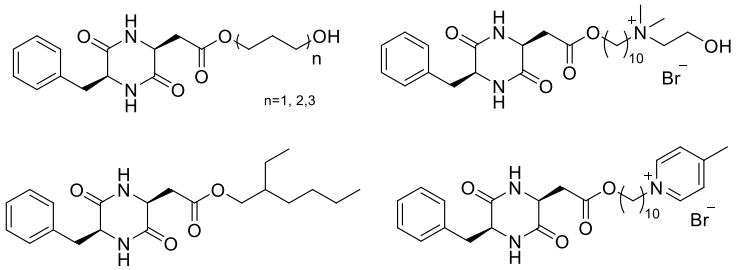

Figure 1.13 Chemical structures of APM-DKP-based gelators.

Bio-based mesoporous were produced by chitosan conjugated with APM-DKP. The novel mesoporous sponges had oil/water emulsion due to the hydrophilic main chain and hydrophobic side chain through hydrogen bonding and π-πinteraction (Scheme 1.3).[64]

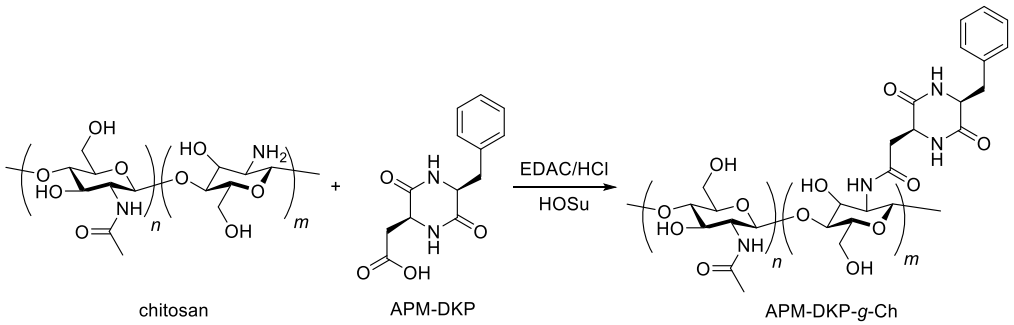

Scheme 1.3 Mesoporous sponges of chitosan conjugated with APM-DKP.

DKP-based polymers

As described above, DKPs in low molecular weight have such attractive properties which have been studied in many fields, so polymers with DKP unit are considered as materials with interesting features. However, due to the difficult synthesis and low solubility of DKP-based monomers, only a few DKP-based polymers have been reported.

Aspartic and glutamic acid-based DKPs have been reported in the polycomdensation with dibromoxylenes and diamines. This method successfully produced DKP-based monomers, and demonstrated the intermolecular hydrogen bond inside monomers. However, it suffered from some problems. Due to the high polarity of the DKP-based monomers, solubility in organic solvents is very low. The polymers obtained from polymerizations with various dibromoxylenes and diamines showed very low molecular weight, from 460 to 4100 (Scheme 1.4)[65]. Due to the low molecular weight, properties of obtained polymers was unclear.

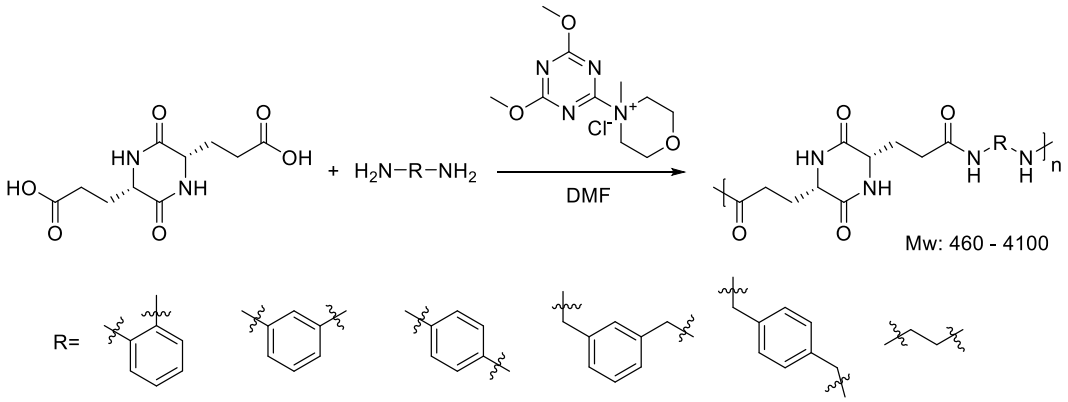

Scheme 1.4 Synthesis of DKP-based polymers with diamines.

A further progress of synthesis of DKP-based polymers was reported. By Masuda and coworkers reported that acyclic diene metathesis (ADMET) polymerization with ruthenium catalysts was applied (Scheme 1.5). In this case, the molecular weight of DKP-based polymer up to 15200. XRD and DSC indicated the crystallization of DKP-based

polymers. Crystalline properties were studied by adding $C_{13}F_{27}COOH$, which could form complex with DKP-based polymers by hydrogen bonding[66]. However, the use of ruthenium catalysts and the low yield of products required development of the synthesis method of DKP-based polymers.

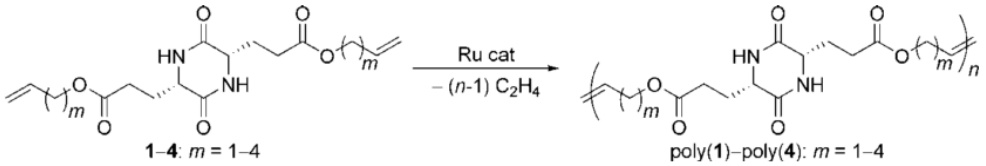

Scheme 1.5 Synthesis of DKP-based polymers by ADMET polycondensation.

DKP monomer from 4-amino phenylalanine was synthesized by Kaneko, by which various polyimides were obtained (Scheme 1.6). These DKP-based polyimides showed high thermal properties. Self-assembly property of DKP-based polymers was firstly demonstrated by particulation. Various morphologies of DKP polyimides particles were observed by changing solvent polarity, which suggested that the self-assembly behavior of DKP unit was deeply affected by environment.[67]

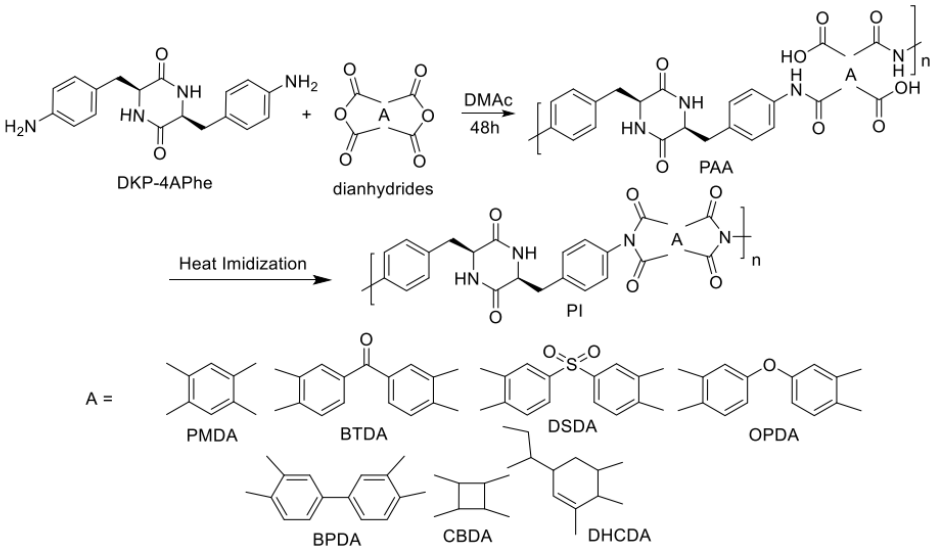

Scheme 1.6 Syntheses of DKP-based polyimides.

1.4 Objects of this thesis

As described above, due to the increasing concerns on oil shock and sustainable society, there are raising attractions on bio-based polymers. DKPs, a kind of cyclic dipeptides, which have multiple hydrogen sites and chirality, attract scientists from various fields. DKP-based polymers are expected to have many properties such as self-assembling, crystalline, and catalytic property, but very few reports about DKP-based polymers are presented, and these polymers all suffer from the low molecular weight which make the effects of DKP moiety on properties of polymer are not clear enough.

In this thesis, novel chiral AB-type DKP monomers and resulting polyamides will be synthesized. This would expand the development of functional bio-based polymer. The objectives of this thesis are as follows:

- Develop novel AB-type DKP stereoisomers, and study their stereo-structures.
- Develop a synthetic pathway of DKP-based monomer from aspartame, and its polyamides for studying the self-assembly properties.
- Develop DKP-based polyamides with stereochemistry and study their stereochemistry-structural relationship.

References

(1) Springate, M. E. Cellulose Nitrate Plastic (Celluloid) in Archaeological Assemblages: Identification and Care. *Northeast Hist. Archaeology* **1997**, *26* (1), 63–72. https://doi.org/10.22191/neha/vol26/iss1/5.

(2) PlasticsEurope. *Plastics - the Facts 2016*; 2016.

(3) Quayle, D. V. Plastics in the Marine Environment: Problems and Solutions. *Chem. Ecol.* **1992**, *6* (1–4), 69–78. https://doi.org/10.1080/02757549208035263.

(4) Monteiro, R. C. P.; Ivar do Sul, J. A.; Costa, M. F. Plastic Pollution in Islands of the Atlantic Ocean. *Environ. Pollut.* **2018**, *238*, 103–110. https://doi.org/10.1016/j.envpol.2018.01.096.

(5) Pivnenko, K.; Eriksen, M. K.; Martín-Fernández, J. A.; Eriksson, E.; Astrup, T. F. Recycling of Plastic Waste: Presence of Phthalates in Plastics from Households and Industry. *Waste Manag.* **2016**, *54*, 44–52. https://doi.org/10.1016/j.wasman.2016.05.014.

(6) Aciu, C.; Ilutiu-Varvara, D. A.; Manea, D. L.; Orban, Y. A.; Babota, F. Recycling of Plastic Waste Materials in the Composition of Ecological Mortars. *Procedia Manuf.* **2018**, *22*, 274–279. https://doi.org/10.1016/j.promfg.2018.03.042.

(7) Saharan, B. S.; Sharma, D. Bioplastics-For Sustainable Development : A Review. **2012**, *1* (1), 11–23.

(8) Jabeen, N.; Majid, I.; Nayik, G. A. Bioplastics and Food Packaging: A Review. *Cogent Food Agric.* **2015**, *1* (1), 1–6. https://doi.org/10.1080/23311932.2015.1117749.

(9) European Bioplastics; Institute for Bioplastics and Biocomposites. Bioplastics market data www.european-bioplastics.org (accessed Nov 10, 2020).

(10) Emadian, S. M.; Onay, T. T.; Demirel, B. Biodegradation of Bioplastics in Natural Environments. *Waste Manag.* **2017**, *59*, 526–536. https://doi.org/10.1016/j.wasman.2016.10.006.

(11) Pan, Y.; Farmahini-Farahani, M.; O'Hearn, P.; Xiao, H.; Ocampo, H. An Overview of Bio-Based Polymers for Packaging Materials. *J. Bioresour. Bioprod.* **2016**, *1* (3), 106–113.

(12) Karan, H.; Funk, C.; Grabert, M.; Oey, M.; Hankamer, B. Green Bioplastics as Part of a Circular Bioeconomy. *Trends Plant Sci.* **2019**, *24* (3), 237–249. https://doi.org/10.1016/j.tplants.2018.11.010.

(13) Jacob, J.; Haponiuk, J. T.; Thomas, S.; Gopi, S. Biopolymer Based Nanomaterials in Drug Delivery Systems: A Review. *Mater. Today Chem.* **2018**, *9*, 43–55. https://doi.org/10.1016/j.mtchem.2018.05.002.

(14) Okamoto, M.; John, B. Synthetic Biopolymer Nanocomposites for Tissue Engineering Scaffolds. *Prog. Polym. Sci.* **2013**, *38* (10–11), 1487–1503. https://doi.org/10.1016/j.progpolymsci.2013.06.001.

(15) Goonoo, N.; Bhaw-Luximon, A.; Bowlin, G. L.; Jhurry, D. An Assessment of Biopolymer- and Synthetic Polymer-Based Scaffolds for Bone and Vascular Tissue Engineering. *Polym. Int.* **2013**, *62* (4), 523–533. https://doi.org/10.1002/pi.4474.

(16) Berezina, N.; Martelli, S. M. Bio-Based Polymers and Materials. *RSC Green Chem. Ser.* **2014**, *27* (Renewable Resources for Biorefineries), 1–28. https://doi.org/10.1039/9781782620181-00001.

(17) Galiano, F.; Briceño, K.; Marino, T.; Molino, A.; Christensen, K. V.; Figoli, A. Advances in Biopolymer-Based Membrane Preparation and Applications. *J. Memb.*

Sci. **2018**, *564* (July), 562–586. https://doi.org/10.1016/j.memsci.2018.07.059.

(18) Dickinson, E. Biopolymer-Based Particles as Stabilizing Agents for Emulsions and Foams. *Food Hydrocoll.* **2017**, *68*, 219–231. https://doi.org/10.1016/j.foodhyd.2016.06.024.

(19) Nitta, S. K.; Numata, K. Biopolymer-Based Nanoparticles for Drug/Gene Delivery and Tissue Engineering. *Int. J. Mol. Sci.* **2013**, *14* (1), 1629–1654. https://doi.org/10.3390/ijms14011629.

(20) Bilal, M.; Iqbal, H. M. N. Naturally-Derived Biopolymers: Potential Platforms for Enzyme Immobilization. *Int. J. Biol. Macromol.* **2019**, *130*, 462–482. https://doi.org/10.1016/j.ijbiomac.2019.02.152.

(21) Majerle, A.; Schmieden, D. T.; Jerala, R.; Meyer, A. S. Synthetic Biology for Multiscale Designed Biomimetic Assemblies: From Designed Self-Assembling Biopolymers to Bacterial Bioprinting. *Biochemistry* **2019**. https://doi.org/10.1021/acs.biochem.8b00922.

(22) Chen, G. Q.; Wu, Q. The Application of Polyhydroxyalkanoates as Tissue Engineering Materials. *Biomaterials* **2005**, *26* (33), 6565–6578. https://doi.org/10.1016/j.biomaterials.2005.04.036.

(23) Guo, L.; Sato, H.; Hashimoto, T.; Ozaki, Y. FTIR Study on Hydrogen-Bonding Interactions in Biodegradable Polymer Blends of Poly(3-Hydroxybutyrate) and Poly(4-Vinylphenol). *Macromolecules* **2010**, *43* (8), 3897–3902. https://doi.org/10.1021/ma100307m.

(24) Lee, S. Y.; Lee, Y.; Wang, F. Chiral Compounds from Bacterial Polyesters: Sugars to Plastics to Fine Chemicals. *Biotechnol. Bioeng.* **1999**, *65* (3), 363–368. https://doi.org/10.1002/(SICI)1097-0290(19991105)65:3<363::AID-

BIT15>3.0.CO;2-1.

(25) Schnitzler, I.; Hausen, C.; Klein, C. Hydrogel for Natural Cosmetic Purposes. *United States Pat. Appl. Publ.* **2012**, *1* (19), 3. https://doi.org/US 20100322867A1.

(26) Ravi Kumar, M. N. V. A Review of Chitin and Chitosan Applications. *React. Funct. Polym.* **2000**, *46* (1), 1–27. https://doi.org/10.1016/S1381-5148(00)00038-9.

(27) Jones, O. G.; McClements, D. J. Recent Progress in Biopolymer Nanoparticle and Microparticle Formation by Heat-Treating Electrostatic Protein-Polysaccharide Complexes. *Adv. Colloid Interface Sci.* **2011**, *167* (1–2), 49–62. https://doi.org/10.1016/j.cis.2010.10.006.

(28) Jones, O. G.; McClements, D. J. Functional Biopolymer Particles: Design, Fabrication, and Applications. *Compr. Rev. Food Sci. Food Saf.* **2010**, *9* (4), 374–397. https://doi.org/10.1111/j.1541-4337.2010.00118.x.

(29) Jones, O. G.; McClements, D. J. Stability of Biopolymer Particles Formed by Heat Treatment of β-Lactoglobulin/Beet Pectin Electrostatic Complexes. *Food Biophys.* **2008**, *3* (2), 191–197. https://doi.org/10.1007/s11483-008-9068-5.

(30) Park, S. Bin; Lih, E.; Park, K. S.; Joung, Y. K.; Han, D. K. Biopolymer-Based Functional Composites for Medical Applications. *Prog. Polym. Sci.* **2017**, *68*, 77–105. https://doi.org/10.1016/j.progpolymsci.2016.12.003.

(31) Cao, Y.; Li, H. Engineered Elastomeric Proteins with Dual Elasticity Can Be Controlled by a Molecular Regulator. *Nat. Nanotechnol.* **2008**, *3* (8), 512–516. https://doi.org/10.1038/nnano.2008.168.

(32) Dou, X. Q.; Feng, C. L. Amino Acids and Peptide-Based Supramolecular Hydrogels for Three-Dimensional Cell Culture. *Adv. Mater.* **2017**, *29* (16). https://doi.org/10.1002/adma.201604062.

(33) Wang, D.; Tong, G.; Dong, R.; Zhou, Y.; Shen, J.; Zhu, X. Self-Assembly of Supramolecularly Engineered Polymers and Their Biomedical Applications. *Chem. Commun.* **2014**, *50* (81), 11994–12017. https://doi.org/10.1039/c4cc03155e.

(34) Bar-On, Y. M.; Phillips, R.; Milo, R. The Biomass Distribution on Earth. *Proc. Natl. Acad. Sci. U. S. A.* **2018**, *115* (25), 6506–6511. https://doi.org/10.1073/pnas.1711842115.

(35) Demirbaş, A. Biomass Resource Facilities and Biomass Conversion Processing for Fuels and Chemicals. *Energy Convers. Manag.* **2001**, *42* (11), 1357–1378. https://doi.org/10.1016/S0196-8904(00)00137-0.

(36) Agbor, V. B.; Cicek, N.; Sparling, R.; Berlin, A.; Levin, D. B. Biomass Pretreatment: Fundamentals toward Application. *Biotechnol. Adv.* **2011**, *29* (6), 675–685. https://doi.org/10.1016/j.biotechadv.2011.05.005.

(37) Gupta, B.; Revagade, N.; Hilborn, J. Poly(Lactic Acid) Fiber: An Overview. *Prog. Polym. Sci.* **2007**, *32* (4), 455–482. https://doi.org/10.1016/j.progpolymsci.2007.01.005.

(38) Lim, L. T.; Auras, R.; Rubino, M. Processing Technologies for Poly(Lactic Acid). *Prog. Polym. Sci.* **2008**, *33* (8), 820–852. https://doi.org/10.1016/j.progpolymsci.2008.05.004.

(39) Corneillie, S.; Smet, M. PLA Architectures: The Role of Branching. *Polym. Chem.* **2015**, *6* (6), 850–867. https://doi.org/10.1039/c4py01572j.

(40) Vasiliou, A. K.; Kim, J. H.; Ormond, T. K.; Piech, K. M.; Urness, K. N.; Scheer, A. M.; Robichaud, D. J.; Mukarakate, C.; Nimlos, M. R.; Daily, J. W.; Guan, Q.; Carstensen, H. H.; Ellison, G. B. Biomass Pyrolysis: Thermal Decomposition Mechanisms of Furfural and Benzaldehyde. *J. Chem. Phys.* **2013**, *139* (10).

https://doi.org/10.1063/1.4819788.

(41) Yao, K.; Tang, C. Controlled Polymerization of Next-Generation Renewable Monomers and Beyond. *Macromolecules* **2013**, *46* (5), 1689–1712. https://doi.org/10.1021/ma3019574.

(42) Deng, W.; Wang, Y.; Zhang, S.; Gupta, K. M.; Hülsey, M. J.; Asakura, H.; Liu, L.; Han, Y.; Karp, E. M.; Beckham, G. T.; Dyson, P. J.; Jiang, J.; Tanaka, T.; Wang, Y.; Yan, N. Catalytic Amino Acid Production from Biomass-Derived Intermediates. *Proc. Natl. Acad. Sci. U. S. A.* **2018**, *115* (20), 5093–5098. https://doi.org/10.1073/pnas.1800272115.

(43) Mallakpour, S.; Dinari, M. Progress in Synthetic Polymers Based on Natural Amino Acids. *J. Macromol. Sci. Part A* **2011**, *48* (8), 644–679. https://doi.org/10.1080/15226514.2011.586289.

(44) Zhao, Y.; Su, H.; Fang, L.; Tan, T. Superabsorbent Hydrogels from Poly(Aspartic Acid) with Salt-, Temperature- and PH-Responsiveness Properties. *Polymer (Guildf).* **2005**, *46* (14), 5368–5376. https://doi.org/10.1016/j.polymer.2005.04.015.

(45) Zhao, Y.; Kang, J.; Tan, T. Salt-, PH- and Temperature-Responsive Semi-Interpenetrating Polymer Network Hydrogel Based on Poly(Aspartic Acid) and Poly(Acrylic Acid). *Polymer (Guildf).* **2006**, *47* (22), 7702–7710. https://doi.org/10.1016/j.polymer.2006.08.056.

(46) Suvannasara, P.; Tateyama, S.; Miyasato, A.; Matsumura, K.; Shimoda, T.; Ito, T.; Yamagata, Y.; Fujita, T.; Takaya, N.; Kaneko, T. Biobased Polyimides from 4-Aminocinnamic Acid Photodimer. *Macromolecules* **2014**, *47* (5), 1586–1593. https://doi.org/10.1021/ma402499m.

(47) Kaneko, T.; Ali, M. A.; Captain, I.; Perlin, P.; Deming, T. J. Polypeptide Gels Incorporating the Exotic Functional Aromatic Amino Acid 4-Amino-l-Phenylalanine. *Polym. Chem.* **2018**, *9* (25), 3466–3472. https://doi.org/10.1039/c8py00427g.

(48) Huang, R.; Zhou, X.; Xu, T.; Yang, X.; Liu, Y. Diketopiperazines from Marine Organisms. *Chem. Biodivers.* **2010**, *7* (12), 2809–2829. https://doi.org/10.1002/cbdv.200900211.

(49) Pérez-Picaso, L.; Escalante, J.; Olivo, H. F.; Rios, M. Y. Efficient Microwave Assisted Syntheses of 2,5-Diketopiperazines in Aqueous Media. *Molecules* **2009**, *14* (8), 2836–2849. https://doi.org/10.3390/molecules14082836.

(50) Hong, Y. P.; Lee, S. H.; Choi, J. H.; Kashima, A.; Nakamura, G.; Suzuki, T. Crystal Structure and Spectroscopic Properties of Cyclic Dipeptide: A Racemic Mixture of Cyclo(D-Prolyl-L-Tyrosyl) and Cyclo(L-Prolyl-D-Tyrosyl). *Bull. Korean Chem. Soc.* **2014**, *35* (8), 2299–2303. https://doi.org/10.5012/bkcs.2014.35.8.2299.

(51) Arunrattiyakorn, P.; Ikeda, B.; Nitoda, T.; Kanzaki, H. Enzymatic Synthesis of Dehydroderivatives from Proline-Containing Cyclic Dipeptides and Their Effects toward Cell Division. *Biosci Biotechnol Biochem* **2007**, *71* (3), 830–833. https://doi.org/10.1271/bbb.60651.

(52) Fischer, P. M. Diketopiperazines in Peptide and Combinatorial Chemistry. *J. Pept. Sci.* **2003**, *9* (1), 9–35. https://doi.org/10.1002/psc.446.

(53) Xu, W. F.; Mao, N.; Xue, X. J.; Qi, Y. X.; Wei, M. Y.; Wang, C. Y.; Shao, C. L. Structures and Absolute Configurations of Diketopiperazine Alkaloids Chrysopiperazines A-C from the Gorgonian-Derived Penicillium Chrysogenum Fungus. *Mar. Drugs* **2019**, *17* (5), 1–10. https://doi.org/10.3390/md17050250.

(54) Pérez-Mellor, A.; Alata, I.; Lepere, V.; Zehnacker, A. Chirality Effects in the Structures of Jet-Cooled Bichromophoric Dipeptides. *J. Mol. Spectrosc.* **2018**, *349*, 71–84. https://doi.org/10.1016/j.jms.2018.02.005.

(55) Li, X.; Hopmann, K. H.; Hudecová, J.; Isaksson, J.; Novotná, J.; Stensen, W.; Andrushchenko, V.; Urbanová, M.; Svendsen, J. S.; Bouř, P.; Ruud, K. Determination of Absolute Configuration and Conformation of a Cyclic Dipeptide by NMR and Chiral Spectroscopic Methods. *J. Phys. Chem. A* **2013**, *117* (8), 1721–1736. https://doi.org/10.1021/jp311151h.

(56) Manchineella, S.; Govindaraju, T. Molecular Self-Assembly of Cyclic Dipeptide Derivatives and Their Applications. *Chempluschem* **2017**, *82* (1), 88–106. https://doi.org/10.1002/cplu.201600450.

(57) Borthwick, A. D. 2,5-Diketopiperazines: Synthesis, Reactions, Medicinal Chemistry, and Bioactive Natural Products. *Chem. Rev.* **2012**, *112* (7), 3641–3716. https://doi.org/10.1021/cr200398y.

(58) Borthwick, A. D.; Liddle, J. The Design of Orally Bioavailable 2, 5-Diketopiperazine Oxytocin Antagonists: From Concept to Clinical Candidate for Premature Labor. *Med. Res. Rev.* **2011**, *31* (4), 576–604. https://doi.org/10.1002/med.20193.

(59) Davie, E. A. C.; Mennen, S. M.; Xu, Y.; Miller, S. J. Asymmetric Catalysis Mediated by Synthetic Peptides. *Chem. Rev.* **2007**, *107* (12), 5759–5812. https://doi.org/10.1021/cr068377w.

(60) Hanabusa, K.; Matsumoto, M.; Kimura, M.; Kakehi, a; Shirai, H. Low Molecular Weight Gelators for Organic Fluids: Gelation Using a Family of Cyclo(Dipeptide)S. *J. Colloid Interface Sci.* **2000**, *224* (2), 231–244.

https://doi.org/10.1006/jcis.1999.6672.

(61) Pianowski, Z. L.; Karcher, J.; Schneider, K. Photoresponsive Self-Healing Supramolecular Hydrogels for Light-Induced Release of DNA and Doxorubicin. *Chem. Commun.* **2016**, *52* (15), 3143–3146. https://doi.org/10.1039/c5cc09633b.

(62) Gaines, S. M.; Bada, J. L. Aspartame Decomposition and Epimerization in the Diketopiperazine and Dipeptide Products as a Function of PH and Temperature. *J. Org. Chem.* **1988**, *53* (12), 2757–2764. https://doi.org/10.1021/jo00247a018.

(63) Yagasaki, M.; Hashimoto, S. Synthesis and Application of Dipeptides; Current Status and Perspectives. *Appl. Microbiol. Biotechnol.* **2008**, *81* (1), 13–22. https://doi.org/10.1007/s00253-008-1590-3.

(64) Takada, K.; Yin, H.; Matsui, T.; Ali, M. A. Bio-Based Mesoporous Sponges of Chitosan Conjugated with Amino Acid-Diketopiperazine through Oil-in-Water Emulsions. *J. Polym. Res.* **2017**.

(65) Terada, K.; Sanda, F.; Masuda, T. Polycondensation of Diketopiperazine-Based Dicarboxylic Acids with Diamines and Dibromoxylenes. *J. Macromol. Sci. Part A Pure Appl. Chem.* **2007**, *44* (8), 789–794. https://doi.org/10.1080/10601320701406971.

(66) Terada, K.; Berda, E. B.; Wagener, K. B.; Sanda, F.; Masuda, T. ADMET Polycondensation of Diketopiperazine-Based Dienes. Polymerization Behavior and Effect of Diketopiperazine on the Properties of the Formed Polymers. *Macromolecules* **2008**, *41* (16), 6041–6046. https://doi.org/10.1021/ma800367z.

(67) Hirayama, T.; Kumar, A.; Takada, K.; Kaneko, T. Morphology-Controlled Self-Assembly and Synthesis of Biopolyimide Particles from 4-Amino-l-Phenylalanine. *ACS Omega* **2020**, *5* (5), 2187–2195. https://doi.org/10.1021/acsomega.9b03231.

CHAPTER II
Syntheses and configurational studies of diketopiperazine stereoisomers

2.1 Introduction

Chirality is the basic attribute of nature and is closely related to life activity.[1] The basic substances of life are chiral, for example, amino acids, proteins, DNA, sugar, and polysaccharide. [2–5] The effects of medicine on living organisms are primarily related to chiral matching and chirality between them and their target molecules in the body.[2,6] Therefore, research on chiral molecules is of particular importance. Different enantiomers of chiral drugs show different efficacy in physiological processes.[7–9] The situation is even more serious, especially if one of the chiral drug enantiomers is therapeutically effective and the other enantiomer shows negative effect.

Diketopiperazines (DKPs) are cyclic dipeptides formed by the condensation of two amino acids via a peptide bond.[10] DKP unit have multiple hydrogen bond acceptor and donor sites in a rigid six-membered ring skeleton with chiral sites, which shows important pharmacological effects, including antibacterial, antifungal, antiviral, antitumor, immunosuppressive neuroprotection, antimalaria, antiprion, antihypertensive, etc.[11,12] The chirality and the molecular configuration of DKPs are important in their bioactivity.[10,13–15] The configuration and structure–activity relationship (SAR) has been studied in numerous DKPs.[7,10,16–18] For instance, stereoisomers of cyclo(Arg-Pro) show different activity for inhibiting cell separation of saccharomyces cerevisiae.[14] Its LD-type isomer shows the highest enzyme activity, and LL-type isomer has middle activity, whereas DL-type is much less active. Moreover, DKPs are not only important in the medicinal chemistry, but also in the catalytic chemistry.[19] Due to the stable ring structure with hydrogen bond sites, DKPs are considered as useful chiral auxiliaries for asymmetric synthesis. Based on a wide range of natural or modified amino acid derivatives, the structural diversity allows DKPs to be applied in various reactions[20,21]. Otherwise, unique

structural characters of DKPs attract interest of scientists. For example, with aromatic side chain, DKP tend to form folded configuration by C-H-π interaction, while with terminal charged group, configuration become complicated.[22] Thus, conformational study of various DKPs has been a hot topic in both pharmacy chemistry and physical chemistry.

Aspartic acid (Asp), which carries an acidic carboxylic acid side chain, is one of amino acids whose both L and D type are naturally presented in mammals. Both L and D type Asp have physiologic effect on human nervous system.[23] 4-aminophenylalanine (4APhe), which carries an ionizable phenylamine side chain, exists in Streptomyces venezuelae as an intermediate of the biosynthetic pristinamycin.[24–26] 4APhe also can be provided by chemical synthesis from phenylalanine or bioconversion from glycerol using metabolic grafting of Escherichia coli.[24] Both L and D type of 4APhe has been applied in the synthesis of medicines, for example, jodomycin.[27] Cyclic dipeptides of (L/D)-Asp and (L/D)-4APhe, cyclo(aspartyl-4-amino-phenylalanyl) (ADKP), which have four stereoisomers, are simple zwitterionic DKPs carrying carboxyl group and phenylamine group. ADKP are considered to have a great potential for developments of medicines, chiral catalysts, and polymeric materials.

This chapter deals with the synthesis and configuration study of four kinds of stereoisomers of ADKP.

2.2 Experimental

2.2.1 Materials

4-Nitro-L-phenylalanine hydrate (L-NPhe·$9H_2O$), 4-nitro-D-phenylalanine hydrate (D-NPhe·$9H_2O$), 4-tert-butyl N-[(9H-fluoren-9-ylmethoxy)carbonyl]- L-aspartate (Fmoc-L-Asp(OtBu)-OH), 4-tert-butyl N-[(9H-fluoren-9-ylmethoxy)carbonyl]-D-aspartate (Fmoc-D-Asp(OtBu)-OH), 1-(3-dimethylaminopropyl)-3-ethylcarbodiimide hydrochloride (EDC·HCl), dichloromethane (DCM) and formic acid were purchased from Tokyo Chemical Industry Co., LTD. Palladium on activated carbon (Pd/C), triethylamine (TEA) and *N*-methylpyrrolidone (NMP) were purchased from FUJIFILM Wako Pure Chemical Corporation. Trimethylsilyl chloride (TMSCl) was purchased from Shinetsu chemical. 1-Hydroxy-1H-benzotriazole, anhydrate was purchased from Dojindo. All the chemicals were directly used as purchased.

2.2.2 Characterization

^{1}H NMR and rotating-frame nuclear overhauser effect spectroscopy (ROESY) spectra were performed by a Bruker Biospin AG 400 MHz, 54 mm spectrometer using DMSO-d_6 as the solvent with the concentration of 4 mg/mL at room temperature.

The FT-IR spectra were recorded with a Perkin-Elmer Spectrum One spectrometer between 4000 and 400 cm^{-1} using a diamond-attenuated total reflection (ATR) accessory.

Circular dichroism (CD) spectra were recorded with a JASCO J-820 spectrometer. All samples were dissolved in DMSO with concentration of 1 mg/mL. Quartz cuvette with 1 cm path length was used. Measured region was 190-300 nm. All spectra were solvent-corrected.

Sample morphologies were characterized with scanning electron microscope (JCM-

6000Plus Versatile Benchtop SEM). Samples were coated with a layer of gold in thickness of 15 nm by a sputter coater (Magnetron sputter MSP-1S). SEM instrument was operated at an acceleration voltage of 10 kV and an emission current of 10 μA.

2.2.3 ADKPs syntheses

Synthetic route of ADKP stereoisomers is shown in Scheme 2.1. LL-, DD-, LD-, DL-type isomers were synthesized by similar protocol (where, ie, LD- refers to L-aspartyl-D-phenylalanyl-.)

a) Synthesis of methyl 4-nitro-phenylalanine hydrochloride (NPhe-Me·HCl)

NPhe·9H_2O (5.5 g, 0.015 mol) was dispersed in methanol (25 mL). After TMSCl (6 mL, 0.060 mol) was added, the milky solution turned into clear solution. The reaction solution was stirred overnight at room temperature. Solvent was evaporated and the crude product was recrystallization from methanol to obtain NPhe-Me·HCl as white powder. L-NPhe-Me·HCl (yield: 92%), ^{1}H NMR (400 MHz, DMSO-d_6, δ, ppm): 3.27 (dd, 2H, J = 4.4, 6.8 Hz), 3.69 (s, 3H), 4.41 (t, 1H, J = 7.0 Hz), 7.56 (d, 2H, J = 8.8 Hz), 8.21 (d, 2H, J = 8.8 Hz), 8.61 (s, 3H); D-NPhe-Me·HCl (yield: 92%), ^{1}H NMR (400 MHz, DMSO-d_6, δ, ppm): 3.28 (t, 2H, J = 6.1 Hz), 3.60 (s, 3H), 4.40 (t, 1H, J = 6.8 Hz), 7.56 (d, 2H, J = 8.6 Hz), 8.21 (d, 2H, J = 8.6 Hz), 8.64 (s, 3H).

b) Synthesis of N-α-Fmoc-aspartyl β-t.-butyl ester-methyl 4-nitro-phenylalanine (Asp-Phe dipeptide)

Fmoc-Asp(OtBu)-OH (4.11 g, 0.010 mol), HOBt (1.62 g, 0.012 mol), and EDC·HCl (2.30 g, 0.012 mol) were added into DMF (30 mL) at 0 ℃. The reaction mixture was stirred for 1 hour under ice bath. Then NPhe-Me·HCl (2.60 g, 0.010 mol) and TEA (5 mL) were added into the reaction mixture. The turbid solution was stirred at room

temperature for overnight. Thereafter, reaction mixture was added into 300 mL water in a 500 mL flask with hand-shaking to obtain sticky precipitate. Then the flask was heated at 50 ℃ with rotation for 1 h, which turned sticky precipitate into solid precipitate. The precipitate was filtered and dried. L-Asp-L-Phe dipeptide (yield, 79%),^{1}H NMR (400 MHz, DMSO-d_6, δ, ppm): 1.35 (s, 9H), 2.39 (dd, 1H, J = 9.6, 16.1 Hz), 2.55 (dd, 1H, J = 4.5, 16.3 Hz), 3.07 (dd, 1H, J = 9.5, 13.4 Hz), 3.20 (dd, 1H, J = 5.1, 13.8 Hz), 3.63, (s, 3H), 4.23 (m, 2H),4.35 (m, 2H), 4.57 (m, 1H), 7.30 (t, 2H, J = 7.5 Hz), 4.35 (t, 2H, J = 7.5 Hz), 7.48 (d, 2H, J = 8.7 Hz), 7.56 (d, 1H, J = 8.6 Hz), 7.69 (d, 2H, J = 7.4 Hz), 7.88 (d, 2H, J = 7.5 Hz), 7.95 (s, 1H), 8.08 (d, 2H, J = 8.6 Hz), 8.40 (d, 1H, J = 7.8 Hz). D-Asp-D-Phe dipeptide (yield, 81%),^{1}H NMR (400 MHz, DMSO-d_6, δ, ppm): 1.35 (s, 9H), 2.39 (dd, 1H, J = 9.6, 16.1 Hz), 2.55 (dd, 1H, J = 4.5, 16.3 Hz), 3.07 (dd, 1H, J = 9.5, 13.4 Hz), 3.20 (dd, 1H, J = 5.1, 13.8 Hz), 3.63, (s, 3H), 4.23 (m, 2H),4.35 (m, 2H), 4.57 (m, 1H), 7.30 (t, 2H, J = 7.5 Hz), 4.35 (t, 2H, J = 7.5 Hz), 7.48 (d, 2H, J = 8.7 Hz), 7.56 (d, 1H, J = 8.6 Hz), 7.69 (d, 2H, J = 7.4 Hz), 7.88 (d, 2H, J = 7.5 Hz), 7.95 (s, 1H), 8.08 (d, 2H, J = 8.6 Hz), 8.40 (d, 1H, J = 7.8 Hz). L-Asp-D-Phe dipeptide (yield, 70%),^{1}H NMR (400 MHz, DMSO-d_6, δ, ppm): 1.32 (s, 9H), 2.26 (dd, 1H, J = 9.6, 16.0 Hz), 2.38 (dd, 1H, J = 4.8, 16.1 Hz), 3.05 (dd, 1H, J = 10.0, 13.6 Hz), 3.22 (dd, 1H, J = 5.1, 13.6 Hz), 3.63, (s, 3H), 4.21 (m, 2H),4.30 (m, 2H), 4.57 (m, 1H), 7.30 (t, 2H, J = 7.5 Hz), 4.35 (t, 2H, J = 7.5 Hz), 7.48 (d, 2H, J = 8.7 Hz), 7.56 (d, 1H, J = 8.6 Hz), 7.69 (d, 2H, J = 7.4 Hz), 7.88 (d, 2H, J = 7.5 Hz), 7.95 (s, 1H), 8.08 (d, 2H, J = 8.6 Hz), 8.40 (d, 1H, J = 8.2 Hz). D-Asp-L-Phe dipeptide (yield, 68%),^{1}H NMR (400 MHz, DMSO-d_6, δ, ppm): 1.32 (s, 9H), 2.26 (dd, 1H, J = 9.6, 16.0 Hz), 2.38 (dd, 1H, J = 4.8, 16.1 Hz), 3.05 (dd, 1H, J = 10.0, 13.6 Hz), 3.22 (dd, 1H, J = 5.1, 13.6 Hz), 3.63, (s, 3H), 4.22 (m, 2H),4.29 (m, 2H), 4.57 (m, 1H), 7.30 (t, 2H, J = 7.5 Hz), 4.35 (t, 2H, J = 7.5 Hz), 7.48 (d, 2H, J = 8.7 Hz),

7.56 (d, 1H, *J* = 8.6 Hz), 7.69 (d, 2H, *J* = 7.4 Hz), 7.88 (d, 2H, *J* = 7.5 Hz), 7.94 (s, 1H), 8.08 (d, 2H, *J* = 8.6 Hz), 8.40 (d, 1H, *J* = 8.2 Hz).

c) Synthesis of cyclo(aspartyl β-t.-butyl ester-4-nitro- phenylalanyl) (NDKP-tBu)

Asp-Phe dipeptide (1.81 g, 0.005 mol) and TEA (8 mL) were added into DCM (16 mL). The reaction solution was stirred overnight at room temperature. The resulting mixture was concentrated under evaporation. Thereafter, the mixture was washed by ethyl ether (200 mL) twice and filtered. LL-NDKP-tBu (yield, 83%), ^{1}H NMR (400 MHz, DMSO-d_6, δ, ppm): 1.31 (s, 9H), 1.96 (dd, 1H, *J* = 5.8, *J* = 16.3 Hz), 2.05 (dd, 1H, *J* = 5.9, 16.3 Hz), 3.08 (dd, 1H, *J* = 5.2, 13.7 Hz), 3.26 (dd, 1H, *J* = 4.2, 13.7 Hz), 4.04 (t, 1H, *J* = 5.2 Hz), 4.35 (t, 1H, *J* = 5.2 Hz), 7.49 (d, 2H, *J* = 8.6 Hz), 8.06 (s, 1H), 8.17 (d, 2H, *J* = 8.7 Hz), 8.26 (s, 1H). DD-NDKP-tBu (yield, 87%), ^{1}H NMR (400 MHz, DMSO-d_6, δ, ppm): 1.31 (s, 9H), 1.96 (dd, 1H, *J* = 5.8, *J* = 16.3 Hz), 2.05 (dd, 1H, *J* = 5.9, 16.3 Hz), 3.08 (dd, 1H, *J* = 5.2, 13.7 Hz), 3.26 (dd, 1H, *J* = 4.2, 13.7 Hz), 4.04 (t, 1H, *J* = 5.2 Hz), 4.35 (t, 1H, *J* = 5.2 Hz), 7.49 (d, 2H, *J* = 8.6 Hz), 8.04 (s, 1H), 8.17 (d, 2H, *J* = 8.7 Hz), 8.25 (s, 1H). LD-NDKP-tBu (yield, 76%), ^{1}H NMR (400 MHz, DMSO-d_6, δ, ppm): 1.35 (s, 9H), 2.43 (dd, 1H, *J* = 5.2, *J* = 16.8 Hz), 2.60 (dd, 1H, *J* = 3.6, 16.9 Hz), 3.05 (dd, 1H, *J* = 5.4, 13.2 Hz), 3.26 (dd, 1H, *J* = 3.9, 14.0 Hz), 3.46 (t, 1H, *J* = 4.8 Hz), 4.23 (t, 1H, *J* = 4.8 Hz), 7.45 (d, 2H, *J* = 8.3 Hz), 8.09 (s, 1H), 8.18 (d, 2H, *J* = 8.3 Hz), 8.28 (s, 1H). DL-NDKP-tBu (yield, 74%), ^{1}H NMR (400 MHz, DMSO-d_6, δ, ppm): 1.35 (s, 9H), 2.43 (dd, 1H, *J* = 5.2, *J* = 16.8 Hz), 2.60 (dd, 1H, *J* = 3.6, 16.9 Hz), 3.05 (dd, 1H, *J* = 5.4, 13.2 Hz), 3.26 (dd, 1H, *J* = 3.9, 14.0 Hz), 3.46 (t, 1H, *J* = 4.8 Hz), 4.23 (t, 1H, *J* = 4.8 Hz), 7.45 (d, 2H, *J* = 8.3 Hz), 8.07 (s, 1H), 8.18 (d, 2H, *J* = 8.3 Hz), 8.26 (s, 1H).

d) Synthesis of cyclo(aspartyl-4-nitro- phenylalanyl) (NDKP)

NDKP-tBu was added into formic acid and stirred for 3 h at room temperature. The resulting mixture was concentrated under evaporation and recrystallize in methanol. LL-NDKP (yield, 80%), ^{1}H NMR (400 MHz, DMSO-d_6, δ, ppm): 2.07 (dd, 1H, J = 5.9, 16.6 Hz), 2.28 (dd, 1H, J = 5.4, 16.6 Hz), 3.10 (dd, 1H, J = 5.3, 14.0 Hz), 3.24 (dd, 1H, J = 4.8, 13.9 Hz), 4.11 (t, 1H, J = 5.6 Hz), 4.34 (t, 1H, J = 5.1 Hz), 7.49 (d, 2H, J = 8.7 Hz), 8.10 (s, 1H), 8.17 (d, 1H, J = 8.7 Hz), 8.23 (s, 1H). DD-NDKP (yield, 78%), ^{1}H NMR (400 MHz, DMSO-d_6, δ, ppm): 2.07 (dd, 1H, J = 5.9, 16.6 Hz), 2.28 (dd, 1H, J = 5.4, 16.6 Hz), 3.10 (dd, 1H, J = 5.3, 14.0 Hz), 3.24 (dd, 1H, J = 4.8, 13.9 Hz), 4.11 (t, 1H, J = 5.6 Hz), 4.34 (t, 1H, J = 5.1 Hz), 7.49 (d, 2H, J = 8.7 Hz), 8.04 (s, 1H), 8.17 (d, 1H, J = 8.7 Hz), 8.22 (s, 1H). LD-NDKP (yield, 80%), ^{1}H NMR (400 MHz, DMSO-d_6, δ, ppm): 2.5 (overlapped with DMSO-$_{d6}$), 2.62 (dd, 1H, J = 4.4, 17.2 Hz), 3.05 (dd, 1H, J = 5.1, 13.4 Hz), 3.27 (dd, 1H, J = 4.5, 13.9 Hz), 3.54 (t, 1H, J = 4.3 Hz), 4.22 (t, 1H, J = 4.3 Hz), 7.47 (d, 2H, J = 8.7 Hz), 8.07 (s, 1H), 8.16 (d, 1H, J = 8.7 Hz), 8.25 (s, 1H). DL-NDKP (yield, 86%), ^{1}H NMR (400 MHz, DMSO-d_6, δ, ppm): 2.5 (overlapped with DMSO-$_{d6}$), 2.62 (dd, 1H, J = 4.4, 17.2 Hz), 3.05 (dd, 1H, J = 5.1, 13.4 Hz), 3.27 (dd, 1H, J = 4.5, 13.9 Hz), 3.54 (t, 1H, J = 4.3 Hz), 4.22 (t, 1H, J = 4.3 Hz), 7.47 (d, 2H, J = 8.7 Hz), 8.03 (s, 1H), 8.16 (d, 1H, J = 8.7 Hz), 8.24 (s, 1H).

e) Synthesis of cyclo(aspartyl-4-amino-phenylalanyl) (ADKP)

NDKP (0.50 g, 1.63 mmol) not subjected to purification was dissolved in pure water, and Pd/C (0.11 g, 22 wt.%) was added. The mixture was connected with a hydrogen generator and reacted with hydrogen at a feed rate of 500 mL/min at 50 °C for 6h. The resulting mixture was filtered and evaporated under vacuum. The resulting solid was recrystallized in water and dried. LL-ADKP (yield, 83%). ^{1}H NMR (400 MHz, DMSO-d_6, δ, ppm):

1.63 (dd, 1H, J=7.4, 11.9 Hz), 2.12 (dd, 1H, *J* = 5.1, 16.4 Hz), 2.72 (dd,1H, *J* = 4.6, 13.8 Hz), 2.91 (dd, 1H, *J* = 4.2, 13.7 Hz), 4.01 (t, 1H, *J* = 6.0 Hz), 4.05 (t, 1H, *J* = 4.7 Hz), 6.46 (d, 2H, *J* =8.3 Hz), 6.80 (d, 2H, *J* =8.3 Hz), 7.84 (s, 1H), 7.98 (s, 1H). DD-ADKP (yield, 83%). ^{1}H NMR (400 MHz, DMSO-d_6, δ, ppm): 1.67 (dd, 1H, J=7.2, 16.5 Hz), 2.13 (dd, 1H, *J* = 5.3, 16.5 Hz), 2.73 (dd,1H, *J* = 4.6, 13.8 Hz), 2.91 (dd, 1H, *J* = 4.5, 13.7 Hz), 4.01 (t, 1H, *J* = 6.0 Hz), 4.05 (t, 1H, *J* = 4.7 Hz), 6.46 (d, 2H, *J* =8.3 Hz), 6.80 (d, 2H, *J* =8.3 Hz), 7.80 (s, 1H), 7.97 (s, 1H). LD-ADKP (yield, 5%). ^{1}H NMR (400 MHz, DMSO-d_6, δ, ppm): 2.40 (d, 2H, *J* = 5 Hz), 2.67 (dd, 1H, *J* = 4.8, 13.6 Hz), 2.93 (dd, 1H, *J* = 3.8, 13.6 Hz), 3.09 (t, 1H, *J* = 5.0 Hz), 3.97 (t, 1H, *J* = 5.0 Hz), 6.44 (d, 2H, *J* =8.4 Hz), 6.79 (d, 2H, *J* =8.4 Hz), 7.95 (s, 1H), 7.99 (s, 1H).

2.3 Results and discussion

2.3.1 Synthesis of ADKP isomers.

DKPs have structural properties such as rigid heterocyclic structure, chirality, and hydrogen bond sites. Charity is provided by two α-carbons of relative amino acids. The chirality and optical activity make DKP become an attractive scaffolding for drug design and chiral catalyst. In peptide chemistry, it is very challenging but important to synthesize peptides and proteins with specific chirality efficiently with chiral amino acids. The condensation reaction between the carboxylic acid and the amine does not undergo easily. Especially, under harsh conditions, such as high temperature, strong acidity, and basicity, racemization of amino acids and peptides will occur, which affect the optical purity of products. Thus, it is necessary to select appropriate condensing agents for reactions under mild conditions. On the other hand, amino acids have functional groups on their side

chains, such as carboxyl, hydroxyl, amino and sulfhydryl groups, these functional groups must be protected from reacting with carboxyl groups. Here, (L/D) aspartic acids carrying typical fluorenylmethyloxycarbonyl (Fmoc) and tertiary butyl (tBu) protecting groups and 4-nitro-phenylalanie were chosen as starting materials. Synthetic route is shown in Scheme 2.1.

In the reaction of coupling of Fmoc-Asp(OtBu)-OH and NPhe-Me·HCl, various condensing agents were tried, such as *N*,*N*'-dicyclohexylcarbodiimide (DCC), EDC and 4-(4,6-dimethoxy-1,3,5-triazin-2-yl)-4-methyl-morpholinium chloride (DMT-MM). As results, DMT-MM gave very low yield of producta, around 20%, where carbodiimides coupling reagents (DCC and EDC) gave higher yield over 80%. DMT-MM did not dissolve in the reaction solvent DMF, therefor, condensation became a hetero-phase reaction, which presumably responses to the low efficiency. On the other hand, when DCC was applied as condensing agents, it was difficult to remove *N*,*N*'-dicyclohexylureais byproducts from the reaction system. *N*,*N*'-Dicyclohexylureais had similar solubility with Asp-Phe linear dipeptide, which was difficult to be separated from desired product. In addition, HOBt was added to avoid racemization during amide formation in the DCC-assisted coupling.

The Fmoc removal and the cyclization of linear peptide were under one-pot synthesis by using TEA as base catalyst. The cleavage of Fmoc protecting group is typically proceeded by basic solution. Pyridine was firstly tried and Fmoc protected group was successfully removed. However, the subsequent intramolecular cyclization did not occur at room temperature. In order to avoid racemization caused by heating under basic condition, the stronger base TEA was used instead. In this case, ester-amide exchange

reaction occurred under mild condition after the Fmoc protecting group cleavage, which resulted in DKP ring formation with high efficiency.

Otherwise, it is known that though stereoisomers have similar chemical structure, they have different physical and chemical properties. In fact, in the last step, the reduction of NDKP to ADKP, was impacted by the stereochemistry, which deeply affected the solubility of NDKP stereoisomers. LL-type and DD-type NDKP have high solubility in water and methanol, while LD-type and DL-type NDKP have very low solubility in these solvents. As results, LL-type and DD-type ADKPs were obtained with more than 80% yield. On the contrary, LD-type and DL-type were barely synthesized with less than 5% yield. However, small amount of LD-ADKP were obtained by large scale synthesis for further characterization and polymerization. All obtained ADKP stereoisomers show high solubility in water and polar organic solvents such as methanol, DMSO, NMP, and DMF.

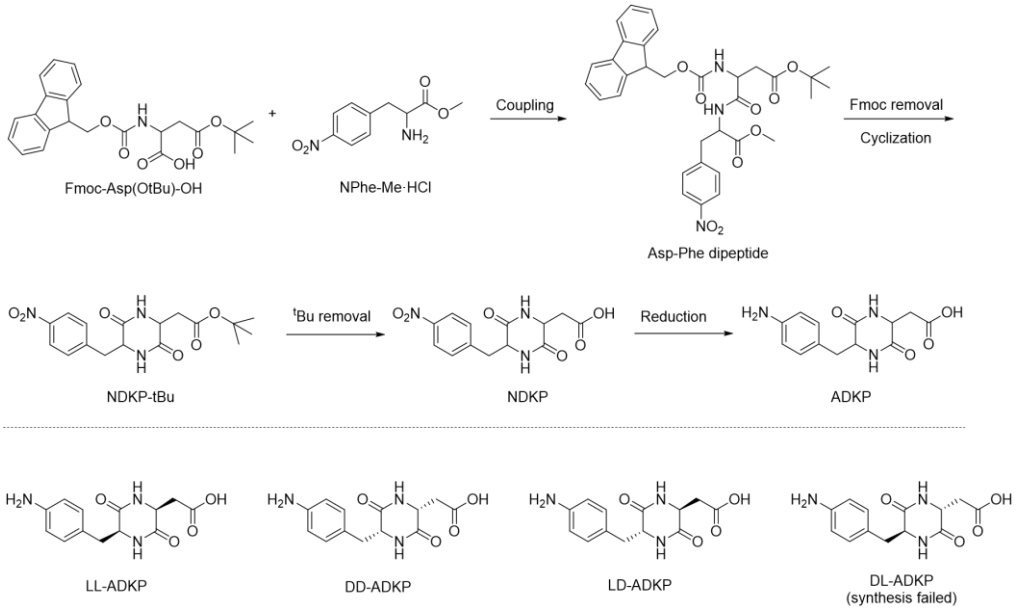

Scheme 2.1 Synthetic route of ADKP stereoisomers form protected aspartic acid and 4-nitro phenylalanine, and structures of ADKP stereoisomers.

2.3.2 Characterization of DKP stereoisomers.

Though DL-ADKP failed to be synthesized, four kinds of NDKP isomers were obtained and examined by ^{1}H NMR shown in Figure 2.1 for the structural discussion of *cis*- and *trans*-stereoisomers. Because both aspartic acid and phenylalanine parts contain chiral carbons, two kinds of α-proton exist in ADKPs and precursors. Two α-protons which have different chemical environment, could be clearly identified by ^{1}H NMR. In *cis*-NDKPs (LL- and DD-type), the aspartic acid-based α-proton and the phenylalanine-based α-proton showed at round 4.11 and 4.34 ppm, respectively. On the other hand, in *trans*-NDKP (LD- and DL-type), the aspartic acid-based α-proton and the phenylalanine-based α-proton showed at around 3.54 and 4.22 ppm. The significant shift of α-proton from aspartic acid part, is considered due to the shielding effect by folded aromatic ring from phenylalanine part, which is observed and reported from other phenylalanine-based DKPs. Peaks at 4.11, 4.34, 3.54, and 4.22 ppm did not occur at the same time in these ^{1}H NMR charts, which indicates that no racemic isomerization occurred during the synthesis of NDKP, though reactions underwent strong basic (TEA) and acidic (formic acid) conditions. In cases of ADKP stereoisomers, difference of α-protons between *cis*- and *trans*-ADKPs was also clearly observed in ^{1}H NMR, shown in Figure 2.2: α-protons in *cis*-ADKPs (LL- and DD-type) shown in a narrow region from 3.98 to 4.13 ppm while *trans*-ADKP shown in a wide region from 3.05 to 4.00 ppm. The shielding effect in α-proton of LD-ADKP is confirmed, which is similar to *trans*-NDKPs. Moreover, LL-ADKP and DD-ADKP which are enantiomers, are considered as mirror images of each other, having same ^{1}H NMR pattern.

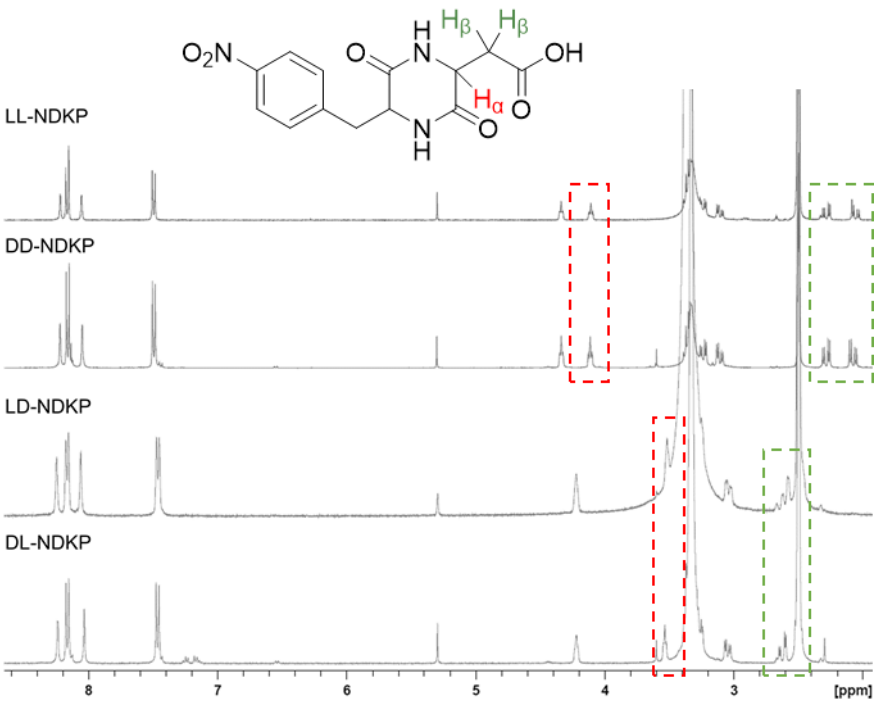

Figure 2.1 ^{1}H NMR spectra of LL-, DD-, LD- and DL-NDKP in DMSO-d_6.

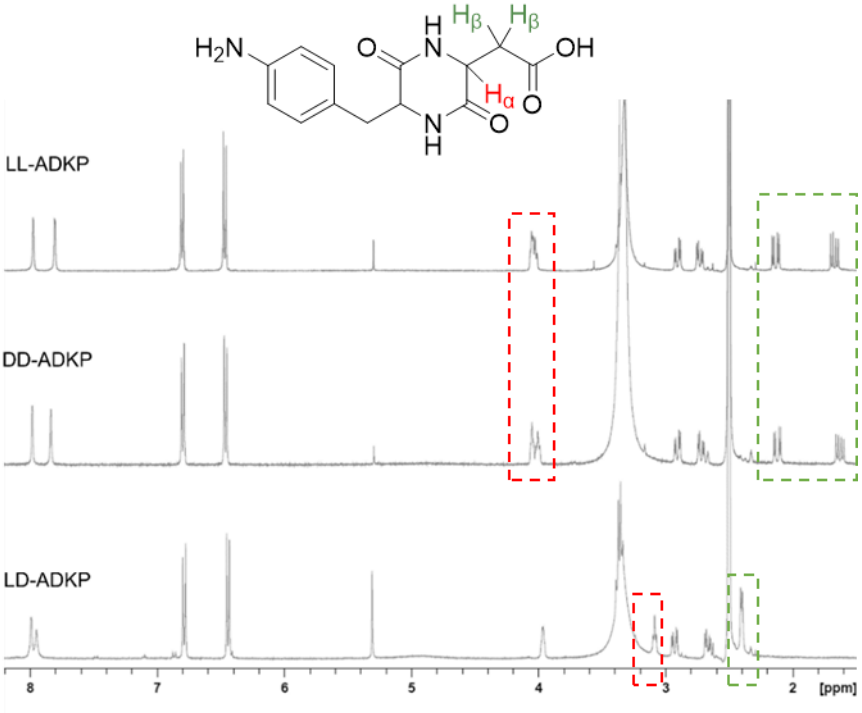

Figure 2.2 ^{1}H NMR spectra of LL-, DD-, LD-ADKP in DMSO-d_6.

Infrared spectra of LL-, DD- and LD-ADKP are presented in Figure 2.3. LL- and DD-ADKP show similar spectra, and LD-ADKP show distinct difference. Peaks of C=O stretching, and N-H bending are shown at 1669 cm^{-1} and 1467 cm^{-1} respectively in all stereoisomers, which indicate the existence of DKP amide. N-H stretching band in around 3200-3500 cm^{-1} is shown in all isomers, but band of LD-ADKP is weaker and shift to higher energy. The C=O stretching band of carboxyl group at around 1710 cm^{-1} is strong in LL- and DD-ADKP, while in LD-ADKP, the band become weaker. Similarly, The C-N stretching band of phenylamine at around 1267 cm^{-1} in LD-ADKP is weaker than LL- and LD-ADKP. The difference between LD-ADKP and *cis*-ADKPs suggests that LD-ADKP tend to form inner salt in solid state. Notably, All IR samples were prepared in same method.

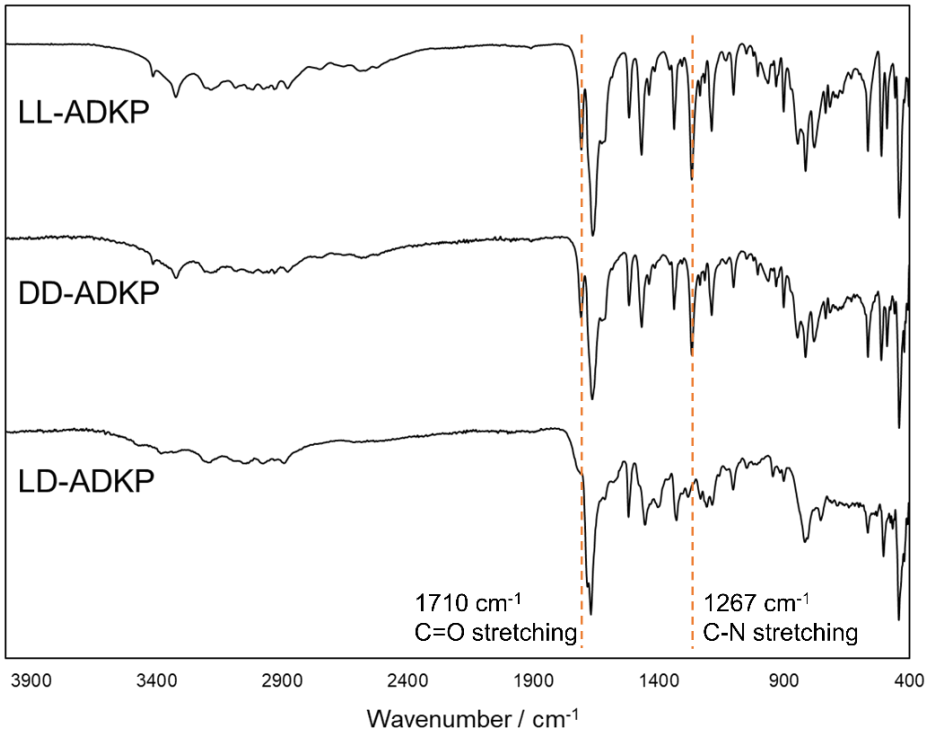

Figure 2.3 IR spectra of LL-, DD- and LD-ADKP.

2.3.3 ROESY study of ADKP stereoisomers.

Nuclear overhauser effect (NOE) which has a strong correlation with molecular configuration, it has been applied to analyze and determine the three-dimensional structure and conformation of molecules, especially in peptide chemistry. When two nuclei are fixed in a molecule while being spatially close to each other, a dipole-dipole interaction acts on the relaxation mechanism of these two nuclei. NOE is a very important measurement method in the current three-dimensional structure determination. Nuclear overhauser effect spectroscopy (NOESY) and rotating-frame nuclear overhauser effect spectroscopy (ROESY) are both two-dimensional space correlation NMR methods using NOE effect. NOESY is a phase sensitivity spectrum, with poor resolution near the diagonal peak, and NOE effect of NOESY in molecule with molecular weight between 600-1000 may be 0, while NOE effect of ROESY is always positive. Thus, ROESY was applied in this study to get more insight into spatial configurations of stereoisomers.

Two-dimensional NMR ROESY spectra of ADKP stereoisomers in DMSO-d_6 were analyzed for spatial configurational study. As enantiomers, LL- and DD-ADKP shows similar cross-peaks correlation, as a result, ROESY of DD-ADKP as a representative of *cis*-ADKP is shown in Figure 2.4.a, while ROESY of LD-ADKP is shown in Figure 2.5.a. In both *cis*- and *trans*-ADKP, protons at ortho site of benzene show cross-peaks with N-*H* of DKP amides, indicating the overlap of DKP ring and benzene ring in both *cis*- and *trans*-ADKP. In the region of β-protons-benzene (shown in red dot frame A in Figure 2.4.a and A' in Figure 2.5.a), β-protons of aspartic acid part only show cross-peaks with protons at ortho site of benzene in *cis*-ADKP, not in *trans*-ADKP, which indicates the β-protons of aspartic acid direct to the benzene ring and the DKP ring, while carboxyl group directs to outside. In the region of α-protons-benzene (shown in red dot frame B in Figure

2.4.a and B' in Figure 2.5.a), α-protons of aspartic acid part show cross-peaks with protons at ortho site of benzene only in *trans*-ADKP, not in *cis*-ADKP, which is characteristic for *trans*-structure. The correlations of β-protons-benzene in cis-ADKP and α-protons-benzene in trans-ADKP suggest configurations are stabilized by C_β-H…π interaction and C_α-H…π interaction, respectively, which is also reported in other aromatic substituted DKP such as cyclo(argininyl-arginine)[28]. Key correlations in *cis*- and *trans*-ADKP are shown in Figure 2.4.b and Figure 2.5.b, respectively.

2.3.4 Computational study of stereoisomers.

For further configurational study, computational structural analysis was applied. LL-, DD- and LD-ADKP were optimized by Gaussian, at the scf-b3lyp/6-31g(d) (IEFPCM, solvent = DMSO) level. As LL- and DD-ADKP are enantiomers, only DD-ADKP as a presentative of cis-structure, and LD-ADKP were presented. As shown in Figure 2.4.c, and Figure 2.5.c, DKP ring in both stereoisomers present in planar structure, which has lower energy compared to boat-like conformers. Otherwise, folded structure of benzene in both stereoisomers is confirmed. Folded structures of *cis*- and *trans*-isomers are stabilized by C_β-H···π and C_α-H···π, respectively. Carboxyl group is oriented to outside in both cases, does not form intramolecular hydrogen bond in both stereoisomers. Optimized structures of *cis*- and *trans*-ADKP support the obtained data from NMR. The C-H···π interaction in both *cis*- and *trans*-isomers explains why racemization did not occur during the synthesis of NDKPs and ADKPs, which occurs in DKP with two aliphatic side chains.

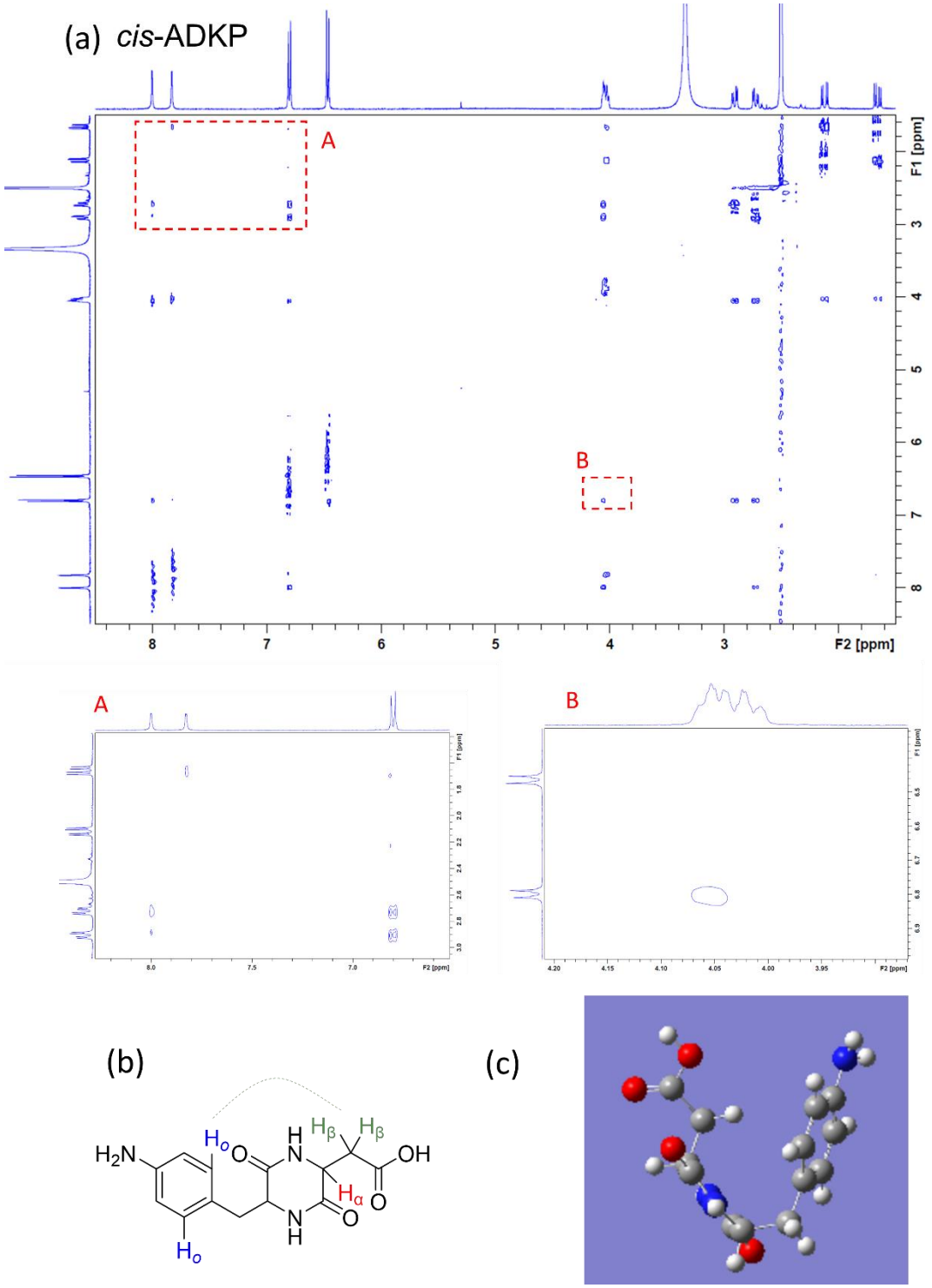

Figure 2.4 (a) ROESY NMR spectra of DD-ADKP in DMSO-d_6. (b) Key correlations of DD-ADKP. (c) Optimized structure of DD-ADKP.

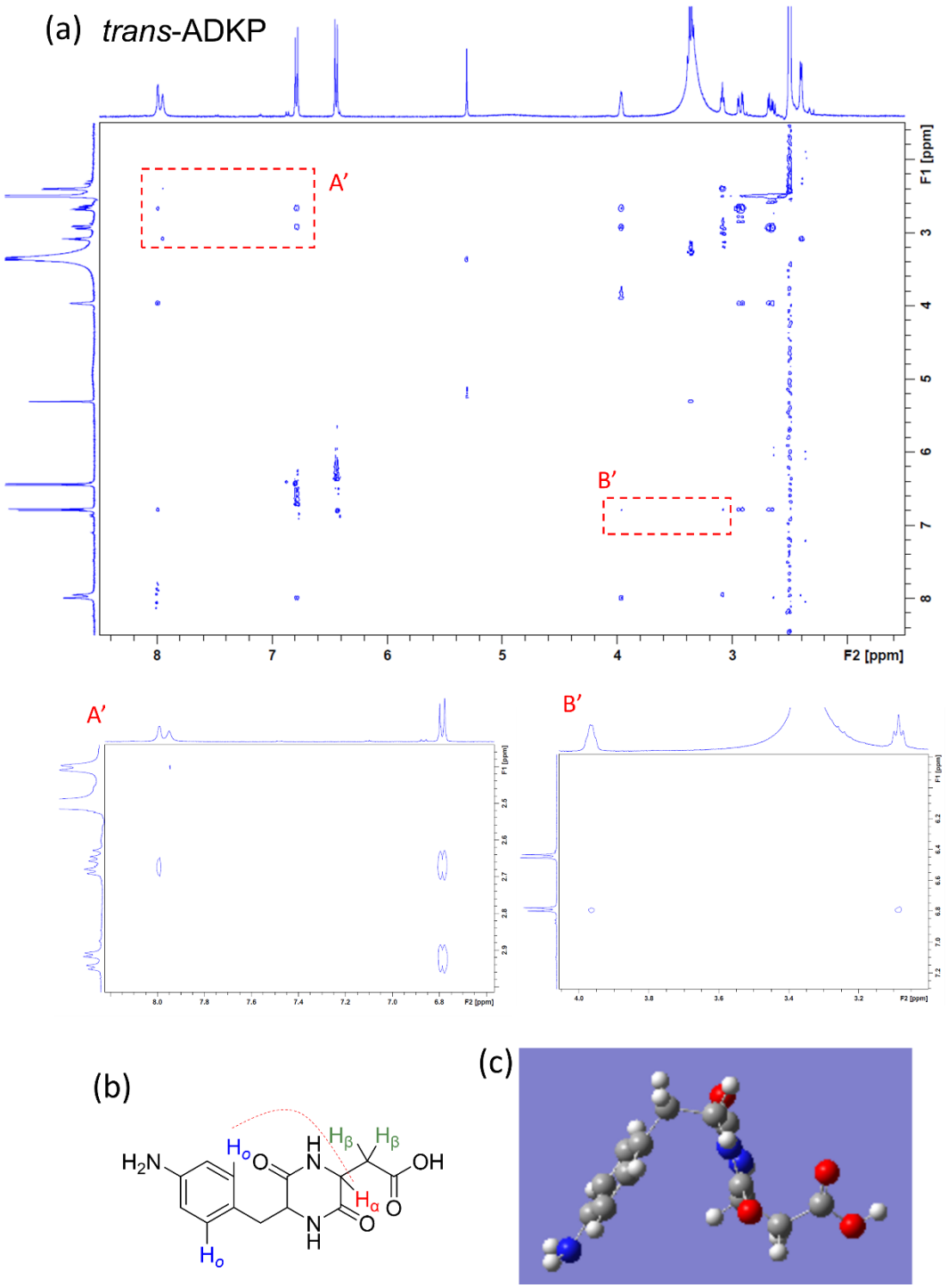

Figure 2.5 (a) ROESY NMR spectra of LD-ADKP in DMSO-d_6. (b) Key correlations of LD-ADKP. (c) Optimized structure of LD-ADKP

2.3.5 Chiroptical property of ADKP stereoisomers.

As chiral molecules, chiroptical property of ADKP stereoisomers is important and measured by CD spectroscopy in the far-UV region, presented in Figure 2.6. LL- and LD-ADKP show negative cotton effect at 210 nm and 208 nm, while DD-ADKP shows a positive cotton effect at a longer wavelength 213 nm, which are assigned to the typical peptide amide n → π* transition. It is known that, hydrogen bond has influence on the excitation energy of amide, resulting in blue shift of n → π* transition.[29] Thus, the shift of DD-ADKP is presumably caused by water absorption of DMSO solution. The CD spectra of LD-ADKP shows similar to the peptide with random coil secondary structure, which has a maximum negative peak shorter than 200 nm (π → π* transition), and a negative peak around 210 nm. Difference of CD spectra shows the different geometry of stereoisomers of ADKP.

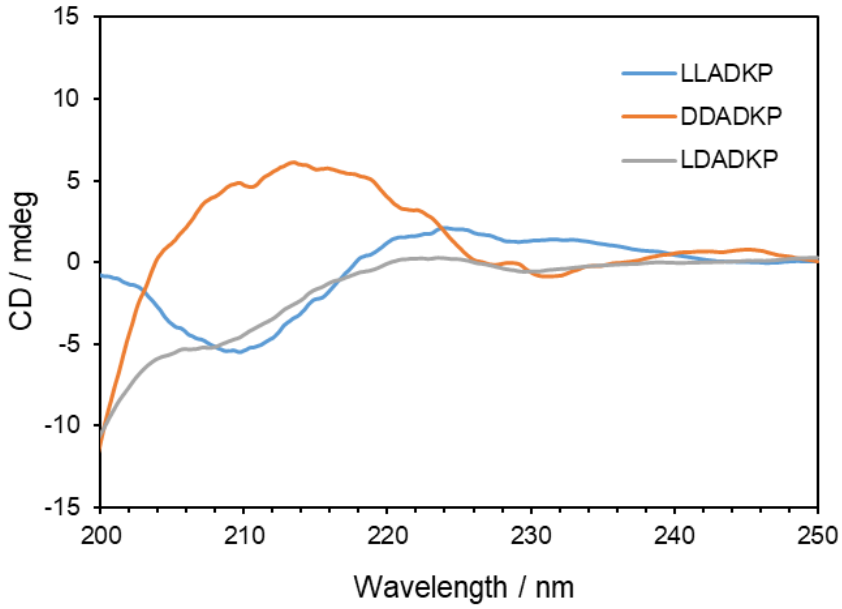

Figure 2.6 CD spectra of LL-, DD- and LD-ADKP in DMSO.

2.3.6 Self-assembly of ADKPs

The geometry is one of the significant factors in the self-assembly / packing of molecules, which further affects functionalities of molecules, such as bioactivity, catalytic activity. Especially in cases of amino acids and peptides, chirality plays an important role in the peptide folding and aggregation, which attracts many scientists[30].

The self-assembly property of ADKP stereoisomers were examined by solvent displacement method as follows: 100 μL DMSO solution of ADKP (2.5 mg/mL) was slowly dropped into 3 mL toluene with stirring to rapidly form particles. As shown in Figure 2.7, LL- and DD-ADKP self-assembled in similar chrysanthemum-like morphology. This behavior was similar to the report from Govindaraju[31], in which LL- and DD-type cyclo(phenylalaninyl-phenylalanine) showed same fibril morphology. In the case of LD-ADKP, rose-like structure was observed. All ADKP particles consisted of two-dimensional petals with a soft and smooth surface. It is suggested that, with continuous hydrogen bonding between DKPs ring, ADKP molecules are considered that arrange into ordered planar tape, resulting in petal-like morphologic substructures. The difference between LL/DD-ADKP and LD-ADKP is suggested that, LD-ADKP may has lower crystallinity than LL- and DD-ADKP.

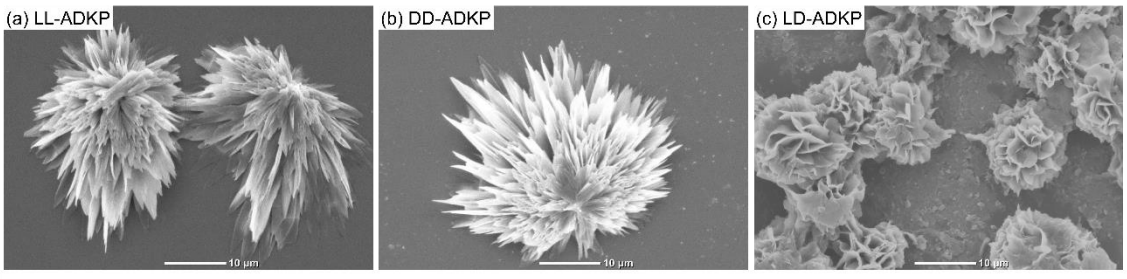

Figure 2.7 SEM images of particles obtained by the dispersion into toluene, (a) LL-ADKP, (b) DD-ADKP, (c) LD-ADKP

2.4 Conclusion

Three kinds of stereoisomers of cyclo(aspartyl-4-amino-phenylalanyl) (ADKP) were synthesized by step-wise protection and deprotection from ($_{L/D}$)-aspartic acid and ($_{L/D}$)-4-nitro phenylalanine. Caused by the solubility problem of precursors of *trans*-ADKPs, LD-ADKP and DL-ADKP were synthesized in low yield. Structural study of stereoisomers was performed by ^{1}H NMR, two-dimensional NMR ROESY, FTIR, TD-DFT and CD. In solid state, LD-type *trans*-ADKP tends to form inner salt form while *cis*-ADKPs are not. In DMSO solution, configurations of *cis*- and *trans*-ADKP were confirmed, in which DKP rings are in planer structure, and benzene ring are stabilized by C_{β}-H$\cdots\pi$ and C_{α}-H$\cdots\pi$ interactions, respectively. Self-assembly property of stereoisomer was study by particle formation. LL- and DD-ADKP show similar chrysanthemum-like morphology, while LD-ADKP shows rose-like morphology. The present study provides a synthesis method for stereoisomers of DKP, and structural insight of phenylalanine-aspartic acid-based DKP, which have potential for drug and catalyst design.

References

(1) Bonner, W. A. Chirality and Life. *Orig. Life Evol. Biosph.* **1995**, *25* (1–3), 175–190. https://doi.org/10.1007/BF01581581.

(2) Mori, K. Bioactive Natural Products and Chirality. *Chirality* **2011**, *23* (6), 449–462. https://doi.org/10.1002/chir.20930.

(3) Wagner, A. J.; Zubarev, D. Y.; Aspuru-Guzik, A.; Blackmond, D. G. Chiral Sugars Drive Enantioenrichment in Prebiotic Amino Acid Synthesis. *ACS Cent. Sci.* **2017**, *3* (4), 322–328. https://doi.org/10.1021/acscentsci.7b00085.

(4) Lee, S. Y.; Lee, Y.; Wang, F. Chiral Compounds from Bacterial Polyesters: Sugars to Plastics to Fine Chemicals. *Biotechnol. Bioeng.* **1999**, *65* (3), 363–368. https://doi.org/10.1002/(SICI)1097-0290(19991105)65:3<363::AID-BIT15>3.0.CO;2-1.

(5) Gekko, K. Carbohydrate Circular Dichroism. *Encycl. Biophys.* **2018**, 1–4. https://doi.org/10.1007/978-3-642-35943-9_86-1.

(6) Amdursky, N.; Stevens, M. M. Circular Dichroism of Amino Acids: Following the Structural Formation of Phenylalanine. *ChemPhysChem* **2015**, *16* (13), 2768–2774. https://doi.org/10.1002/cphc.201500260.

(7) Pérez-Mellor, A.; Alata, I.; Lepère, V.; Zehnacker, A. Conformational Study of the Jet-Cooled Diketopiperazine Peptide Cyclo Tyrosyl-Prolyl. *J. Phys. Chem. B* **2019**, *123* (28), 6023–6033. https://doi.org/10.1021/acs.jpcb.9b04529.

(8) Zipper, C.; Suter, M. J. F.; Haderlein, S. B.; Gruhl, M.; Kohler, H. P. E. Changes in the Enantiomeric Ratio of (R)- to (S)-Mecoprop Indicate in Situ Biodegradation

of This Chiral Herbicide in a Polluted Aquifer. *Environ. Sci. Technol.* **1998**, *32* (14), 2070–2076. https://doi.org/10.1021/es970880q.

(9) D'Amato, R. J.; Loughnan, M. S.; Flynn, E.; Folkman, J. Thalidomide Is an Inhibitor of Angiogenesis. *Proc. Natl. Acad. Sci. U. S. A.* **1994**, *91* (9), 4082–4085. https://doi.org/10.1073/pnas.91.9.4082.

(10) Hong, Y. P.; Lee, S. H.; Choi, J. H.; Kashima, A.; Nakamura, G.; Suzuki, T. Crystal Structure and Spectroscopic Properties of Cyclic Dipeptide: A Racemic Mixture of Cyclo(D-Prolyl-L-Tyrosyl) and Cyclo(L-Prolyl-D-Tyrosyl). *Bull. Korean Chem. Soc.* **2014**, *35* (8), 2299–2303. https://doi.org/10.5012/bkcs.2014.35.8.2299.

(11) JIANG, C. S.; ZHOU, Z. F.; YANG, X. H.; LAN, L. F.; GU, Y. C.; YE, B. P.; GUO, Y. W. Antibacterial Sorbicillin and Diketopiperazines from the Endogenous Fungus Penicillium Sp. GD6 Associated Chinese Mangrove Bruguiera Gymnorrhiza. *Chin. J. Nat. Med.* **2018**, *16* (5), 358–365. https://doi.org/10.1016/S1875-5364(18)30068-2.

(12) Ding, Y.; Zhu, X.; Hao, L.; Zhao, M.; Hua, Q.; An, F. Bioactive Indolyl Diketopiperazines from the Marine Derived Endophytic Aspergillus Versicolor DY180635. *Mar. Drugs* **2020**, *18* (7). https://doi.org/10.3390/md18070338.

(13) Daugan, A.; Grondin, P.; Ruault, C.; Le Monnier de Gouville, A.-C.; Coste, H.; Kirilovsky, J.; Hyafil, F.; Labaudinière, R. The Discovery of Tadalafil: A Novel and Highly Selective PDE5 Inhibitor. 1: 5,6,11,11a-Tetrahydro-1 H -Imidazo[1',5':1,6]Pyrido[3,4- b]Indole-1,3(2 H)-Dione Analogues. *J. Med. Chem.* **2003**, *46* (21), 4525–4532. https://doi.org/10.1021/jm030056e.

(14) Houston, D. R.; Synstad, B.; Eijsink, V. G. H.; Stark, M. J. R.; Eggleston, I. M.; Van Aalten, D. M. F. Structure-Based Exploration of Cyclic Dipeptide Chitinase Inhibitors. *J. Med. Chem.* **2004**, *47* (23), 5713–5720. https://doi.org/10.1021/jm049940a.

(15) Sharma, S.; Singh, R.; Rana, S. Bioactive Peptides: A Review. *Int. J. Bioautomation* **2011**, *15* (4), 223–250. https://doi.org/10.1093/fqs/fyx006.

(16) Xu, W. F.; Mao, N.; Xue, X. J.; Qi, Y. X.; Wei, M. Y.; Wang, C. Y.; Shao, C. L. Structures and Absolute Configurations of Diketopiperazine Alkaloids Chrysopiperazines A-C from the Gorgonian-Derived Penicillium Chrysogenum Fungus. *Mar. Drugs* **2019**, *17* (5), 1–10. https://doi.org/10.3390/md17050250.

(17) Pérez-Mellor, A.; Le Barbu-Debus, K.; Zehnacker, A. Solid-State Synthesis of Cyclo LD-Diphenylalanine: A Chiral Phase Built from Achiral Subunits. *Chirality* **2020**, *32* (5), 693–703. https://doi.org/10.1002/chir.23195.

(18) Pérez-Mellor, A.; Zehnacker, A. Vibrational Circular Dichroism of a 2,5-Diketopiperazine (DKP) Peptide: Evidence for Dimer Formation in Cyclo LL or LD Diphenylalanine in the Solid State. *Chirality* **2017**, *29* (2), 89–96. https://doi.org/10.1002/chir.22674.

(19) Fuchida, S.; Naraoka, H.; Masuda, H. Formation of Diastereoisomeric Piperazine-2,5-Dione from Dl-Alanine in the Presence of Olivine and Water. *Orig. Life Evol. Biosph.* **2017**, *47* (1), 83–92. https://doi.org/10.1007/s11084-016-9500-7.

(20) Tanaka, K. T.; Mori, A.; Inoue, S.; Tanaka, K. The Cyclic Dipeptide Cyclo[(S)-Phenylalanyl-(S)-Histidyl] as a Catalyst for Asymmetric Addition of Hydrogen

Cyanide to Aldehydes. *J. Org. Chem.* **1990**, *55* (1), 181–185. https://doi.org/10.1021/jo00288a030.

(21) Davie, E. A. C.; Mennen, S. M.; Xu, Y.; Miller, S. J. Asymmetric Catalysis Mediated by Synthetic Peptides. *Chem. Rev.* **2007**, *107* (12), 5759–5812. https://doi.org/10.1021/cr068377w.

(22) Nakao, M. Development of Novel Functional Molecules Based on the Molecular Structure Characteristics of Diketopiperazines. *YAKUGAKU ZASSHI* **2017**, *137* (12), 1505–1516.

(23) Topo, E.; Soricelli, A.; D'Aniello, A.; Ronsini, S.; D'Aniello, G. The Role and Molecular Mechanism of D-Aspartic Acid in the Release and Synthesis of LH and Testosterone in Humans and Rats. *Reprod. Biol. Endocrinol.* **2009**, *7* (October). https://doi.org/10.1186/1477-7827-7-120.

(24) Mohammadi Nargesi, B.; Trachtmann, N.; Sprenger, G. A.; Youn, J. W. Production of P-Amino-l-Phenylalanine (l-PAPA) from Glycerol by Metabolic Grafting of Escherichia Coli. *Microb. Cell Fact.* **2018**, *17* (1), 1–11. https://doi.org/10.1186/s12934-018-0996-6.

(25) Masuo, S.; Zhou, S.; Kaneko, T.; Takaya, N. Bacterial Fermentation Platform for Producing Artificial Aromatic Amines. *Sci. Rep.* **2016**, *6* (May), 1–9. https://doi.org/10.1038/srep25764.

(26) Kaneko, T.; Ali, M. A.; Captain, I.; Perlin, P.; Deming, T. J. Polypeptide Gels Incorporating the Exotic Functional Aromatic Amino Acid 4-Amino-l-Phenylalanine. *Polym. Chem.* **2018**, *9* (25), 3466–3472.

https://doi.org/10.1039/c8py00427g.

(27) Martinez-Farina, C. F.; Robertson, A. W.; Yin, H.; Monro, S.; Mcfarland, S. A.; Syvitski, R. T.; Jakeman, D. L. Isolation and Synthetic Diversification of Jadomycin 4-Amino-l-Phenylalanine. *J. Nat. Prod.* **2015**, *78* (6), 1208–1214. https://doi.org/10.1021/np5009398.

(28) Li, X.; Hopmann, K. H.; Hudecová, J.; Isaksson, J.; Novotná, J.; Stensen, W.; Andrushchenko, V.; Urbanová, M.; Svendsen, J. S.; Bouř, P.; Ruud, K. Determination of Absolute Configuration and Conformation of a Cyclic Dipeptide by NMR and Chiral Spectroscopic Methods. *J. Phys. Chem. A* **2013**, *117* (8), 1721–1736. https://doi.org/10.1021/jp311151h.

(29) Feng, W.; Kim, J. Y.; Wang, X.; Calcaterra, H. A.; Qu, Z.; Meshi, L.; Kotov, N. A. Assembly of Mesoscale Helices with Near-Unity Enantiomeric Excess and Light-Matter Interactions for Chiral Semiconductors. *Sci. Adv.* **2017**, *3* (3), 1–13. https://doi.org/10.1126/sciadv.1601159.

(30) Bera, S.; Xue, B.; Rehak, P.; Jacoby, G.; Ji, W.; Shimon, L. J. W.; Beck, R.; Král, P.; Cao, Y.; Gazit, E. Self-Assembly of Aromatic Amino Acid Enantiomers into Supramolecular Materials of High Rigidity. *ACS Nano* **2020**, *14* (2), 1694–1706. https://doi.org/10.1021/acsnano.9b07307.

(31) Manchineella, S.; Murugan, N. A.; Govindaraju, T. Cyclic Dipeptide-Based Ambidextrous Supergelators: Minimalistic Rational Design, Structure-Gelation Studies, and In Situ Hydrogelation. *Biomacromolecules* **2017**, acs.biomac.7b00924. https://doi.org/10.1021/acs.biomac.7b00924.

CHAPTER III

Synthesis and solvent-controlled self-assembly of diketopiperazine-based polyamides from aspartame

3.1 Introduction

Amino acids are important renewable resources for food, medical, and biological studies, as well as synthetic materials.[1–5] Amino acids and their derivatives have been used as monomers for functional and high-performance polymers.[6–8] Notably, 2,5-Diketopiperazines (DKPs), which are cyclic *α*-amino acid dimers, contain two centrosymmetric s-*cis*-amide bonds in a six-membered ring. DKPs have multiple hydrogen bonding acceptor and donor sites in a rigid ring, which enable the formation of regular molecular assemblies through continuous intermolecular hydrogen bonding.[9–12] This remarkable DKP assembling behavior has been attracting the attention of scientists in crystal engineering, gelators, and supramolecular architectures.[13–19] As described above, DKPs exhibit a unique particle morphology, even when they are used as monomers; it can be expected that they still exhibit such morphologies when they adopt a polymer structure. In addition, the rigid structure of DKP may impart high thermal and mechanical properties to polymeric materials.[20,21] The continuous hydrogen bonding site of DKPs may lead to unique self-assembly.[22] However, only a few DKP-based polymers have been reported, and their self-assembly properties have not been adequately studied.[20–24] The main problem in the development of DKP-based polymers is the low solubility, which induces lower molecular weight and complicates property evaluation. Thus, the design of DKP monomers with high solubility is important for obtaining self-assembled DKP polymers. Almost all DKP monomers used in the literature have been obtained from the homo-coupling of amino acids, which exhibit high symmetry and tend to increase the crystallinity and decrease the solubility of many solvents. The use of asymmetric AB-type monomers of two different amino acids is envisaged to be one of the efficient methods to control solubility.[16,25,26] Masuda et al. reported various synthesis approaches

of DKP-based polymers and confirmed that the hydrogen bonding of DKP moieties affected polymer properties.[23] We recently reported DKP-based polyimides whose particles showed high heat resistance and polymorphism properties.[24] However, the self-assembly mechanism of the DKP moiety in polymers remains unclear, while self-assembly is a bottom-up formation of ordered structures under thermodynamic and kinetic conditions[5,27–30]. The self-assembly behavior of DKPs with low molecular weight has been reported to be deeply affected by conditions and environment. In a solution system, DKP–DKP interactions always compete with DKP-solvent interactions; therefore, investigating the interaction nature of both DKP-based polymers and solvents is important.[31,32]

Solvent parameters have been applied to select solvents for gelation, crystal growth, protein aggregation and other solubility or mixture matters. Hildebrand was firstly connected the solubility to cohesive energy density, which gives Hildebrand solubility parameter. However, as we known, various intermolecular interactions act between molecules. Only one simple parameter cannot tell the proportion of interactions between molecules, which is important for self-assembly study. Hansen developed Hildebrand solubility parameter by breaking it into three parts as Hansen solubility parameters (HSPs), dispersion (δ_D), polarity (δ_P) and hydrogen bonding (δ_H). Recently, HSPs have been applied to understand self-assembly behaviours of gelator in various solvents. Gelation behaviour of several low-molecular-weight DKPs were studied by HSPs, which gave insight of the relationship between HSPs of molecules and states. HSPs is a very powerful tool for studying self-assembly not only in solution and gelation, but also in particle formation.

In chapter II, three kinds of AB-type DKP with amine and carboxylic group, LL, DD, and LD-type cyclo(aspartyl-4-amino-phenylalanyl) (ADKP), were successfully synthesized. However, yields of these ADKP were very low. Among these three kinds of ADKP, LL-ADKP is dipeptide from L-type amino acids, which is important in biochemistry. As a result, it is necessary to have efficient synthetic pathway. The L-aspartyl-L-phenylalanine methyl ester is a synthetic sweetener that is commercially known as aspartame; it is one of the most highly produced peptides worldwide[33,34]. Further, it is known that intramolecular cyclocondensation of aspartame occurs through heating, and aspartame diketopiperazine (APM-DKP) with an asymmetric structure is produced.[35,36] Therefore, aspartame can be a promising candidate for synthesizing the above-mentioned highly soluble DKP and its polymer.

This chapter deals with the synthesis of AB-type DKP monomer and polyamides from aspartame, as well as the self-assembly properties of both monomer and polymers.

3.2 Experimental

3.2.1 Materials

L-Aspartyl-L-phenylalanine methyl ester was supplied by Ajinomoto Co., Inc. Triphenyl phosphite ($P(OPh)_3$), L-phenylalanine (Phe), succinic acid, ethylene diamine and *p*-phenylenediamine were purchased from Tokyo Chemical Industry Co., LTD. 5% Palladium on activated carbon (Pd/C) and *N*-methylpyrrolidone (NMP) were purchased from FUJIFILM Wako Pure Chemical Corporation. Dimethyl sulfoxide (DMSO), dimethylacetamide (DMAc), *N*,*N*-dimethylformamide (DMF), sulfuric acid, nitric acid, pyridine, ethanol, tetrahydrofuran (THF), ethyl acetate, acetone and toluene were

purchased from Kanto Chemical Co., Inc. All the chemicals were directly used as purchased.

3.2.2 Characterization

^{1}H NMR and ^{13}C NMR spectra were performed by a Bruker Biospin AG 400 MHz, 54 mm spectrometer using DMSO-d_6 as the solvent.

The FT-IR spectra were recorded with a Perkin-Elmer Spectrum One spectrometer between 4000 and 400 cm^{-1} using a diamond-attenuated total reflection (ATR) accessory.

The mass spectra were measured using a FT-ICR MS (Solarix) equipped with a Nanospray source operating in the nebulizer-assisted ESI mode used in the negative ion mode and scanned from m/z 50 to m/z 1000.

The number-average molecular weight (M_n), weight-average molecular weight (M_w) and the molecular weight distribution (M_w/M_n) were determined by gel permeation chromatography (GPC, concentration 1 g/L, 10 mM LiBr/DMF eluent) after calibration with polystyrene standards using two of OHpack SB-806M HQ column (Shodex).

Thermogravimetric analysis (TGA) and differential scanning calorimetry (DSC) were carried out by Seiko Instruments SII, SSC/5200 and Seiko Instruments SII, X-DSC7000T, respectively, at a heating rate of 5 °C/min under a nitrogen atmosphere. Remaining solvent and absorbed moisture in polymer samples were removed at 200 °C for 1 hour before TGA and DSC measurement.

Monomer and polymer particles morphology were characterized with scanning electron microscope (JCM-6000Plus Versatile Benchtop SEM). Samples were coated with a layer of gold in thickness of 15 nm by a sputter coater (Magnetron sputter MSP-

1S). SEM instrument was operated at an acceleration voltage of 10 kV and an emission current of 10 μA.

Hansen solubility parameters of polymer and solvents are calculated by Hansen Solubility Parameters in Practice (HSPiP) 5th Edition software.

3.2.3 Monomer synthesis

a) Synthesis of cyclo(L-aspartyl-L-phenylalanyl) (AMP-DKP).

L-Aspartyl-L-phenylalanine methyl ester (5.86 g, 20.0 mmol) was dissolved in DMSO (20 mL) and stirred at 80 °C for 8 h. The resulting solution was added into a mixture of acetone (300 mL) and hexane (300 mL) to obtain a precipitate. The white precipitate was obtained by filtration and dried in a vacuum oven at 100 °C with a yield of 4.61 g (88%).

b) Synthesis of cyclo(L-aspartyl-4-nitro-L-phenylalanyl) (NDKP).

Here, APM-DKP (1.30 g, 4.96 mmol) was dissolved in concentrated sulfuric acid (30 mL) in an ice bath. A prepared solution mixture of nitric acid (1 mL) and sulfuric acid (4 mL) was added dropwise to the APM-DKP sulfuric acid solution at 0 °C. Subsequently, the solution was stirred for 5 min. The resulting solution was poured into ice water (300 mL) dropwise and the pH was adjusted to approximately 5 by adding sodium hydroxide solution. Thereafter, the solution was extracted with ethyl acetate (200 mL) three times and vapor was removed using a vacuum evaporator and vacuum oven at 100 °C. The objective product was obtained as a white powder with a 73% yield (1.10 g). ^{1}H NMR (400 MHz, DMSO-d_6, δ, ppm): 2.07 (dd, 1H, J = 5.9, 16.6 Hz), 2.28 (dd, 1H, J = 5.4, 16.6 Hz), 3.10 (dd, 1H, J = 5.3, 14.0 Hz), 3.24 (dd, 1H, J = 4.8, 13.9 Hz), 4.11 (t, 1H, J = 5.6 Hz), 4.34 (t, 1H, J = 5.1 Hz), 7.49 (d, 2H, J = 8.7 Hz), 8.1 (s, 1H), 8.17 (d, 1H, J = 8.7 Hz), 8.23 (s, 1H).

c) Synthesis of cyclo(L-aspartyl- 4-amino-L-phenylalanyl) (ADKP).

NDKP (0.50 g, 1.63 mmol) not subjected to purification was dissolved in pure water, and Pd/C (0.11 g, 22 wt.%) was added. The mixture was connected with a hydrogen generator and reacted with hydrogen at a feed rate of 500 mL/min at 50 °C for 6h. The resulting mixture was filtered and evaporated under vacuum. The resulting solid was recrystallized in water and dried in a vacuum oven at 100 °C with an 88% yield (0.40 g). ^{1}H NMR (400 MHz, DMSO-d_6, δ, ppm): 1.63 (dd, 1H, J=7.4, 11.9 Hz), 2.12 (dd, 1H, J = 5.1, 16.4 Hz), 2.72 (dd,1H, J = 4.6, 13.8 Hz), 2.91 (dd, 1H, J = 4.2, 13.7 Hz), 4.01 (t, 1H, J = 6.0 Hz), 4.05 (t, 1H, J = 4.7 Hz), 6.46 (d, 2H, J =8.3 Hz), 6.80 (d, 2H, J =8.3 Hz), 7.83 (s, 1H), 7.98 (s, 1H). FT-ICR MS (ESI): calcd for $[C_{13}H_{14}N_3O_4]^-$, 276.10626, found 276.09867.

3.2.4 ADKP-based polyamide syntheses

A typical polymerization procedure for DKP-based polyamides is shown below. ADKP (0.055 g, 0.2 mmol) was mixed with $P(OPh)_3$ (40 μL, 0.15 mmol), pyridine (50 μL, 0.6mmol), and NMP (100 μL). The reaction solution was stirred at 100 °C for 48 h under nitrogen atmosphere. After the reaction finished, the resulting solution was precipitated in acetone, and the resulting solid was washed with acetone and dried in a vacuum oven at 100 °C to give PA1 as a yellow powder with an 84% yield. Following the same protocol, ADKP (0.027 g, 0.1 mmol) was treated with other monomers such as L-phenylalanine (0.016 g, 0.1 mmol) to synthesize PA2 with a 79% yield; further, succinic acid (0.012 g, 0.1 mmol) was treated with ethylene diamine (67 μL, 0.1 mmol) to synthesize PA3 with an 81% yield, and succinic acid (0.012 g, 0.1 mmol) was treated with *p*-phenylenediamine (0.011 g, 0.1 mmol) to synthesize PA4 with an 84% yield.

3.2.5 Preparation of particles of ADKP and ADKP-based polyamides

The obtained ADKP or PAs (ca. 2.5 mg) were dissolved in 1 mL DMSO as a stock solution. A 0.1 mL stock solution was dispersed into 3 mL of different poor solvents, under vigorous magnetic stirring. A droplet of the dispersion liquid was dropped on a glass slide and air-dried at room temperature to assess the SEM images.

3.3 Results and Discussion

3.3.1 Monomer syntheses

The solubility of DKP derivatives is low due to the rigid six-membered ring and the strong intermolecular hydrogen bond, although monomer solubility is a key factor for efficient polymerization. Almost all of the reported AA-type DKP monomers exhibiting low solubility were converted into polymers with low molecular weights and poor performances. AA-type DKP monomers are homo-coupling of amino acids, which have high symmetry and crystallinity. Thus, AB-type DKP monomer, which have lower crystallinity, is expected to demonstrate higher solubility.

Scheme 3.1 Synthesis of AB-type DKP-based monomer from aspartame.

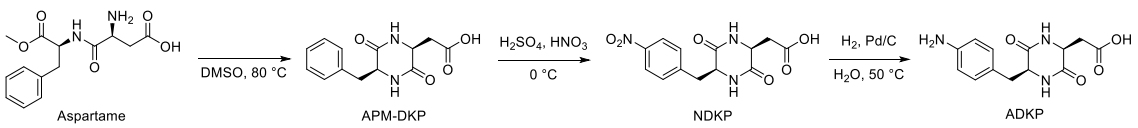

The AB-type DKP-based monomer LL-ADKP was obtained from the L-aspartyl-L-phenylalanine methyl ester, following intramolecular condensation, nitration, and reduction (Scheme 3.1). Notably, after the nitration of APM-DKP, both para-substituted and ortho-substituted products were confirmed (Figure 3.1). The ratio of the para-substituted product to the ortho-substituted product was 9:1, as calculated by NMR. Recrystallization of the crude product could not completely remove the ortho-substituted product. However, the reduction product could be easily recrystallized to give pure para-substituted LL-ADKP. The structure of LL-ADKP was confirmed by ^{1}H NMR, ^{13}C NMR, and FTIR (Figure 3.1-3.3), which has same structure with the LL-ADKP from Chapter II.

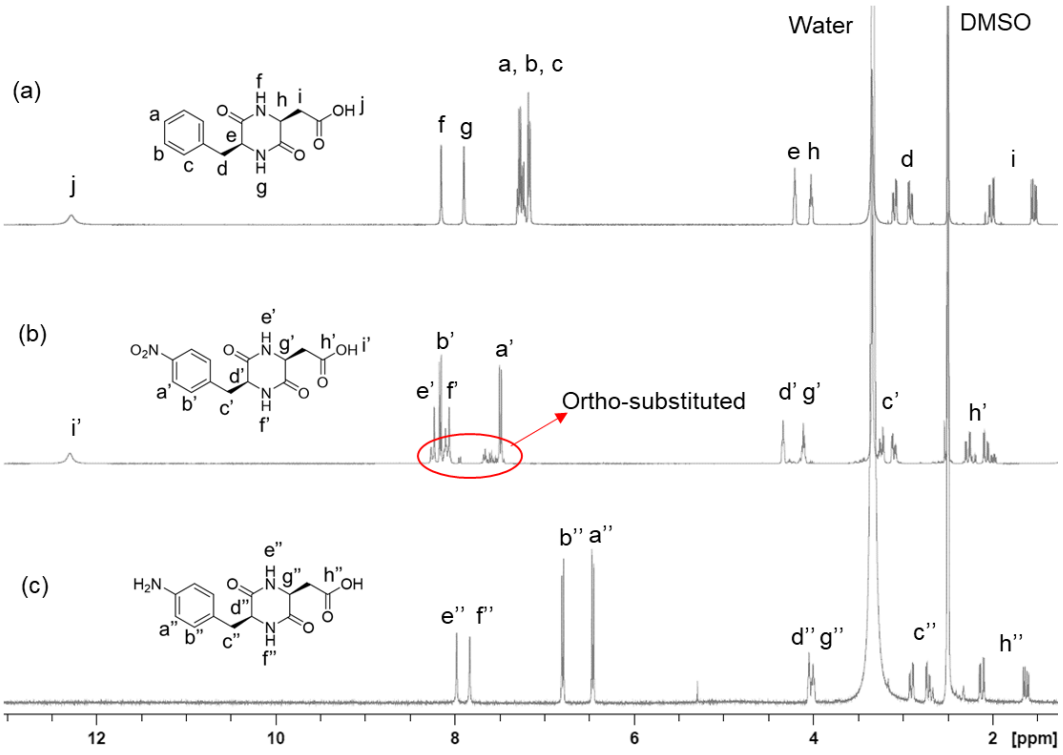

Figure 3.1 ^{1}H NMR spectra of (a) APM-DKP, (b) LL-NDKP, and (c) LL-ADKP in DMSO-d_6

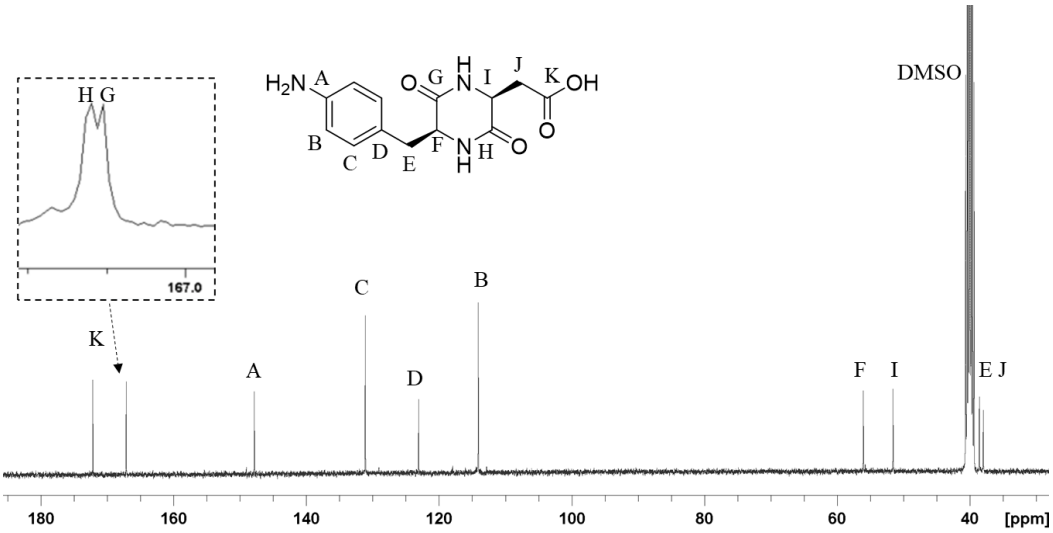

Figure 3.2 ^{13}C NMR spectrum of LL-ADKP

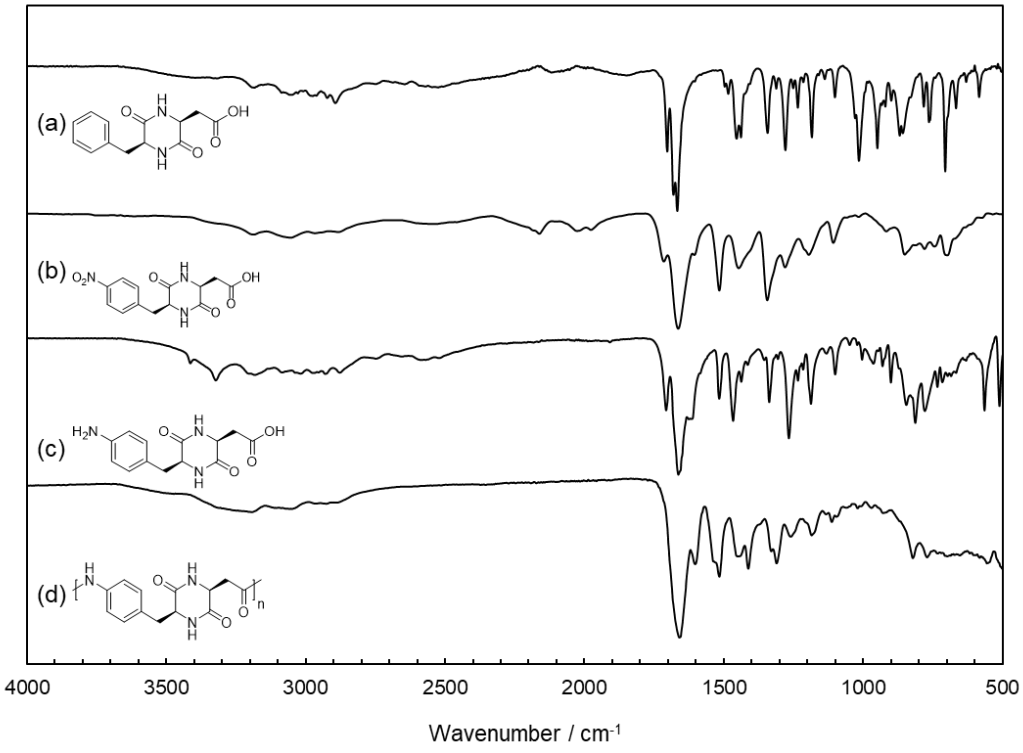

Figure 3.3 FT-IR spectra of (a) APM-DKP, (b) LL-NDKP, (c) LL-ADKP and (d) PA1

As a result, the obtained LL-ADKP showed high solubility in water and polar organic solvents such as methanol, NMP, DMF, and DMSO (Table 3.1). The high solubility of LL-ADKP is attributable to the asymmetric structure, which increases the solvation entropy of LL-ADKP.[37] Otherwise, the existence of ionic amine and carboxylic groups can contribute to solubility, which disturbs the formation of intermolecular hydrogen bonds between the DKP moieties in solvated states[38].

Table 3.1. Solubility of LL-NDKP and LL-ADKP [a]

Solvent	NDKP	ADKP	Solvent	NDKP	ADKP
Water	±	+	DMSO	+	+
Methanol	±	+	DMF	+	+
Ethanol	±	+	DMAc	+	+
Acetone	±	±	NMP	+	+

[a] Conditions; samples, 10 mg; solvent, 2 ml; temperature, r.t.; +, soluble; ±, partially soluble; −, insoluble.

3.3.2 Properties of Polymers

Scheme 3.2 Synthesis of DKP-based polyamides from cyclo(L-aspartyl-4-amino-L-phenylalanyl)

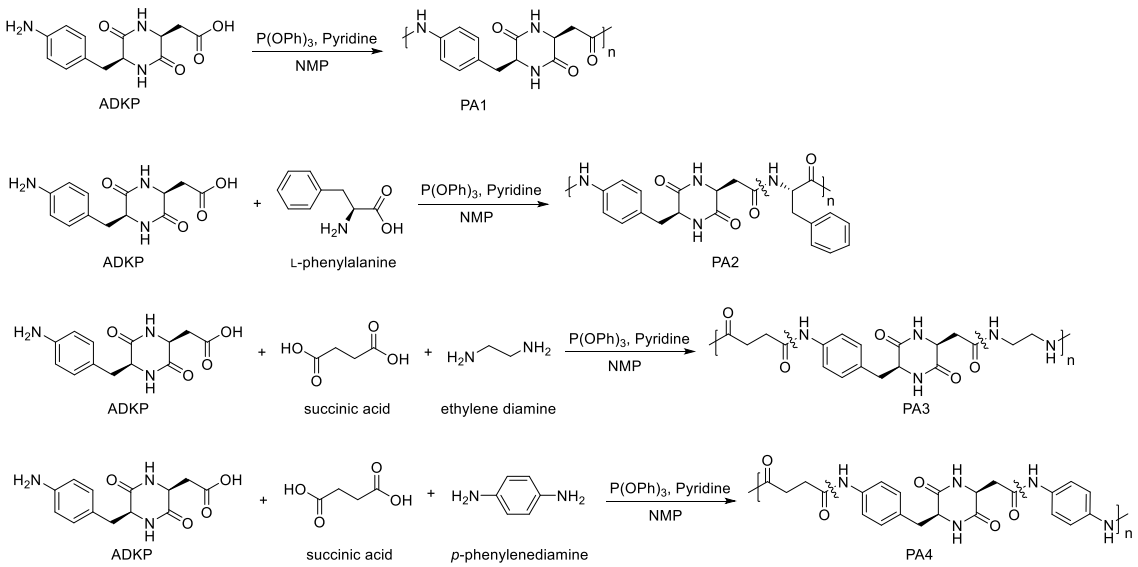

PAs were prepared by homopolymerization or co-polymerization of ADKP as an AB-type monomer (with or without other comonomers) using $P(OPh)_3$ and pyridine as condensation reagents (Scheme 3.2). ^{1}H NMR spectra of the obtained PAs showed a new peak at 9.5 ppm due to the phenyl amide proton, which indicated the beginning of the polymerization of ADKP. The amide protons in the DKP moiety remained unchanged at 7.9 and 8.1 ppm, and phenyl protons appeared for all the PA ^{1}H NMR spectra at 7.1 and 7.4 ppm, which confirmed the presence of the ADKP moiety in the polymer chains (Figure 3.4).

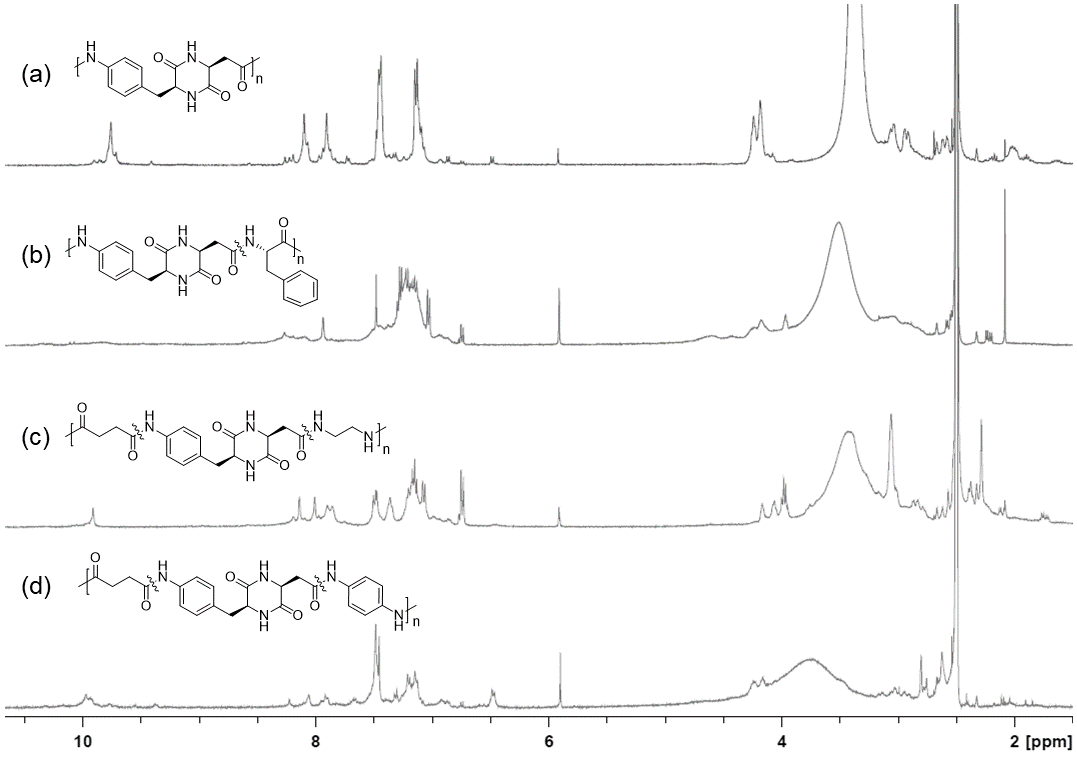

Figure 3.4 ^{1}H NMR spectra of (a) PA1, (b) PA2, (c) PA3 and (d) PA4 in DMSO-d_6

The weight average molecular weight (M_w) and number average molecular weight (M_n) of PAs were determined by GPC, which are summarized in Table 3.2. Based on these results, the polymerizations of ADKP successfully proceeded, and the molecular weights were observed to be in the range of 1.59–1.98 × 10^4 g/mol; the M_w/M_n ratio was 1.17–1.36. Furthermore, the obtained PAs are soluble in NMP, DMSO, DMAc, and concentrated sulfuric acid (Table 3.3). The high molecular weight of PAs contributes to the high solubility of the monomers and polymers in the organic solvents.

Table 2.2 Molecular weights and thermal properties of PAs derived from ADKP

Polymers	M_w [a] ($\times 10^4$ g/mol)	M_n [a] ($\times 10^4$ g/mol)	M_w/M_n [a]	T_{d5} (°C) [b]	T_{d10} (°C) [b]
PA1	1.93	1.64	1.18	326	348
PA2	1.59	1.36	1.17	276	296
PA3	1.76	1.36	1.29	272	289
PA4	1.98	1.46	1.36	280	302

[a] Determined by GPC measurements based on polystyrene standards; eluent, 10 mmol L^{-1} of LiBr DMF solution. [b] T_{d5} and T_{d10} were observed from TGA curve scanned at a heating rate of 5 °C/min under nitrogen atmosphere.

TGA was utilized to evaluate the thermal decomposition of PAs in a nitrogen atmosphere. As shown in Table 2, the 5% and 10% weight-loss temperatures (*T_{d5}* and T_{d10}) of PAs ranged from 272–326 °C. Remarkably, although all PAs had similar molecular weights, the homopolymer PA1 revealed the highest T_{d5} and T_{d10} values, which was approximately 50 °C higher than the others. Moreover, the thermal physical transformation of PAs was investigated via DSC in a nitrogen atmosphere. The glass transition temperature (T_g), melting temperature (T_m), and recrystallization temperature were detected to not be in the range of 50–250 °C, which indicated that all the PA transition temperatures were higher than 250 °C. These results indicate that PA1 has the simplest chemical structure among all PAs, with the most abundant DKP moiety and benzene ring, which is considered to contribute to its relatively superior thermal properties.

Table 3.3. Solubility of PA1[a]

Water	Methanol	Ethanol	THF	Toluene	Ethyl acetate
-	±	-	-	-	-
Acetone	DMSO	DMF	DMAc	NMP	Con. H_2SO_4
-	+	+	+	+	+

[a] Conditions; samples, 10 mg; solvent, 2 ml; temperature, r.t.; +, soluble; ±, partially soluble; −, insoluble.

3.3.3 Self-assembly behaviors of DKP-based monomer and PA1

DKP derivatives with low molecular weights are well known for their orderly aggregation through parallel hydrogen bonds, which are utilized to fabricate crystals or semi-crystals with various morphologies. Long chains reduce the crystallinity of polymeric systems[39], which may lead to different self-assembling behaviors that originate from small DKP derivatives. In this study, the simple DKP-based polymer (PA1) was considered a suitable model for carrying out the self-assembly study; subsequently, it was used for particle fabrication. The solvent displacement method was adopted for the self-assembly studies PA1. To evaluate the effects of poor solvents on particulation, a DMSO solution of PA1 was dropped into water, ethanol, tetrahydrofuran, ethyl acetate, acetone, and toluene to precipitate particles. In the case of water, ethanol, and THF, irregular network-like morphologies were observed (Figure 3.5.a-c). However, in ethyl acetate, ellipsoids were formed (Figure 3.5.d). In case of acetone and toluene, particles with hollow structures were observed (Figure 3.5.e and f). Notably, in contrast to other hollow particles reported in the literature[40–43], the PA1 homopolymer (without any side chain and template) spontaneously self-assembled into a hollow morphology, which is a unique case for polymeric hollow particles. The particle sizes from acetone and toluene were

approximately 1 μm and 12 μm, respectively. Because of the thin shell, these hollow particles show a porous structure or collapse into a bow-like structure.

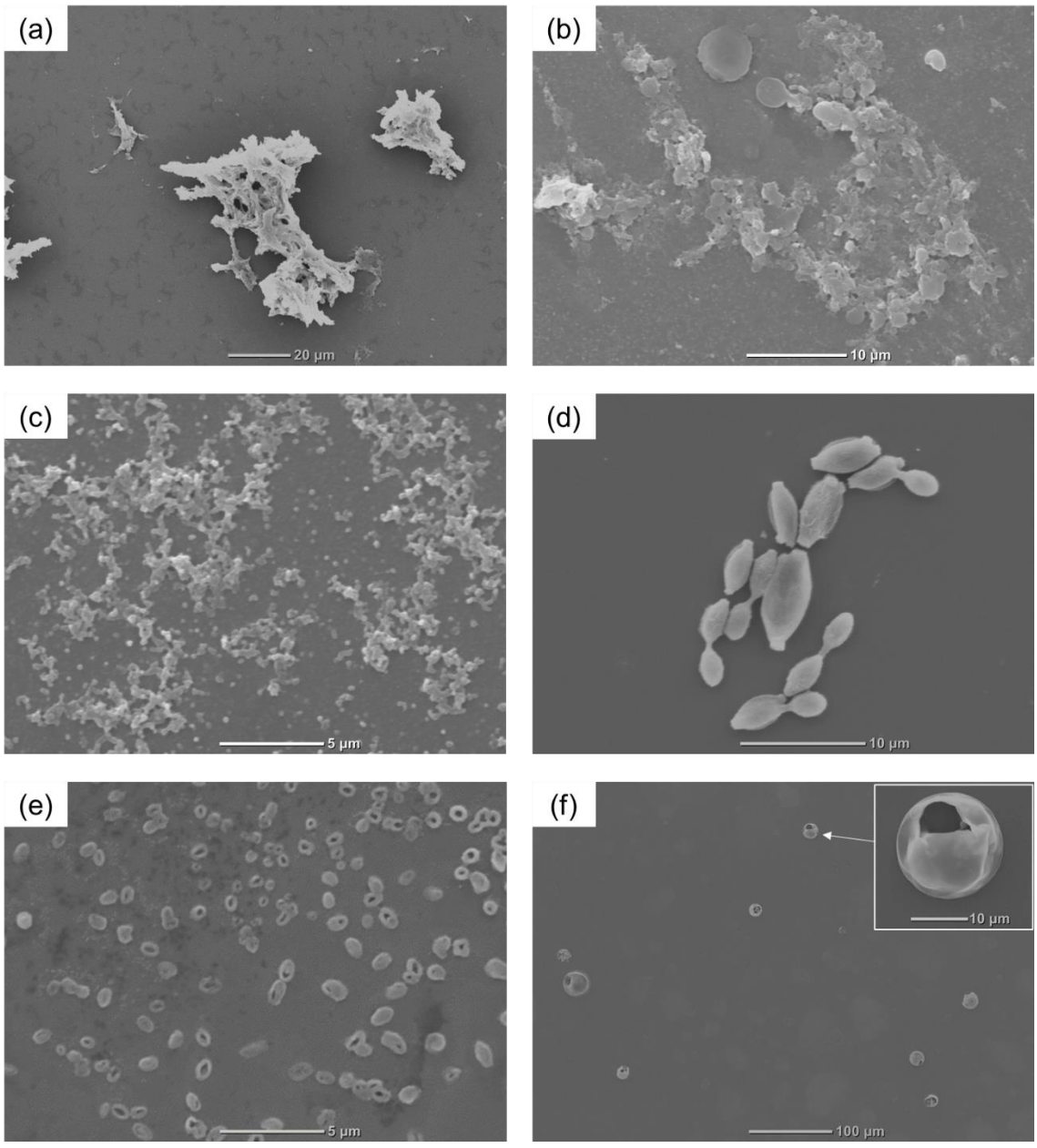

Figure 3.5 SEM images of particles obtained by the dispersion of PA1 into (a) water, (b) ethanol, (c) THF, (d) ethyl acetate, (e) acetone, and (f) toluene.

3.3.4 Morphology transformation.

The self-assembly of PA1 was highly sensitive to the solvent environment as observed in the solvent displacement method, which provided primitive thermodynamic conditions. Notably, self-assembly is a thermodynamic process to reduce the free energies of the systems. Therefore, if the environment changes, a morphological transformation of PA1 particles may occur.[24] The morphological transformation was further investigated through the secondary solvent treatment of the formed particles. The treatment procedures are shown in Figure 3.6.a. By adding one drop of acetone to the particles formed over toluene and subsequent drying, hollow particles (same form of Figure 3.5.d) were deformed to petal-like particles (Route 1, Figure 3.6.b). Similarly, by simply changing the precipitate solvent to acetone and adding one drop of toluene on the particles formed, irregular particles were formed after drying (Route 2, Figure 3.6.c). Nonetheless, when toluene was added to the droplet of the acetone sample without drying, cubic particles were formed (Route 3, Figure 3.6.d). Cubic particles are expected to have high crystallinity based on hydrogen bonds. However, X-ray diffraction did not show any distinct diffraction due to the small amount of cubic particles used for measurement (Figure 3.7). A similar behavior to cube formation has been previously reported for amphipathic polypeptides poly{γ-glutamic acid-*g*-(L-phenylalanine ethyl)}, but PA1 is not amphipathic.[44] However, both results indicated that molecular assembly through the π-stacking of phenylalanine moiety was important to form cubic morphology. In addition, based on such morphological changes that depend on the solvent, the addition of one drop of acetone on the cubic particles after drying transformed the cubic particles into a spherical morphology that appeared porous or hollow (Route 3, Figure 3.6.e). These hollow particles had a disordered shape because they were not vigorously stirred.

Furthermore, it was envisaged that the shape would be the same as that shown in Figure 3.5.f, if the same experimental operation as that used for the particle preparation was performed.

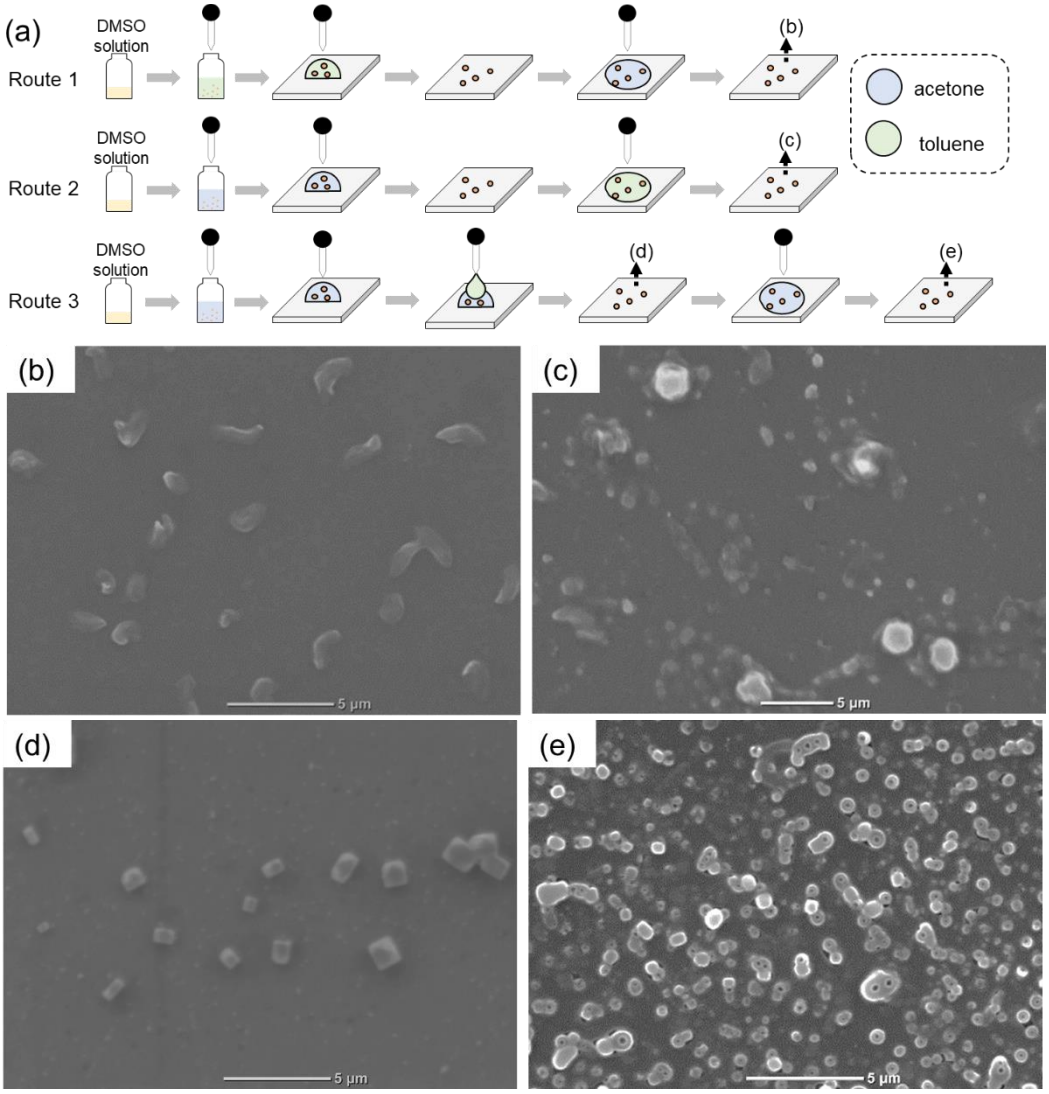

Figure 3.6 (a) Process illustration of particle formation and transformation. SEM images of particles obtained in different processes related to the process illustration: particles obtained by (b) adding acetone into particles formed from toluene, (c) adding toluene into particles formed from acetone, (d) adding toluene into the suspension of the acetone sample, and (e) adding acetone into particles formed from mixture of acetone and toluene.

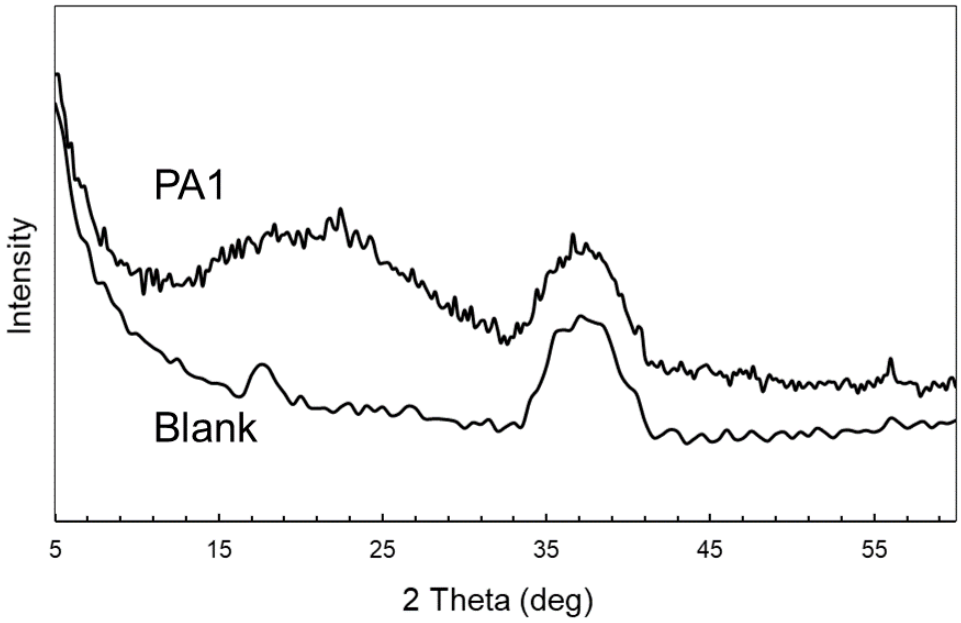

Figure 3.7 XRD spectrum of PA1 and substrate blank

3.3.5 Evaluation of the strength of hydrogen bond by FTIR spectroscopy.

In the previous section, particle formations were dependent on the solvent, which in turn were dependent on the strength of the hydrogen bond for the solvent and PA.[45] Thus, the FTIR spectra were studied to evaluate the hydrogen bond behavior in the self-assembled particles formed in different solvents. Three types of morphologies were observed for the four solvents: irregular networks of water, hollow particles of acetone or toluene, and cubic particles of the solvent produced by mixing acetone and toluene. Figure 3.8 shows the IR absorption in the N–H stretching vibration region. A shoulder peak for N–H stretching appears in all particles, whereby the band around 3191 cm^{-1} indicates a moderate hydrogen bond, and the band at 3240 cm^{-1} indicates the free N–H group.[46] In particles formed from water, the shoulder peak is flat, indicating that the number of free N–H and the hydrogen bond-interacted N–H was approximately equal. The distinct band

around 3191 cm^{-1} in the particles formed from acetone and toluene indicated a strong hydrogen bond, thereby suggesting a continuous hydrogen bond in the PA intra/inter molecules. However, for the particles formed from the solvent mixture of acetone and toluene, the bands at 3191 cm^{-1} and 3240 cm^{-1} became weaker and stronger, respectively. It is considered that acetone and toluene produce particles with strong hydrogen bonds, while their solvent mixture results in particles with weak hydrogen bonds. It is suspected that in particles that are formed from a mixed solvent, π-stacking becomes a dominant interaction rather than hydrogen bonding, thereby resulting in different morphologies.

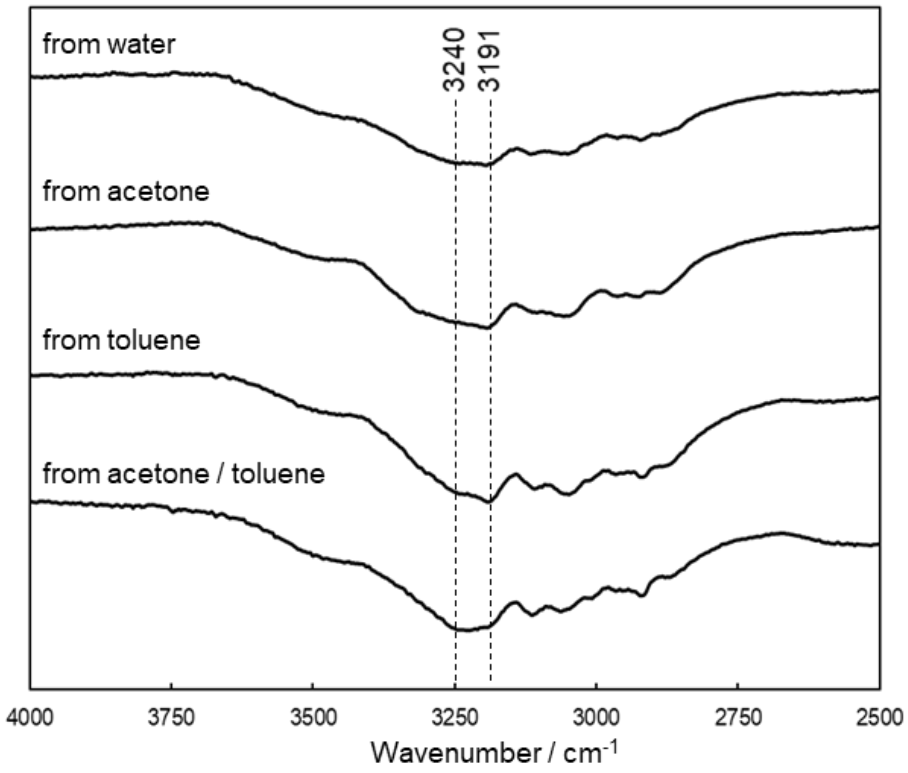

Figure 3.8 IR spectra of PA1 particles precipitated from water, acetone, toluene, and mixture of acetone/toluene.

3.3.6 Hansen solubility parameters.

As discussed above, the self-assembly of PA1 was strongly affected by the polymorphism of the solvent composition. Solvent parameter evaluation has become a powerful tool to explain gelation, crystal growth, polymer aggregation, and other colloidal phenomena.[31,32,47,48] Here, we use Hansen solubility parameters (HSP), which include dispersion (δ_D), polarity (δ_P), and hydrogen bond (δ_H), to explain such a complicated polymorphism.[49,50] The HSPs of PA1 and the solvents used for elucidating the morphologies are summarized in Table 3.4. The δ_D and δ_P values for solvents seem to have little relation with particle morphology. Compared to the hydrogen bond, the dispersion interaction and dipole–dipole interaction are weak, which are considered to have minimal influence on the self-assembly of PA1 with multiple hydrogen bonding sites. As for δ_H, when solvents have higher δ_H than PA1 (δ_H = 7.9 $MPa^{0.5}$), precipitates produce irregular aggregates, which is in contrast to the results obtained for individual particles. In water with the highest δ_H, the DKP moieties in PA1 tend to form hydrogen bonds much more easily with water molecules than with themselves, thereby resulting in the formation of random hydrogen bonds (Figure 3.5.a). As for ethanol, with the decrease in the δ_H value for the solvent, the probability of DKP–DKP interaction increases, leading to the emergence of a two-dimensional substructure (Figure 3.5.b). As for THF, the δ_H value for the solvent approaches PA1, which implies that the DKP moieties have a similar chance to form hydrogen bonds with the solvent and themselves, resulting in a median morphology between the network and individual particles (Figure 3.5.c). When solvents exhibit lower δ_H values than PA1, the DKP moieties have a greater chance to form hydrogen bonds with themselves rather than with solvent molecules, resulting in individual particles.

Table 3.4 Hansen solubility parameters of PA1 and solvents

Molecules	δ_D ($MPa^{0.5}$)	δ_P ($MPa^{0.5}$)	δ_H ($MPa^{0.5}$)
PA1	22.2	13.1	7.9
Water	15.5	16	42.3
Ethanol	15.8	8.8	19.4
Tetrahydrofuran	16.8	5.7	8
Ethyl Acetate	15.8	5.3	7.2
Acetone	15.5	10.4	7
Toluene	18	1.4	2

3.3.7 Mechanism of self-assemble behavior for PA1.

Based on the morphological study of PA1, the formation of both hollow and cubic particles exhibits unique characteristics because they are not typical for a homopolymer without side chains. It is important and challenging to analyze this self-assembly mechanism. Based on the above-mentioned IR and HSP studies, hydrogen bonds and π-stacking are considered as driving forces of self-assembly (especially, the hydrogen bonds). The mechanism of the self-assembly of PA1 is shown in Figure 3.9. When PA1 DMSO solution is added into poor solvents with low δ_H, polymer chains aggregate regularly due to the parallel hydrogen bonding formed by DKP moieties in the molecules, thereby resulting in a two-dimensional sheet-like substructure. Following vigorous stirring, the sheet-like substructure eventually bends to form a vesicle. When toluene is added to the acetone droplet sample, the thermodynamic environment of the particles changes, thereby resulting in the unfolding of the sheet-like substructure. Notably, in this

case, no stirring is performed. And π-stacking of the aromatic ring moiety of PA1 occurs guadually, resulting in the stacking of substructures to form cubic morphology. When acetone is added to the cubic particles, the cubic particles decompose again to form the sheet-like substructure. Along with the relatively fast drying of acetone, the sheet-like substructures tend to bend to form hollow particles again. However, acetone dries rapidly and cannot impart sufficient bending energy as compared to that provided by vigorous stirring. The hydrogen bond/π-stacking dominated self-assembly system of vesicle particle also was reported by Haldar, in which thiocoumarin based-amino ester was used as a building block[51].

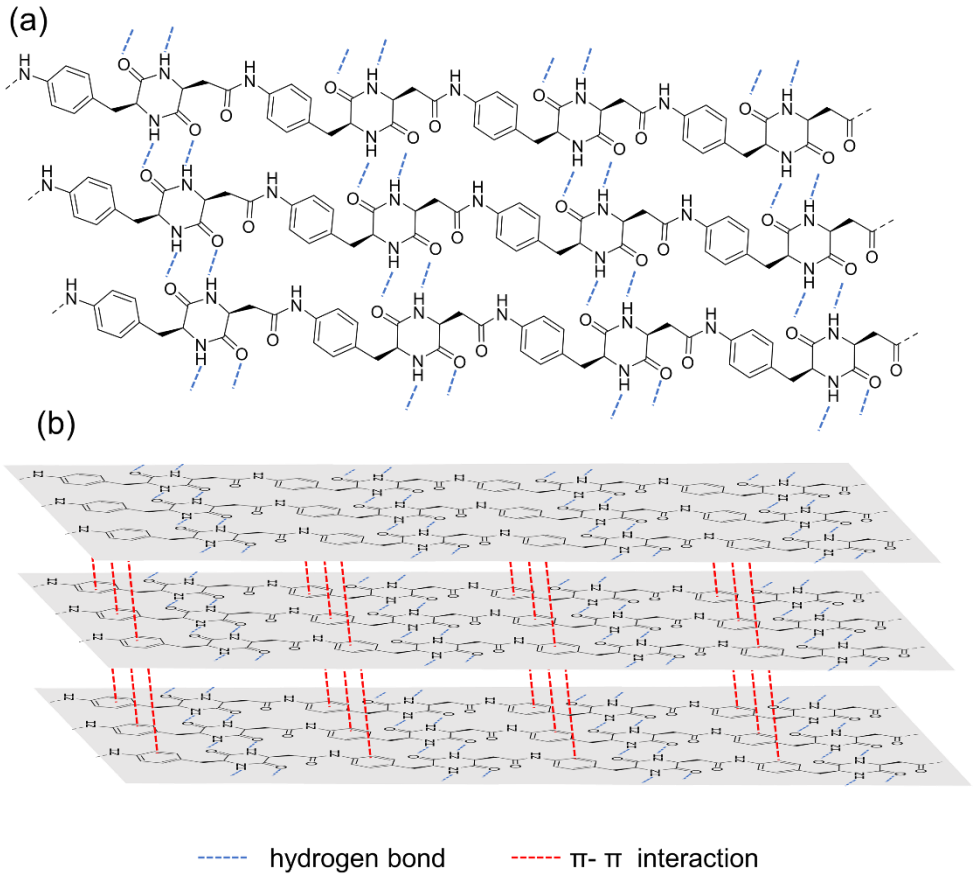

Figure 3.9 Schematic illustration of formations of vesicle and cubic particles.

3.4 Conclusion

We have established an AB-type DKP-based monomer with high solubility from a commercial dipeptide sweetener. Various DKP-based PAs, with or without other monomers, were synthesized. All the PAs showed high molecular weights and high thermal resistances. Their morphologies were elucidated using solvent displacement methods that employed a variety of solvents ranging from a DMSO solution to various poor solvents, thereby resulting in particles with various morphologies; for example, irregular networks as well as rugby-like and hollow particles. In particular, the preparation of hollow particles was achieved without any additive or fabrication. Furthermore, PA1 particles underwent a morphological transformation by secondary solvent treatment using the acetone and toluene dropping technique. To investigate the role of hydrogen bonds in self-assembly, IR and HSP approaches were applied to define the mechanism governing the morphology formation of DKP-based PAs. The present study provides a high potential as a self-assembly building block for functional nanomaterials.

References

(1) Dou, X.-Q.; Feng, C.-L. Amino Acids and Peptide-Based Supramolecular Hydrogels for Three-Dimensional Cell Culture. *Adv. Mater.* **2017**, *29* (16), 1604062. https://doi.org/10.1002/adma.201604062.

(2) Sharma, S.; Singh, R.; Rana, S. Bioactive Peptides: A Review. *Int. J. Bioautomation* **2011**, *15* (4), 223–250. https://doi.org/10.1093/fqs/fyx006.

(3) Adhikari, B.; Singh, C.; Shah, A.; Lough, A. J.; Raatz, H. B. Amino Acid Chirality and Ferrocene Conformation Guided Self-Assembly and Gelation of Ferrocene-Peptide Conjugates. *Chem. - A Eur. J.* **2015**, *21* (32), 11560–11572. https://doi.org/10.1002/chem.201501395.

(4) Basak, S.; Nanda, J.; Banerjee, A. A New Aromatic Amino Acid Based Organogel for Oil Spill Recovery. *J. Mater. Chem.* **2012**, *22* (23), 11658. https://doi.org/10.1039/c2jm30711a.

(5) Yan, X.; Zhu, P.; Li, J. Self-Assembly and Application of Diphenylalanine-Based Nanostructures. *Chem. Soc. Rev.* **2010**, *39* (6), 1877–1890. https://doi.org/10.1039/b915765b.

(6) Mallakpour, S.; Dinari, M. Progress in Synthetic Polymers Based on Natural Amino Acids. *J. Macromol. Sci. Part A* **2011**, *48* (8), 644–679. https://doi.org/10.1080/15226514.2011.586289.

(7) Okamura, A.; Hirai, T.; Tanihara, M.; Yamaoka, T. Synthesis and Properties of Novel Biodegradable Polyamides Containing α-Amino Acids. *Polymer (Guildf).* **2002**, *43* (12), 3549–3554. https://doi.org/10.1016/S0032-3861(02)00111-8.

(8) Suvannasara, P.; Tateyama, S.; Miyasato, A.; Matsumura, K.; Shimoda, T.; Ito, T.; Yamagata, Y.; Fujita, T.; Takaya, N.; Kaneko, T. Biobased Polyimides from 4-Aminocinnamic Acid Photodimer. *Macromolecules* **2014**, *47* (5), 1586–1593. https://doi.org/10.1021/ma402499m.

(9) Fischer, P. M. Diketopiperazines in Peptide and Combinatorial Chemistry. *J. Pept. Sci.* **2003**, *9* (1), 9–35. https://doi.org/10.1002/psc.446.

(10) Luo, T.-J. M.; Palmore, G. T. R. Influence of Structure on the Kinetics of Assembly of Cyclic Dipeptides into Supramolecular Tapes. *J. Phys. Org. Chem.* **2000**, *13* (12), 870–879. https://doi.org/10.1002/1099-1395(200012)13:12<870::AID-POC324>3.0.CO;2-O.

(11) Palacin, S.; Chin, D. N.; Simanek, E. E.; MacDonald, J. C.; Whitesides, G. M.; McBride, M. T.; Palmore, G. T. R. Hydrogen-Bonded Tapes Based on Symmetrically Substituted Diketopiperazines: A Robust Structural Motif for the Engineering of Molecular Solids. *J. Am. Chem. Soc.* **1997**, *119* (49), 11807–11816. https://doi.org/10.1021/ja962905b.

(12) Ressurreição, A. S. M.; Delatouche, R.; Gennari, C.; Piarulli, U. Bifunctional 2,5-Diketopiperazines as Rigid Three-Dimensional Scaffolds in Receptors and Peptidomimetics. *European J. Org. Chem.* **2011**, No. 2, 217–228. https://doi.org/10.1002/ejoc.201001330.

(13) Manchineella, S.; Govindaraju, T. Molecular Self-Assembly of Cyclic Dipeptide Derivatives and Their Applications. *Chempluschem* **2017**, *82* (1), 88–106. https://doi.org/10.1002/cplu.201600450.

(14) Borthwick, A. D. 2,5-Diketopiperazines: Synthesis, Reactions, Medicinal Chemistry, and Bioactive Natural Products. *Chem. Rev.* **2012**, *112* (7), 3641–3716. https://doi.org/10.1021/cr200398y.

(15) Takada, K.; Yin, H.; Matsui, T.; Ali, M. A. Bio-Based Mesoporous Sponges of Chitosan Conjugated with Amino Acid-Diketopiperazine through Oil-in-Water Emulsions. *J. Polym. Res.* **2017**.

(16) Hanabusa, K.; Matsumoto, M.; Kimura, M.; Kakehi, a; Shirai, H. Low Molecular Weight Gelators for Organic Fluids: Gelation Using a Family of Cyclo(Dipeptide)S. *J. Colloid Interface Sci.* **2000**, *224* (2), 231–244. https://doi.org/10.1006/jcis.1999.6672.

(17) Hanabusa, K.; Suzuki, M. Development of Low-Molecular-Weight Gelators and Polymer-Based Gelators. *Polym. J.* **2014**, *46* (11), 776–782. https://doi.org/10.1038/pj.2014.64.

(18) Ohta, Y.; Terada, K.; Masuda, T.; Sanda, F. Diketopiperazine Supramolecule Derived from Hydroxyphenylglycine. *Heterocycles* **2009**, *78* (6), 1477–1483. https://doi.org/10.3987/COM-08-11635.

(19) Davie, E. A. C.; Mennen, S. M.; Xu, Y.; Miller, S. J. Asymmetric Catalysis Mediated by Synthetic Peptides. *Chem. Rev.* **2007**, *107* (12), 5759–5812. https://doi.org/10.1021/cr068377w.

(20) Terada, K.; Sanda, F.; Masuda, T. Polycondensation of Diketopiperazine-Based Dicarboxylic Acids with Diamines and Dibromoxylenes. *J. Macromol. Sci. Part A Pure Appl. Chem.* **2007**, *44* (8), 789–794.

https://doi.org/10.1080/10601320701406971.

(21) Akerlund, J.; Harmeier, S.; Pumphrey, J.; Timm, D. C.; Brand, J. I. Diketopiperazine-Based Polymers from Common Amino Acids. *J. Appl. Polym. Sci.* **2000**, *78* (12), 2213–2218. https://doi.org/10.1002/1097-4628(20001213)78:12<2213::AID-APP190>3.0.CO;2-8.

(22) Terada, K.; Berda, E. B.; Wagener, K. B.; Sanda, F.; Masuda, T. ADMET Polycondensation of Diketopiperazine-Based Dienes. Polymerization Behavior and Effect of Diketopiperazine on the Properties of the Formed Polymers. *Macromolecules* **2008**, *41* (16), 6041–6046. https://doi.org/10.1021/ma800367z.

(23) Terada, K.; Masuda, T.; Sanda, F. Synthesis and Secondary Structure of Polyacetylenes Carrying Diketopiperazine Moieties. The First Example of Helical Polymers Stabilized by s - Cis -Amide-Based Hydrogen Bonding. *Macromolecules* **2009**, *42* (4), 913–920. https://doi.org/10.1021/ma8023552.

(24) Hirayama, T.; Kumar, A.; Takada, K.; Kaneko, T. Morphology-Controlled Self-Assembly and Synthesis of Biopolyimide Particles from 4-Amino-l-Phenylalanine. *ACS Omega* **2020**, *5* (5), 2187–2195. https://doi.org/10.1021/acsomega.9b03231.

(25) Ishikawa, M.; Hashimoto, Y. Improvement in Aqueous Solubility in Small Molecule Drug Discovery Programs by Disruption of Molecular Planarity and Symmetry. *J. Med. Chem.* **2011**, *54* (6), 1539–1554. https://doi.org/10.1021/jm101356p.

(26) Pinal, R. Effect of Molecular Symmetry on Melting Temperature and Solubility. *Org. Biomol. Chem.* **2004**, *2* (18), 2692. https://doi.org/10.1039/b407105k.

(27) Busseron, E.; Ruff, Y.; Moulin, E.; Giuseppone, N. Supramolecular Self-Assemblies as Functional Nanomaterials. *Nanoscale* **2013**, *5* (16), 7098. https://doi.org/10.1039/c3nr02176a.

(28) Li, Y.; Yan, L.; Liu, K.; Wang, J.; Wang, A.; Bai, S.; Yan, X. Solvothermally Mediated Self-Assembly of Ultralong Peptide Nanobelts Capable of Optical Waveguiding. *Small* **2016**, *12* (19), 2575–2579. https://doi.org/10.1002/smll.201600230.

(29) Wang, D.; Tong, G.; Dong, R.; Zhou, Y.; Shen, J.; Zhu, X. Self-Assembly of Supramolecularly Engineered Polymers and Their Biomedical Applications. *Chem. Commun.* **2014**, *50* (81), 11994–12017. https://doi.org/10.1039/c4cc03155e.

(30) Qing, G.; Shan, X.; Chen, W.; Lv, Z.; Xiong, P.; Sun, T. Solvent-Driven Chiral-Interaction Reversion for Organogel Formation. *Angew. Chemie - Int. Ed.* **2014**, *53* (8), 2124–2129. https://doi.org/10.1002/anie.201308554.

(31) Lan, Y.; Corradini, M. G.; Liu, X.; May, T. E.; Borondics, F.; Weiss, R. G.; Rogers, M. A. Comparing and Correlating Solubility Parameters Governing the Self-Assembly of Molecular Gels Using 1,3:2,4-Dibenzylidene Sorbitol as the Gelator. *Langmuir* **2014**, *30* (47), 14128–14142. https://doi.org/10.1021/la5008389.

(32) Lan, Y.; Lv, M.; Guo, S.; Nasr, P.; Ladizhansky, V.; Vaz, R.; Corradini, M. G.; Hou, T.; Ghazani, S. M.; Marnangoni, A.; Rogers, M. A. Molecular Motifs Encoding Self-Assembly of Peptide Fibers into Molecular Gels. *Soft Matter* **2019**, *15* (45), 9205–9214. https://doi.org/10.1039/c9sm01793c.

(33) Stegink, F. *Aspartame: Physiology and Biochemistry*; CRC Press, 1984; Vol. 12.

(34) Lindeberg, G. A Convenient Synthesis of Aspartame. *J. Chem. Educ.* **1987**, *64* (12), 1062. https://doi.org/10.1021/ed064p1062.

(35) Berset, J. D.; Ochsenbein, N. Stability Considerations of Aspartame in the Direct Analysis of Artificial Sweeteners in Water Samples Using High-Performance Liquid Chromatography-Tandem Mass Spectrometry (HPLC-MS/MS). *Chemosphere* **2012**, *88* (5), 563–569. https://doi.org/10.1016/j.chemosphere.2012.03.030.

(36) Gaines, S. M.; Jeffrey, L. B. Aspartame Decomposition and Epimerization in the Diketopiperazine and Dipeptide Products as a Function of PH and Temperature. *J. Org. Chem.* **1988**, *53* (12), 2757–2764. https://doi.org/10.1021/jo00247a018.

(37) Lynden-Bell, R. M.; Rasaiah, J. C. From Hydrophobic to Hydrophilic Behaviour: A Simulation Study of Solvation Entropy and Free Energy of Simple Solutes. *J. Chem. Phys.* **1997**, *107* (6), 1981–1991. https://doi.org/10.1063/1.474550.

(38) Omta, A. W.; Kropman, M. F.; Woutersen, S.; Bakker, H. J. Negligible Effect of Ions on the Hydrogen-Bond Structure in Liquid Water. *Science (80-.).* **2003**, *301* (5631), 347–349. https://doi.org/10.1126/science.1084801.

(39) Perego, G.; Cella, G. D.; Bastioli, C. Effect of Molecular Weight and Crystallinity on Poly(Lactic Acid) Mechanical Properties. *J. Appl. Polym. Sci.* **1996**, *59* (1), 37–43. https://doi.org/10.1002/(sici)1097-4628(19960103)59:1<37::aid-app6>3.0.co;2-n.

(40) Ramli, R. A. Hollow Polymer Particles: A Review. *RSC Adv.* **2017**, *7* (83), 52632–52650. https://doi.org/10.1039/c7ra10358a.

(41) Zhang, T.; Jin, C.; Wang, L.; Yin, Q. One-Step Synthesis of Hollow Polymeric Nanospheres: Self-Assembly of Amphiphilic Azo Polymers via Hydrogen Bond Formation. *RSC Adv.* **2014**, *4* (69), 36882–36889. https://doi.org/10.1039/c4ra06415a.

(42) Cao, Y.; You, B.; Wu, L. Facile Fabrication of Hollow Polymer Microspheres through the Phase-Inversion Method. *Langmuir* **2010**, *26* (9), 6115–6118. https://doi.org/10.1021/la100450y.

(43) Han, J.; Song, G.; Guo, R. A Facile Solution Route for Polymeric Hollow Spheres with Controllable Size. *Adv. Mater.* **2006**, *18* (23), 3140–3144. https://doi.org/10.1002/adma.200600282.

(44) Kaneko, T.; Higashi, M.; Matsusaki, M.; Akagi, T.; Akashi, M. Self-Assembled Soft Nanofibrils of Amphipathic Polypeptides and Their Morphological Transformation. *Chem. Mater.* **2005**, *17* (10), 2484–2486. https://doi.org/10.1021/cm048196f.

(45) Hong, B. H.; Lee, J. Y.; Lee, C.-W.; Kim, J. C.; Bae, S. C.; Kim, K. S. Self-Assembled Arrays of Organic Nanotubes with Infinitely Long One-Dimensional H-Bond Chains. *J. Am. Chem. Soc.* **2001**, *123* (43), 10748–10749. https://doi.org/10.1021/ja016526g.

(46) Molla, M. R.; Ghosh, S. Structural Variations on Self-Assembly and Macroscopic Properties of 1,4,5,8-Naphthalene-Diimide Chromophores. *Chem. Mater.* **2011**, *23* (1), 95–105. https://doi.org/10.1021/cm102343r.

(47) Yin, Y.; Gao, Z.; Bao, Y.; Hou, B.; Hao, H.; Liu, D.; Wang, Y. Gelation

Phenomenon during Antisolvent Crystallization of Cefotaxime Sodium. *Ind. Eng. Chem. Res.* **2014**, *53* (3), 1286–1292. https://doi.org/10.1021/ie403539d.

(48) Panayiotou, C. Redefining Solubility Parameters: The Partial Solvation Parameters. *Phys. Chem. Chem. Phys.* **2012**, *14* (11), 3882–3908. https://doi.org/10.1039/c2cp23966c.

(49) Abbott, S.; Hansen, C. M.; Yamamoto, H. *Hansen Solubility Parameters in Practice Complete with EBook , Software and Data*; 2013.

(50) Hansen, C. M. *Hansen Solubility Parameters: A User's Handbook*; 2011; Vol. 118.

(51) Debnath, M.; Sasmal, S.; Haldar, D. Fabrication of Egg Shell-like Nanovesicles from a Thiocoumarin-Based ε-Amino Ester: A Potential Carrier. *J. Mater. Chem. B* **2017**, *5* (27), 5450–5457. https://doi.org/10.1039/C7TB00025A.

CHAPTER IV

Synthesis and stereochemistry-property study of diketopiperazine-based polyamides

4.1 Introduction

Stereochemistry is an important factor which deeply affect the physical and biological properties of polymeric materials.[1–4] For example, tacticity which is one of the structural stereochemistry, plays a vital role in mechanical properties on poly(propene) and poly(latic acid).[2] Isotactic polymers consist of only one constitutive basic unit and are generally semi-crystalline with helical structure. Syndiotactic polymers consist of alternating arrangements of basic units which are enantiomerical, and mostly have high crystallinity. Atactic polymers have disordered arrangement of basic units, and consequently are generally amorphous. In peptide science, since the advent of structural biology, accurate understanding of the relationship between protein structure and bioactivities has been an important issue in biophysics.[1] The spatial arrangement of backbone amide hydrogen bonds, the planar peptide bonds and side chains determine the local structure of peptide[5].

Diketopiperazines (DKPs), are a kind of simple peptides and widely found in natural and food production. DKPs are biodegraded products of peptides and also an important core series of bioactive molecules.[6–8] DKPs have two hydrogen bonding acceptor and two donor sites in a six-membered ring, which enable to form regular molecular assemblies through continuous intermolecular hydrogen bonding.[9] The self-assemble properties of DKPs have been widely studied, and nano-fiber or particles with various morphologies have been fabricated.[10,11] As a result, DKP unit has been considered as a vital building block with potential use in drug delivery system. As cyclic dipeptide of two amino acids, DKPs have two chiral carbon, which provide stereochemistry. The stereochemistry of DKPs is reported that have important effect on their bioactivity, self-assemble behavior and also their chiral catalytic properties.[12]

DKPs have interest properties of self-assembly and chirality, which also attract scientists from polymer field. DKPs have been introduced in to polymer side chain, which exhibited several functions. For instant, DKP was introduced into chitosan side chain, which provided a porous sponge.[13] Polyacetylene with DKP side chain was reported by Sanda et. al, in which hydrogen bonding of DKP unit stabilized the helix structure of polymer[14]. In addition, study in the introduction of DKP into polymer main chain normally meet with a problem of low solubility of DKPs, which result to low molecular weight of resulting polymers. However, most of researches on DKP-containing polymers focus on the hydrogen bond and self-assembly, while the stereochemistry, which is an important feature of DKP unit, is barely investigated. The stereochemistry of DKP-containing polymers is considered to have crucial effect on polymer properties, especially the optical and self-assemble properties.

In Chapter II, AB-type DKP cyclo(aspartyl-4-amino-phenylalanyl) (ADKP) with stereochemistry were synthesized, which are suitable for producing DKP-based polymers to study polymeric stereochemistry. And also, in Chapter III, self-assembly of LL-type DKP-based polyamide was study, which shows potential for medical use.

This chapter deals with the synthesis of DKP-based polyamides with stereochemistry, as well as the stereochemistry-property relationship of resulting polymers.

4.2 Experimental

4.2.1 Materials

5% Palladium on activated carbon (Pd/C) and *N*-methylpyrrolidone (NMP) were purchased from FUJIFILM Wako Pure Chemical Corporation. Dimethyl sulfoxide (DMSO), acetone and toluene were purchased from Kanto Chemical Co., Inc. All the chemicals were directly used as purchased. LL-, DD- and LD-type cyclo(aspartyl-4-amino-phenylalanyl) (LL-ADKP, DD-ADKP, and LD-ADKP) were obtained from Chapter II.

4.2.2 Characterization

^{1}H NMR spectra were performed by a Bruker Biospin AG 400 MHz, 54 mm spectrometer using DMSO-d_6 as the solvent.

The FT-IR spectra were recorded with a Perkin-Elmer Spectrum One spectrometer between 4000 and 400 cm^{-1} using a diamond-attenuated total reflection (ATR) accessory.

The number-average molecular weight (M_n), weight-average molecular weight (M_w) and the molecular weight distribution (M_w/M_n) were determined by gel permeation chromatography (GPC, concentration 1 g/L, 10 mM LiBr/DMF eluent) after calibration with polystyrene standards using two of OHpack SB-806M HQ column (Shodex).

Thermogravimetric analysis (TGA) and differential scanning calorimetry (DSC) were carried out by Seiko Instruments SII, SSC/5200 and Seiko Instruments SII, X-DSC7000T, respectively, at a heating rate of 5 °C/min under a nitrogen atmosphere. Remaining solvent and absorbed moisture in polymer samples were removed at 200 ^{o}C for 1 hour before TGA and DSC measurement.

Circular dichroism (CD) spectra were recorded with a JASCO J-820 spectrometer. All samples were dissolved in DMSO with concentration of 1 mg / ml. Quartz cuvette with 1 cm path length was used. Measured region was 190-300 nm. All spectra were solvent-corrected.

Polymer particles morphology were characterized with scanning electron microscope (JCM-6000Plus Versatile Benchtop SEM). Samples were coated with a layer of gold in thickness of 15 nm by a sputter coater (Magnetron sputter MSP-1S). SEM instrument was operated at an acceleration voltage of 10 kV and an emission current of 10 μA.

4.2.3 Polyamides syntheses

A typical polymerization procedure for DKP-based polyamides is shown below (Scheme 4.1). ADKP (0.055 g, 0.2 mmol) was mixed with $P(OPh)_3$ (40 μL, 0.15 mmol), pyridine (50 μL, 0.6 mmol), and NMP (100 μL). The reaction solution was stirred at 100 °C for 48 h under nitrogen atmosphere. After the reaction finished, the resulting solution was precipitated in acetone and methanol, and the resulting solid was dried in a vacuum oven at 100 °C. The polyamide from LL-ADKP (LL-PA) was obtained with 81% yield; the polyamide from DD-ADKP (DD-PA) was obtained with 83% yield; the polyamide from LD-ADKP (LD-PA) was obtained with 76% yield; the polyamide from co-polymerization of LL-ADKP and DD-ADKP (LLcoDD-PA) was obtained with 72% yield.

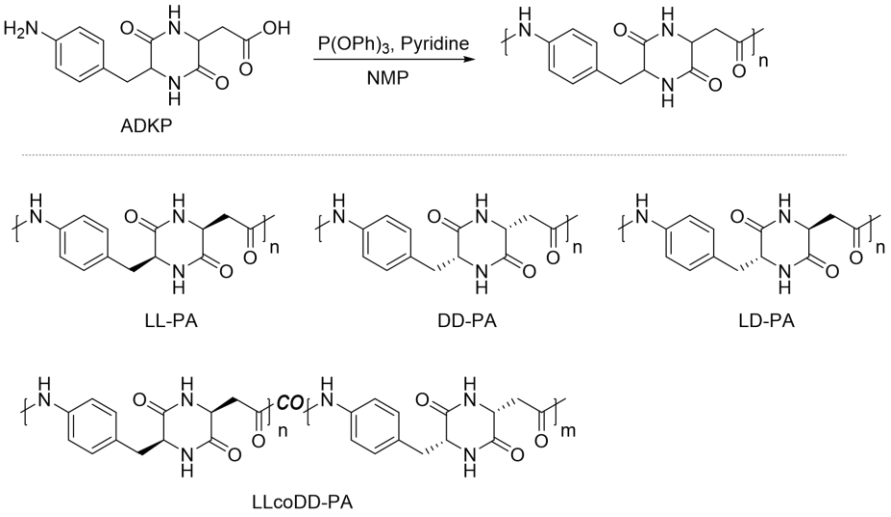

Scheme 4.1 Synthesis of ADKP-based polyamides, and structures of polyamides.

4.3 Results and discussion

4.3.1 Characterization of polymers.

Four kinds of polyamides were prepared by homo-polymerization or co-polymerization of ADKP stereoisomers. Among these polymers, LL-PA was already prepared in Chapter III. For structural analysis, obtained polymers were measured by ^{1}H NMR, shown in Figure 4.1. Spectra of all polymers show peaks of DKP amide N-*H* unchanged at 7.9 and 8.1 ppm. A characteristic peak from phenyl amide N-*H* appears in all spectra, where, peak of polymers from *cis*-ADKP locates at 9.7 ppm, while peak of PA-LD locates at lower field 9.9 ppm. Meanwhile, α-protons in LD-PA locate at the higher field, 4.10 and 4.12 ppm, compared to 4.18 and 4.25 ppm in LL-PA, DD-PA and LLcoDD-PA. Moreover, β-protons from phenylalanine part in LD-PA have higher *J*-coupling constant than LL-PA, DD-PA and LLcoDD-PA. *J*-Coupling constant is controlled by geometry of molecules, in which *trans*-structure normally has high than *cis*-structure.[15] Differences of α- and β-protons between LD-PA and other three polymers

were also observed between *cis*- and *trans*-ADKP monomers, which were discussed in Chapter II. As a result, from ^{1}H NMR spectra, it is suggested that stereo-structures of ADKP unit still maintain in polymers.

Infrared spectra of PAs are shown in Figure 4.2. No significant difference among all PAs is presented. Spectra exhibit characteristic peaks of DKP and polyamide: band of N-H stretching in around 3100-3600 cm^{-1}, band of C-H stretching in around 2800-3000 cm^{-1}, amide I (C=O stretching) at 1665 cm^{-1}, amide II (N-H bending) at 1606 and 1540 cm^{-1}, aromatic C=C at 1516 cm^{-1}, and C-N stretching at 1440, 1413 and 1267 cm^{-1}. The newly amide II peak at 1540 cm-1 indicates the amide formation of phenyl amine.

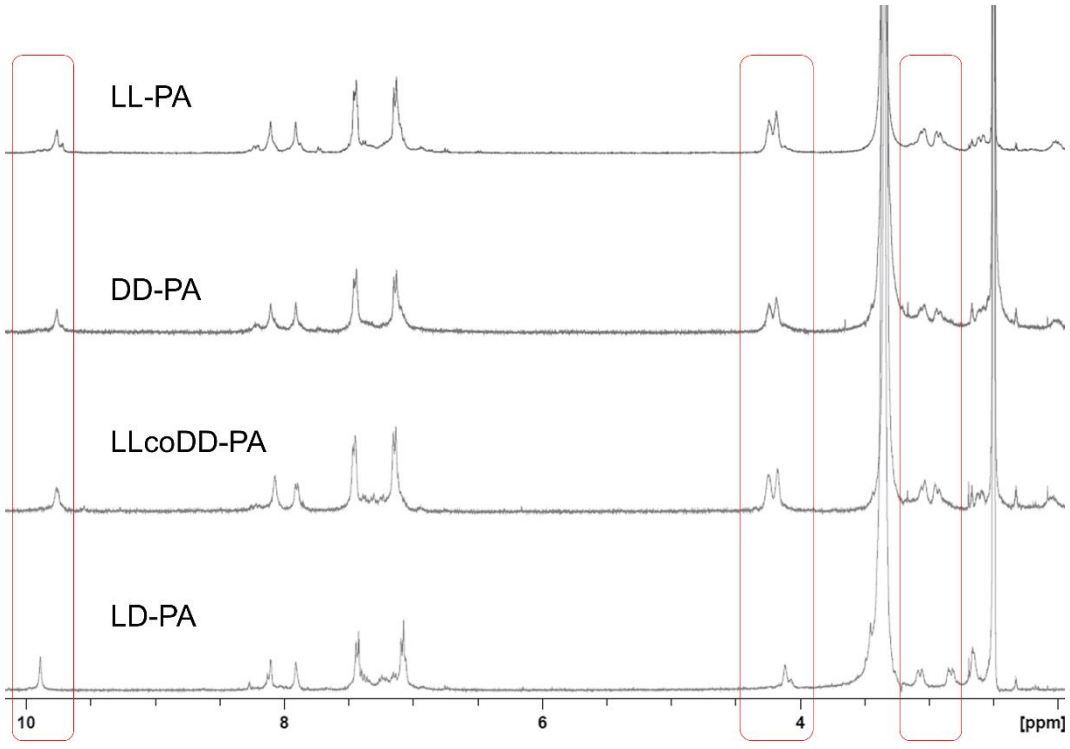

Figure 4.1 ^{1}H NMR spectra of LL-PA, DD-PA, LLcoDD-PA and LD- PA in DMSO-d_6

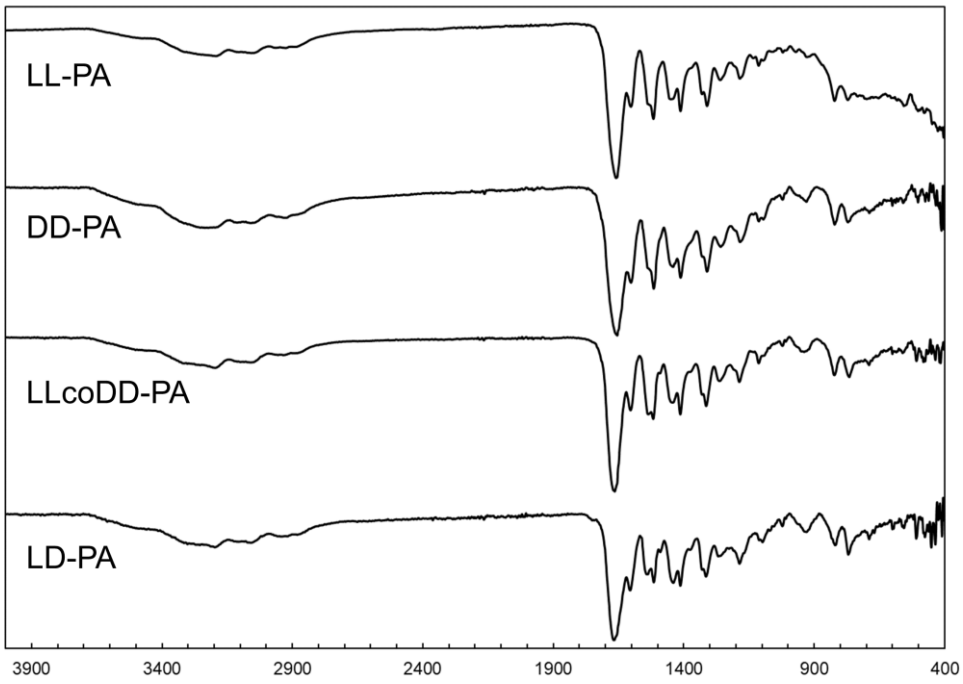

Figure 4.2 IR spectra of LL-PA, DD-PA, LLcoDD-PA, and LD-PA.

Molecular weight of obtained PAs were measured by GPC, which are summarized in Table 4.1. Notably, LL-PA was synthesized again from LL-ADKP obtained by coupling methods in Chapter III, thus, molecular weight of this LL-PA is a little bit different from Chapter II. Weight average molecular weights of all PAs are higher than 1×10^4 g/mol, from 1.33 to 1.51 g/mol. Obtained Pas have close molecular weight, which indicates the close reactivity of ADKP stereoisomers. In addition, all PAs have narrow polydispersity index, from 1.08-1.20, which is presumably due to the absolute stoichiometric ratio of AB-type monomer.

Thermal degradation analysis was applied to evaluate the thermal decomposition of PAs in a nitrogen atmosphere, and summarized in Table 4.1 and Figure 4.3. 5% degradation temperature (T_{d5}) and 10% degradation temperature (T_{d10}) are in the range of 283-305 °C, and 314-334 °C, respectively. Due to the same chemical structure, thermal

properties of obtained PAs show close thermal properties. LL-PA and LLcoDD-PA have slightly higher heat-resistance, that may be caused by the higher molecular weight. Moreover, the thermal physical transformation of PAs was investigated by DSC. The glass transition temperature (T_g) of all PAs were not detected in the range of 50–250 °C, which suggest that all PAs transition temperatures are close to their decomposition temperatures.

The solubility of PAs was summarized in Table 4.2. All PAs show similar solubility, which dissolve in high polar organic solvents such as DMSO, DMF, and NMP. In methanol, PAs partially dissolve.

As results, ADKP stereoisomers show similar activity on polymerization, and PAs with stereochemistry have no significant difference in thermal properties and solubility.

Table 4.1 Molecular weights and thermal properties of PAs derived from ADKP

Polymers	M_w [a] ($\times 10^4$ g/mol)	M_n [a] ($\times 10^4$ g/mol)	M_w/M_n [a]	T_{d5} (°C) [b]	T_{d10} (°C) [b]
LL-PA	1.51	1.26	1.20	305	334
DD-PA	1.45	1.23	1.18	283	314
LLcoDD-PA	1.45	1.28	1.13	301	326
LD-PA	1.33	1.23	1.08	287	323

[a] Determined by GPC measurements based on polystyrene standards; eluent, 10 mmol L^{-1} of LiBr DMF solution. [b] T_{d5} and T_{d10} were observed from TGA curve scanned at a heating rate of 5 °C/min under nitrogen atmosphere.

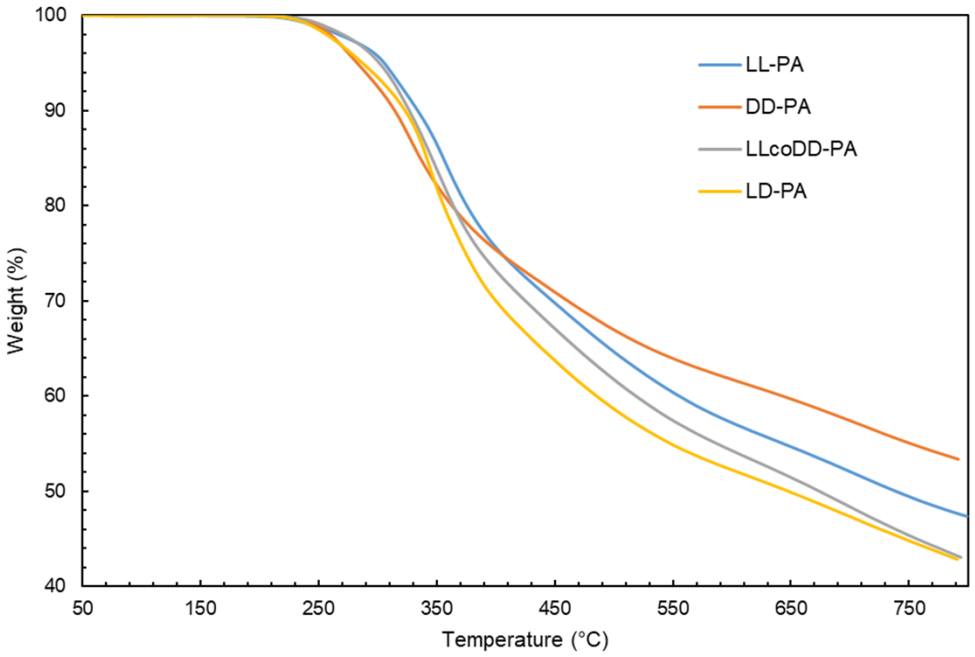

Figure 4.3 TGA curves of LL-PA, DD-PA, LLcoDD-PA, LD-PA

Table 4.2 Solubility of PAs[a]

	Water	Methanol	Ethanol	Acetone	DMSO	DMF	NMP
LL-PA	-	±	-	-	+	+	+
DD-PA	-	±	-	-	+	+	+
LLcoDD-PA	-	±	-	-	+	+	+
LD-PA	-	±	-	-	+	+	+

[a] Conditions; samples, 10 mg; solvent, 2 mL; temperature, r.t.; +, soluble; ±, partially soluble; −, insoluble.

4.3.2 Optical study of PAs.

Circular dichroism (CD) spectroscopy was used to detect the optical properties of PAs with stereochemistry (Figure 4.4). In LL-PA, CD spectrum display a negative Cotton effect at 202 nm, while DD-PA show a positive Cotton effect. These CD curves suggest that main chains of LL-PA and DD-PA have oppositive orientations. In LD-PA, negative Cotton effect was exhibited at 208 and 190 nm. In the case of LLcoDD-PA, the copolymer of enantiomers, display a positive Cotton effect at 202 nm, and a strong negative Cotton effect at 190 nm. The Cotton curve of LLcoDD-PA suggests that the co-polymerization was successful, and the obtained polymer was not a mixture of LL-PA and DD-PA. These CD spectra indicate that all PAs are optical active.

As we known, solvent has a great impact on the secondary structure of polymer. Moreover, molecular interactions also affect the configuration of polymer, especially in peptide science. As mentioned in Chapter III, DKP-based polymer showed different self-assemble behaviors in different solvents, resulting in different morphologies. Thus, solvent/third molecules effect was studied by CD spectroscopy. In this study, 0.1 ml of poor solvents, such as water, ethanol, acetone and toluene, were added into the LL-PA DMSO solution (1 mg of LL-PA in 1 ml DMSO). Resulting solutions were detected by CD spectroscopy. In the case of using toluene, precipitation occurred immediately after toluene being added, so the solution was not used in CD spectroscopy. As shown in Figure 4.5, by adding water and ethanol, LL-PA was optical deactivated, while by adding acetone, LL-PA shows different Cotton effect from pure DMSO solution. It indicates that, hydrogen-bond play an important role in stabilizing secondary structure of DKP-based polymer. When molecules with high hydrogen bond formation property were added, hydrogen bond between DKP was broken, which supports the analysis in Chapter III.

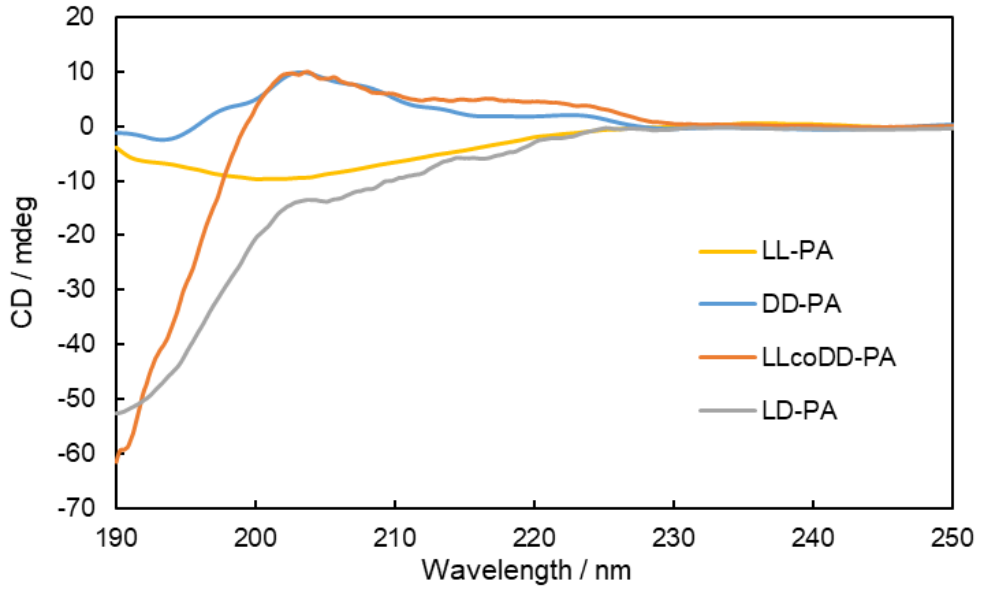

Figure 4.4 CD spectra of LL-, DD-, LLcoDD- and LD-PA in DMSO.

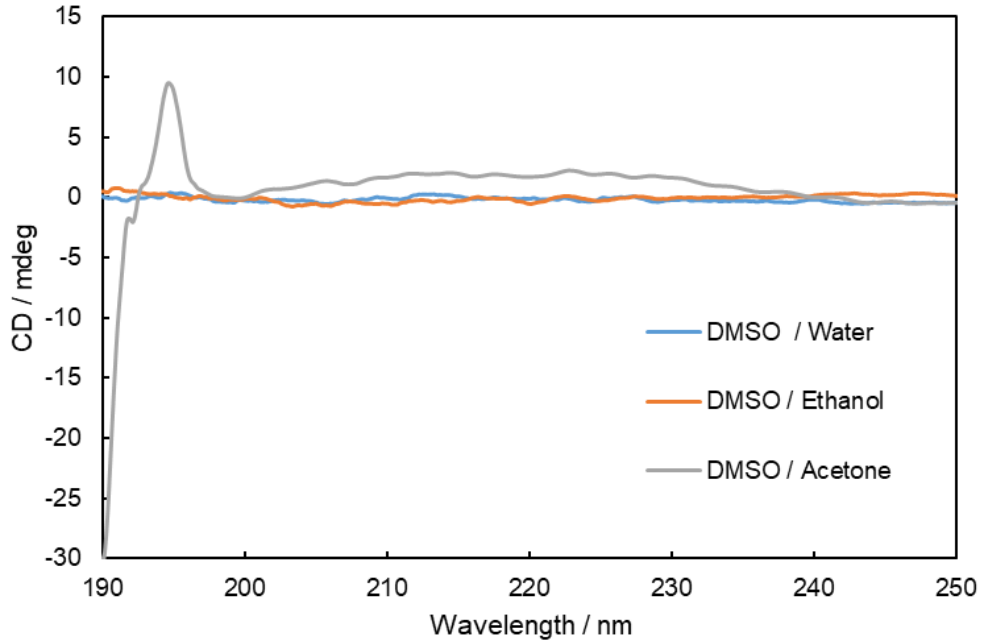

Figure 4.5 CD spectra of LL-PA in DMSO/water, DMSO/ethanol and DMSO/acetone.

4.3.3 Self-assembly properties of PAs

In Chapter III, LL-type ADKP polyamide LL-PA showed polymorphism property of self-assembly behavior in different solvents. Especially in acetone and toluene, hollow spheres with different sizes were observed. In other PAs from ADKP stereoisomers, how the stereochemistry affects the self-assembly behavior is in interest.

In this study, self-assembly of homopolymer from *cis*-ADKPs, LL-PA and DD-PA, the copolymer from cis-ADKPs, LLcoDD-PA, and homopolymer from *trans*-ADKP, LD-PA were investigated by particle formation (Figure 4.6). Morphological study was only performed by using acetone and toluene. In acetone, LL-PA, DD-PA, and LLcoDD-PA all self-assembled in similarly hollow spheres, with the diameter of approximate 0.5-1 μm. In contrary, LD-PA self-assembled in cubic structure in acetone, with the size of about 300 nm. In toluene, hollow spheres with the diameter of 7-14 μm were observed in samples of LL-PA, DD-PA, and LLcoDD-PA. In the case of LD-PA, cubic particles were observed, with the size of 0.5-1 μm.

As results, polymers from *cis*-stereoisomers, LL-ADKP or DD-AKPD, regardless of homo-polymers or co-polymer, exhibit similarly self-assemble behavior. However, LD-PA which is form *trans*-stereoisomer, LD-ADKP, show totally different self-assembly properties. LD-PA prefer to self-assemble into cubic structure, which is similar to particles of LL-PA from transformation in Chapter III. The different self-assemble behavior between PAs from *cis*-ADKP and PLD is the first exhibition of the effect of stereochemistry of DKP polymer on morphology.

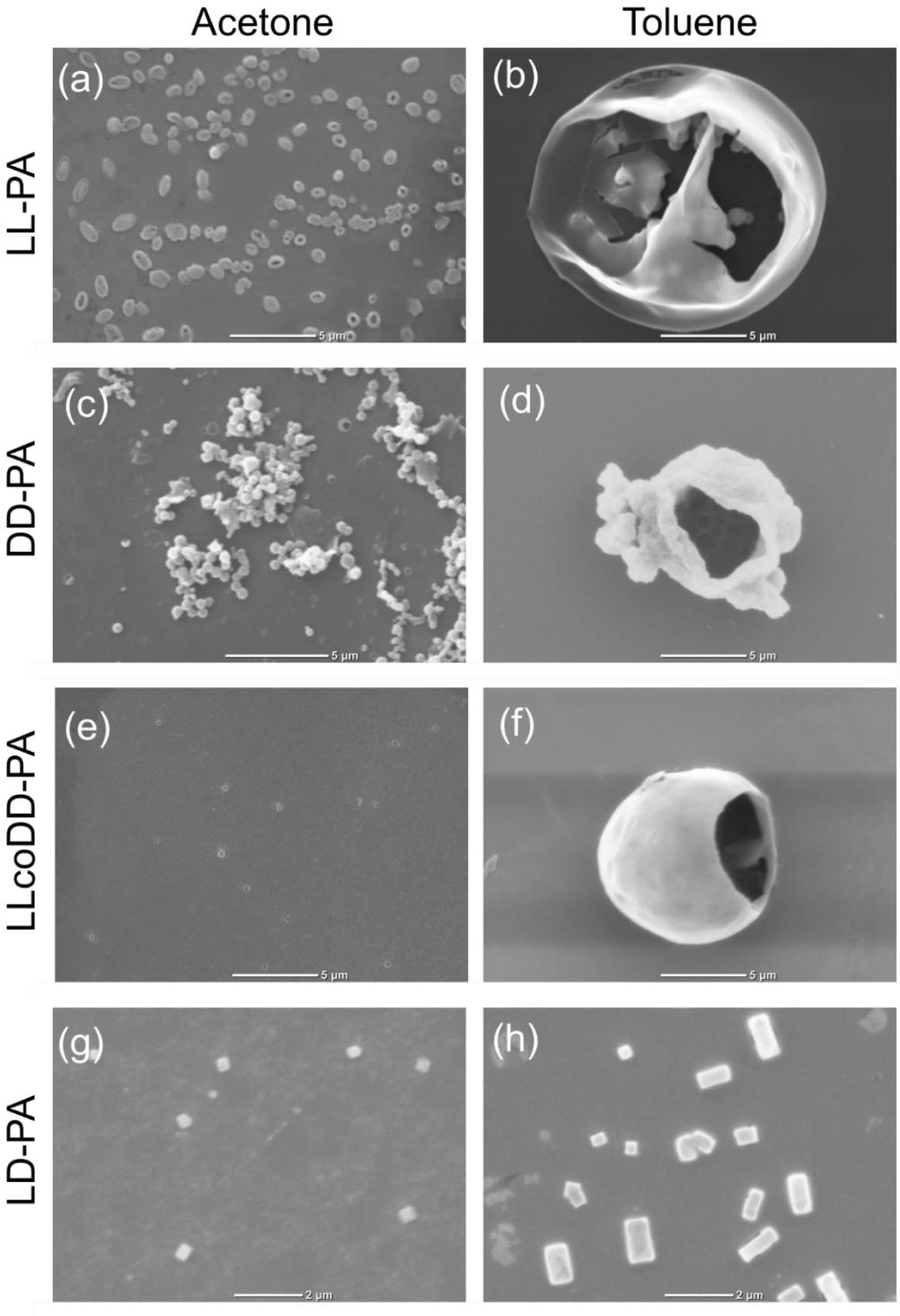

Figure 4.6 SEM images of particles obtained by (a) LL-PA in acetone, (b) LL-PA in toluene (c) DD-PA in acetone, (d) DD-PA in toluene, (e) LLcoDD-PA in acetone, (f) LLcoDD-PA in toluene, (g) LD-PA in acetone, and (h) LD-PA in toluene.

4.4 Conclusion

Homo-polymerizations of ADKP stereoisomers and co-polymerization of LL-ADKP and DD-ADKP were performed to synthesize DKP-based polyamides with stereochemistry, LL-PA, DD-PA, LD-PA and LLcoDD-PA. All PAs showed similar molecular weight, thermal properties and solubility, due to their same chemical structure. Optical properties of PAs were determined by CD spectroscopy. All PAs were optical active, and LL-PA and DD-PA exhibited opposite Cotton effect. Moreover, solvent/third molecule effect on LL-PA was investigated by adding other solvents in the LL-PA DMSO solution. When water and ethanol were added, LL-PA in DMSO became optical inactivity, which suggested the hydrogen bond play an important role in stabilizing secondary structure of DKP-based polymer. Self-assembly of PAs were investigated. Particles of LL-PA, DD-PA and LLcoDD-PA showed similar morphologies of hollow structure, indicating the similar self-assemble behavior, while LD-PA self-assembled into cubic structure in toluene and acetone. The present study provides structural insights of DKP-based polymers with stereochemistry, and reveals their optical and self-assemble properties.

Refences

(1) Garcia, A. M.; Iglesias, D.; Parisi, E.; Styan, K. E.; Waddington, L. J.; Deganutti, C.; De Zorzi, R.; Grassi, M.; Melchionna, M.; Vargiu, A. V.; Marchesan, S. Chirality Effects on Peptide Self-Assembly Unraveled from Molecules to Materials. *Chem* **2018**, *4* (8), 1862–1876. https://doi.org/10.1016/j.chempr.2018.05.016.

(2) Ovitt, T. M.; Coates, G. W. Stereochemistry of Lactide Polymerization with Chiral Catalysts: New Opportunities for Stereocontrol Using Polymer Exchange Mechanisms. *J. Am. Chem. Soc.* **2002**, *124* (7), 1316–1326. https://doi.org/10.1021/ja012052+.

(3) Robert, J. L.; Aubrecht, K. B. Green Chemistry: Ring-Opening Polymerization of Lactide to Form a Biodegradable Polymer. *J. Chem. Educ.* **2008**, *85* (2), 258–260. https://doi.org/10.1021/ed085p258.

(4) Nagahama, S.; Tanaka, T.; Matsumoto, A. Supramolecular Control over the Stereochemistry of Diene Polymers. *Angew. Chemie* **2004**, *116* (29), 3899–3902. https://doi.org/10.1002/ange.200453738.

(5) Mori, K. Bioactive Natural Products and Chirality. *Chirality* **2011**, *23* (6), 449–462. https://doi.org/10.1002/chir.20930.

(6) Schnabel, T.; Barbu, M.-C.; Windeisen-Holzhauser, E.; Petutschnigg, A.; Tondi, G. Impact of Leather on the Fire Resistance of Leather-Wood Fibreboard: FT-IR Spectroscopy and Pyrolysis-GC-MS Investigation. *Adv. Mater. Sci. Eng.* **2019**, *2019* (i), 1–8. https://doi.org/10.1155/2019/2473927.

(7) Borthwick, A. D.; Liddle, J. The Design of Orally Bioavailable 2, 5-

Diketopiperazine Oxytocin Antagonists: From Concept to Clinical Candidate for Premature Labor. *Med. Res. Rev.* **2011**, *31* (4), 576–604. https://doi.org/10.1002/med.20193.

(8) Borthwick, A. D. 2,5-Diketopiperazines: Synthesis, Reactions, Medicinal Chemistry, and Bioactive Natural Products. *Chem. Rev.* **2012**, *112* (7), 3641–3716. https://doi.org/10.1021/cr200398y.

(9) Corey, R. B. The Crystal Structure of Diketopiperazine. *J. Am. Chem. Soc.* **1938**, *60* (7), 1598–1604. https://doi.org/10.1021/ja01274a023.

(10) Pérez-Mellor, A.; Le Barbu-Debus, K.; Zehnacker, A. Solid-State Synthesis of Cyclo LD-Diphenylalanine: A Chiral Phase Built from Achiral Subunits. *Chirality* **2020**, *32* (5), 693–703. https://doi.org/10.1002/chir.23195.

(11) Lan, Y.; Lv, M.; Guo, S.; Nasr, P.; Ladizhansky, V.; Vaz, R.; Corradini, M. G.; Hou, T.; Ghazani, S. M.; Marnangoni, A.; Rogers, M. A. Molecular Motifs Encoding Self-Assembly of Peptide Fibers into Molecular Gels. *Soft Matter* **2019**, *15* (45), 9205–9214. https://doi.org/10.1039/c9sm01793c.

(12) Schoenebeck, F.; Houk, K. N.; Schoenebeck, F.; Houk, K. N. Theoretical Study of the Catalysis of Cyanohydrin Formation by the Cyclic Dipeptide Catalyst Cyclo [(S) -His- (S) -Phe] Theoretical Study of the Catalysis of Cyanohydrin Formation by the Cyclic Dipeptide Catalyst Cyclo [(S) -His- (S) -Phe]. **2009**, No. 5, 1464–1472. https://doi.org/10.1021/jo801958r.

(13) Takada, K.; Yin, H.; Matsui, T.; Ali, M. A. Bio-Based Mesoporous Sponges of Chitosan Conjugated with Amino Acid-Diketopiperazine through Oil-in-Water

Emulsions. *J. Polym. Res.* **2017**.

(14) Terada, K.; Masuda, T.; Sanda, F. Synthesis and Secondary Structure of Polyacetylenes Carrying Diketopiperazine Moieties. The First Example of Helical Polymers Stabilized by s - Cis -Amide-Based Hydrogen Bonding. *Macromolecules* **2009**, *42* (4), 913–920. https://doi.org/10.1021/ma8023552.

(15) Zhang, D.; Wang, W. A Facile Synthesis of Cysteine-Based Diketopiperazine from Thiol-Protected Precursor. *R. Soc. Open Sci.* **2018**, *5* (6), 180272. https://doi.org/10.1098/rsos.180272.

CHAPTER V

General conclusions

Diketopiperazine (DKP) unit is an important building block for medicines, catalysts, supramolecules, and has enormous potential for development of functional materials. The synthesis and property study of DKP-based monomers and polymers could create a new insight on stereochemistry and self-assembly of both DKP monomers and polymers. This study focuses on the synthesis and properties of DKP-based monomers and relative polyamides from aspartame or coupling of aspartic acid and phenylalanine derivatives.

In chapter II, as chirality is one of important features of DKPs, cyclo(L-aspartyl-4-amino-L-phenylalanyl) (ADKP) stereoisomers were synthesized by the coupling of aspartic acid and phenylalanine derivatives. Structural study of ADKP stereoisomers was performed by ^{1}H NMR, two-dimensional NMR ROESY, FTIR, TD-DFT and CD, which suggested that C-H$\cdots\pi$ interaction plays an important role in stabilizing aromatic DKP configurations.

In chapter III, LL-type ADKP, as an analog of aspartame, was synthesized and applied into syntheses of DKP-based polyamides. Self-assembly of DKP-based polyamide was studied by particles fabrication from different poor solvents. Various morphologies of particles were observed, including irregular networks, hollow spheres, and cubic structures, which are rare cases for homopolymer without side chain. Hansen solubility parameters were applied to studied the solvent-morphology relationship.

In chapter IV, homo-polyamides and co-polyamide were synthesized from ADKP stereoisomers, which were synthesized in Chapter II, and their stereochemistry-property

relationship was investigated. Polymers with stereochemistry showed similar molecular weight, thermal properties and solubility, due to their same chemical structure. All PAs were optical active; however, the addition of water or ethanol could make polymers became optical inactive by interrupting DKP-DKP hydrogen bond, which supported the analysis of Hansen solubility parameter in Chapter III. Moreover, PAs with different stereochemistry show different self-assemble behaviors, which was presumably due to *cis*- and *trans*-structure of DKP unit.

Academic achievements

Publications:

1) Takada, K.; **Yin, H**.; Matsui, T.; Ali, M. A.; Kaneko, T. Bio-Based Mesoporous Sponges of Chitosan Conjugated with Amino Acid-Diketopiperazine through Oil-in-Water Emulsions. *J. Polym. Res.* **2017**, *24* (12), 216. https://doi.org/10.1007/s10965-017-1372-7.
2) **Yin, H.**; Takada, K.; Kumar, A.; Hirayama, T.; Kaneko, T. Synthesis and Solvent-Controlled Self-Assembly of Diketopiperazine-Based Polyamides from Aspartame. *RSC Adv.* 2021, *11* (11), 5938–5946. https://doi.org/10.1039/D0RA10086B.

Conferences:

1) 10th International Conference of Modification, Degradation and Stabilization of Polymers (MoDeSt2018), Tokyo, “Aspartame Diketopiperazine for Synthesis of Biopolymers”. (Poster)
2) 14th IUPAC International Conference on Novel Materials and their Synthesis (NMS-XIV), Guangzhou, “Syntheses of Diketopiperazine-Based Polyamides and Morphology Control of Their Particles”. (Poster)
3) The 12th SPSJ International Polymer Conference (IPC2018), Hiroshima, “Syntheses and Morphological Studies of Diketopiperazine-Based Polyamides”. (Oral)